

THE UNIVERSITY *of* EDINBURGH

This thesis has been submitted in fulfilment of the requirements for a postgraduate degree (e. g. PhD, MPhil, DClinPsychol) at the University of Edinburgh. Please note the following terms and conditions of use:

- This work is protected by copyright and other intellectual property rights, which are retained by the thesis author, unless otherwise stated.
- A copy can be downloaded for personal non-commercial research or study, without prior permission or charge.
- This thesis cannot be reproduced or quoted extensively from without first obtaining permission in writing from the author.
- The content must not be changed in any way or sold commercially in any format or medium without the formal permission of the author.
- When referring to this work, full bibliographic details including the author, title, awarding institution and date of the thesis must be given.

The role of Retinoblastoma protein in the development of liver cancer

Louise Treanor

Submitted for the degree of PhD

University of Edinburgh 2006

Declaration

This thesis and the work described herein are my own. Where contributions have been made by others this is stated in the text.

Louise Treanor

June 2006

Acknowledgements

First of all I would like to thank my supervisors Sandrine Prost, Chris Bellamy and Sarah Howie. Many thanks to Sandrine for giving me this project to work on which I enjoyed greatly. I am also extremely grateful for all the contributions she made with her expertise, time and also for guiding me so much. Also I am hugely grateful to David Harrison for all his help and contributions to the project. A special thank you goes to Helen for her patience with me, her assistance on Monday mornings with the perfusions and for all the cups of tea. A special thank you to Pin Lu for his help with the real-time PCR and also for his advice on various aspects of the project. Thanks to Sarah Howie for all her guidance. I am also indebted to Bob Morris for helping me with just about everything. Also thanks to Kirsty, Nass and Linda in the office.

I would like to thank the girls Ada, Amanda, Aoife, Cathy, Catherine, Elaine, Kathleen, Helen, Kathryn and Muireann for all their visits across the Irish sea or in Kathryn's case escaping from Dundee. Thanks to Vincent for the never ending supply of cookies. Lastly I would like to thank my family my sisters Eileen and Caroline and my brother John for all the chats and words of encouragement. This thesis is dedicated to Mum and Dad, thanks for all your love and support.

Abstract 3

Abbreviations 4

CHAPTER 1: INTRODUCTION 9

1.1 Human hepatocellular carcinoma (HCC) 9

1.2 The Cre-lox system 12

1.3 Retinoblastoma protein (Rb) 14

1.4 Rb function 14

1.4.1 Regulation of transcription by Rb 14

The regulation of E2F transcription factors *15*

Acetylation and methylation by Rb *19*

1.4.2 Cell cycle regulation by Rb 21

Cyclin D1 ..... *23*

Regulation of the G1/S transition *23*

Cyclin E *24*

Cyclin A *26*

Regulation of G_2/M by Rb *28*

Regulation of mitosis by Rb *30*

1.4.3 Anti-apoptotic function of Rb 30

1.4.4 Regulation of differentiation by Rb 31

1.4.5 Regulation of senescence by Rb 31

1.5 Regulation of Rb 32

1.5.1 Cyclins 32

1.5.2 Cyclin dependent kinase inhibitors (CDKi) 33

1.5.3 Altered RB regulation in HCC 35

1.6 The p53 connection 35

1.6.1 Alterations of p53 in HCC 36

1.6.2 Regulation of p53 stabilisation and activation 37

Phosphorylation of p53 ..... *37*

Acetylation of p53 40
Sumoylation of p53 44
Murine double minute 2 (MDM2) 45
p19 Alternative reading frame (p19ARF) 47
1.6.3 Uncontrolled p53 regulation in HCC 52
1.6.4 Intra S-phase checkpoint 52
1.6.5 The mitotic checkpoint 57
1.7 Aims and hypothesis 61

CHAPTER 2: MATERIALS AND METHODS 62

2.1 Hepatocyte culture 62
2.2 Immunoblotting 65
2.2.1 Preparation of samples 65
2.2.2 Immunoprecipitation 66
2.2.3 Quantification of protein 66
2.2.4 Protein electrophoresis 67
2.2.5 Detection 68
2.3 Immunofluorescence 72
2.4 RNA 75
2.4.1 RNA extraction 75
2.4.2 Reverse-transcription PCR 76
2.4.3 Real-time RT-PCR 76
2.5 DNA 77
2.5.1 DNA extraction 77
2.5.2 PCR 78
2.5.3 DNA Damage Kit (Biovision) 80
2.5.4 8-oxo-dG Measurement 80
2.6 Reactive oxygen species (ROS) measurement 81
2.6.1 CM-H_2DCFDA measurement of ROS 81
2.6.2 Dihydroethidium (DHE) measurement of superoxide anion 82

2.7 Preparation of mouse embryonic fibroblasts (MEFS)..... 83

CHAPTER 3: THE MECHANISM FOR THE ACUTE STABILISATION OF p53 IN *Rb*-/- HEPATOCYTES. 84

3.1 Introduction 84

3.2 Results..... 86

3.2.1 A transient stabilisation of p53 following deletion of *Rb* by cre recombinase..... 86

3.2.2 MDM2 expression and localisation in WT and *Rb*-/- hepatocytes..... 88

3.2.3 $p19^{ARF}$ is overexpressed in *Rb*-/- hepatocytes compared to WT 93

3.2.4 Interactions of $p19^{ARF}$, MDM2 and p53 99

3.2.5 Nucleophosmin expression in WT and *Rb*-/- hepatocytes 100

3.3 Discussion 105

CHAPTER 4: LOSS OF *Rb* LEADS TO AN INCREASE IN DNA DAMAGE IN HEPATOCYTES.....107

4.1 Introduction 107

4.2 Results..... 111

4.2.1 ATR, the DNA damage response kinase, expression and localisation in ..... hepatocytes 111

4.2.2 Expression and phosphorylation of checkpoint kinase 1 and 2..... 114

4.2.3 MnSOD expression is decreased in *Rb*-/- hepatocytes..... 116

4.2.4 Reactive oxygen species (ROS) production is increased in Rb-/- cells ..... and leads to an increase in DNA injury..... 118

4.2.5 Two DNA damage response proteins, H2A.X and p53 are ..... phosphorylated in *Rb* null cells 122

4.3 Discussion 127

CHAPTER 5: LOSS OF *Rb* LEADS TO ABERRANT CELL CYCLE ACTIVITY. 131

5.1 Introduction 131

5.2 Results 135

5.2.1 The expression of the cyclin family of proteins 135

5.2.2 Centrosomes number and Mad2 expression in WT and *Rb*-/- hepatocytes 139

5.2.3 A decrease in CDC25a is found in *Rb*-/- hepatocytes. 143

5.2.4 Gadd45a expression and localisation in the cytoplasm in *Rb*-/hepatocytes 145

5.3 Discussion 149

CHAPTER 6: FINAL DISCUSSION 153

6.1 A novel mechanism for the transient stabilisation of p53 in *Rb*-/- hepatocytes 153

6.2 The response to the upregulation of ROS in *Rb*-/- hepatocytes 155

6.3 A lack of cell cycle arrest in *Rb*-/- hepatocytes 158

6.4 Conclusion 160

6.5 Future work 161

REFERENCES 163

Appendix 1 190

Appendix 2 192

Abstract

Hepatocelluar carcinoma is the sixth most common cancer worldwide with a diverse aetiology. Dysregulation of the *Rb* pathway can occur in as high as 92% of liver cancers implicating Rb as an important factor in the progression of the disease. The impact *Rb* loss has on the development of liver cancer was determined using an in vitro system, with Cre-lox technology. The Cre-lox technology enables the lethality of *Rb* loss in the embryo to be overcome. The regulation of p53, extent of DNA damage and cell cycle control were investigated in *Rb-/-* hepatocytes. The tumor suppressor $p19^{ARF}$, previously reported to induce stabilisation of p53 was found upregulated. This combined with the localisation of MDM2 in the nucleolus implicates $p19^{ARF}$ as an important factor in the stabilisation of p53 in the *Rb-/-* hepatocytes. The elevated levels of ROS were found to be sufficient to induce DNA damage as measured by an increase in 8-oxo-dG and apurinic and apyrimdinic sites. The regulation of three cyclins, cyclin A, cyclin B and cyclin E is found to lack governance. Analysis of the G2/M checkpoint proteins such as Gadd45a, MAD2 and CDC25a all show a dysregulation in their activities. In conclusion *Rb* loss leads to aberrant regulation of p53 and induces DNA damage, this superimposed on a background of a lack of cell cycle control predisposes the hepatocyte to becoming a cancerous cell.

Abbreviations

APC	Anaphase promoting complex
ARF	Alternative reading frame
ATM	Ataxia telangiectasia-mutated protein
ATP	Adenosine triphosphate
ATR	Ataxia telangiectasia-related
ATRIP	ATR interacting protein
BAX	BCL-associated X protein
BRCA1	Breast cancer-associated gene 1
BRCA2	Breast cancer-associated gene 2
BRDU	5-bromodeoxy-uridine
BRG1	Brm-related gene 1
Brm	Brahma
Bub1	Budding inhibited by benzimadozles 1
BubR1	Spindle assembly checkpoint protein
C	Cysteine
CBP	CREB binding protein
CDC20	Cell divison cycle protein 20 homolog
CDC25a	Cell division cycle 25a
CDC25c	Cell division cycle 25c
CDC6	Cell division control protein 6
CDK	Cyclin dependent kinase
CDKI	Cyclin dependent kinase inhibitor
Chk1	Checkpoint kinase 1
Chk2	Checkpoint kinase 2
Cip/Kip	Cdk-inhibitory protein/kinase inhibitory protein
CK2	Cyclin kinase 2
CM-H_2DCFDA	5,6 chloro-methyl-2, 7 dihydrofluoroscein diacetate
CNS	Central nervous system
C_pG	Cytosine-phospho-Guanine

Cre	Cre recominbase
Cu/ZnSOD	Copper/Zinc superoxide dismutase
DAB	Diaminobenzidine
DHE	Dihydroethidium
DMSO	Dimethylsufoxide
DNA	Deoxyribonucleic acid
DNA-PK	DNA-dependent protein kinase
DNMT	DNA methyl transferase
DP	Dimerisation protein
DSB	Double strand breaks
E2F	Early region factor 2
EDTA	Ethylene diamine tetraacetic acid
ER	Endoplasmic reticulum
GADD45a	Growth arrest and DNA damage inducible protein 45 a
GSK3β	Glycogen synthase kinase 3 beta
HATs	Histone acetyltransferases
HBc	Hepatitis B virus C protein
HBV	Hepatitis B virus
HBx	Hepatitis B virus X protein
HCC	Hepatocellular carcinoma
HCV	Hepatitis C virus
HDAC	Histone deacetylase
HIPK2	Homedomain interacting kinase 2
HLH	Helix-loop-helix transcription factors
HP1	Heterochromatin protein 1
HRP	Horse radish peroxidase
Id2	Inhibitor of DNA binding 2
IGF	Insulin growth factor
IgG_{2A}	Immunoglobulin 2A
INK4	Inhibitors of the CDK4 kinases
IPTG	Isopropyl-thiogalactoside
IR	Ionising radiation

JNK	C-Jun N-terminal kinase
kDa	kilodaltons
L	Leucine
LOH	Loss of heterozygosity
Lox-p	Locus of crossover of P1
Lys	Lysine
Mad2	Mitotic spindle assembly checkpoint protein
MAPK	Mitogen activated protein kinase
MCM	Mini chromosome maintenance
MDM2	Minute double murine 2
MDMX	MDM2-related protein X
MDS	Myelodysplastic Syndromes
mM	Milimolar
MnSOD	Manganese superoxide dismutase
MOI	Multiplicity of infection
Mre11	Meiotic recombination 11
mRNA	Messenger ribonucleic acid
NBS	Nijimegen break syndrome
NES	Nuclear export sequence
NF-κB	Nuclear factor κ B
NLS	Nuclear localisation sequence
NMR	Nuclear magnetic resonance
NPM	Nucleophosmin
NS3	Non-structural protein 3
NS5b	Non-structural protein 5b
OD	Optical density
OGG1	8-oxoguanine DNA glycosylase
ORC	Origin recognition complex
P/CAF	P300/CBP associated factor
$p14^{ARF}$	14kilodalton alternative reading frame protein (Human)
$p19^{ARF}$	19 kilodalton alternative reading frame protein (Mouse)
PBS	Phosphate buffered saline

PCNA	Proliferating nuclear cell antigen
MEF	Mouse embryonic fibroblast
PCR	Polymerase chain reaction
PEST	Proline-Glutamine-Serine-Threonine
PIAS	Protein inhibitor of STAT1
PML	promyelocytic leukemia (PML)
p-p53 ser15	p53 Phosphorylated on serine 15
PRMT2	Protein arginine methyltransferase 2
p-s317Chk1	Checkpoint kinase 1 phosphorylated on serine 317
PTEN	Phophatidylinositol-3,4 5-triphosphate 3-phosphatase
R	Arginine
RanBP2	Ran binding protein 2
Rb	Retinoblastoma gene
Rb	Retinoblastoma protein
RE-PCR	Restriction enzyme-related PCR
RNA	Ribonucleic acid
ROS	Reactive oxygen species
RPA	Replication protein A
RPC	Replication protein C
RT-PCR	Reverse transcription PCR
S/Q	Serine /Glutamine
Ser	Serine
SMYD3	SET and MYND domain-containing protein 3
SOD	Superoxide dismutase
ssDNA	Single stranded DNA
SUMO	Small ubiquitin modifier
SWI/SWN	Switch defective 12\sucrose non-fermenting
TBST	Tris buffered saline with tween 20
TFIID	Transcription factor II H
TFIIH	Transcription factor II H
TGF	Transforming growth factor
Thr	Threonine

TNF	Tumour necrosis factor
TOPORS	Topoisomerase I and p53-binding protein
UTR	Untranslated region
UV	Ultraviolet radiation
VEGF	vascular endothelial growth factor
WT	Wild type
γ-H2A.X	H2A.X phosphorylated on serine 139
8-oxo-dG	8-oxo-7, 8 dihydro-2'deoxyguanosine

Chapter 1: Introduction

The development of cancer is described as a multistage process[1] . The ability of a cell to control its cells cycle is disrupted through the emergence of mutations. Essentially cancer is a shattering of the regulation of the checkpoints. Mutations affecting pathways involving checkpoint proteins, such as Retinoblastoma (Rb) and p53 impact on the integrity of the cells DNA, as it is replicated even after the DNA is damaged. Rb loss of function is found in a high proportion of liver cancers. This study investigates outcomes after *Rb* loss in hepatocytes to determine if *Rb* loss alone is sufficient to induce development of liver cancer.

1.1 Human hepatocellular carcinoma (HCC)

Hepatocellular carcinoma is the sixth most common cancer in the world. Once diagnosed there is a poor prognosis making it the third leading cause of cancer death worldwide. It has a strong aetiological association with viral hepatitis; over 80% of HCC is associated with Hepatitis C and Hepatitis B. Other causative agents include environmental carcinogens, such as aflatoxin, alcohol, inherited metabolic disorders such as haemochromatosis (iron overload) and Wilson's disease (copper overload)[2]. Many of the causative factors of liver cancer are known, but the molecular mechanisms leading to the development of HCC have yet to be fully understood.

Chronic hepatitis B (HBV) and C (HCV) infections are major risk factors for HCC. Hepatitis B virus is member of the hepadnaviridae virus family the virus encodes double stranded DNA, of approximately 3.5kb in size that can integrate into the host's genome. The integration of the viral DNA can activate a number of cellular genes that may lead to chromosomal instability. Hepatitis C virus is a 9.6kb single stranded positive sense RNA virus therefore not capable of integrating into the host's genome. Upon entry into the cell the RNA is translated into a single-stranded polyprotein of about 3,010 amino acids in length by ER bound ribosome, processed

by proteases into three structural (Core protein, E1 and E2) and six non-structural proteins each with different functions[3]. HCV replicates in the cytoplasm of hepatocytes, the majority of the core protein is located in the endoplasmic reticulum, and is known to interrupt the TNF-α signalling pathway in hepatocytes by binding to the TNF-α receptor in the cells, thereby preventing FAS induced apoptosis of the infected hepatocyte. Both HBV and HCV induce an indirect host cell immune response resulting in the liver being in a state of constant inflammation, leading on to cell proliferation, necrosis, and ultimately to cirrhosis.[4] This chronic inflammation of the liver induces the production of cytokines TGF-α and IGF-2, thus promoting the proliferation of the hepatocytes.

Carcinogenesis is not produced simply as a result of an increase in DNA synthesis this increase must be accompanied by the appearance and accumulation of genetic alterations induced by various factors. In HCC the aetiology is known thus it is important to assess the extent of disruption in expression and regulation of important tumour suppressors such as Rb.

Rb is a critical regulator of the cell cycle and therefore is subject to rigorous control by CDK and CKI (Section 1.4). Studies show components of the RB regulation pathway to be altered in between 72%-93% of HCC cases dependent on the stage of the HCC[5].

These alterations are found at various stages of the RB regulatory pathway leading to reduced RB protein expression (loss of heterozygosity (LOH), homozygous deletion, and hypermethylation of Rb gene) or inactivation by hyperphosphorylation of Rb (cyclin D gene amplification, p16 hypermethylation or LOH). Although they depend on the aetiology, they are mutually exclusive, showing that a single alteration is sufficient for disruption of the pathway. For example Edamoto et al showed that Rb promoter methylation occurred in 28% of HCC cases without cyclin D1 but only 5% of HCC cases with cyclin D1 amplification [6].

LOH of Rb is found in cirrhosis indicating that it is an early event[7]. On average LOH of Rb is inbetween 25-48% in cases of HCC. RB expression has been assessed using immunohistochemistry and showed a decrease in between 28-55% of HCC cases[8,5]. Methylation of the Rb promoter differs according to aetiology. HCC with aetiology of HCV had the lowest level at 16%, HBV had 27% and alcohol had 39% of cases with Rb promoter methylation in HCC. This promoter methylation is associated with a loss of expression of RB[6].

Two of the main causative factors associated with HCC are HBV and HCV. Both viruses produce proteins that can interact with Rb. In vitro studies using proteins produced by the viruses have led to insights on their effects on Rb. Oncogenes produced by DNA viruses such as E1A use their LxCxE consensus motif to bind RB [9]. Non-structural protein 5 b (NS5b) is a RNA polymerase, produced as a result of infection with HCV and uses this same motif to bind RB. NS5b downregulates Rb by targeting it for degradation prior to Rb entering the nucleus[10]. Another protein produced as a result of HCV infection is the core protein. It downregulates RB levels in rat embryonic cells, although the mechanism is not yet defined [11]. In HepG2 cells, the hepatitis B virus X protein (HBx) produced as a result of HBV infection binds the Rb promoter. This decreases Rb levels with HBx overcoming Rb inhibition of E2F activity[12].

An oncoprotein, gankryin, which has seven-ankryin repeats, is homologous to the p28 subunit of the 26S proteasome. It promotes phosphorylation and degradation of Rb through the ubiquitin-proteasome pathway and it is overexpressed in 60% of HCC. This leads to a decrease in Rb expression [8].

The high extent of disruption of the Rb pathway reported in HCC emphasises Rb's importance in the development of this cancer. However the direct consequences of this disruption are poorly understood and it is for these reasons that we wished to use conditional targeting in primary murine hepatocytes to study the effects of *Rb* deletion. (Details of alterations to Rb regulation in HCC are in section 1.5.4)

1.2 The Cre-lox system

The manipulation of the mouse genome has proved to be an invaluable tool in cancer biology. It facilitates addition and removal of genes giving an insight into the role these genes play in the initiation and pathogenesis of the disease. Conditional gene targeting adds another level of complexity to this. It enables deletion of genes in a tissue specific manner and also deletion of genes post-partum whose loss is embryo lethal. Their role post-development can now be analysed. *Rb* is one such gene [13, 14]. In the present study we took advantage of the cre-lox system to analyse the consequences of *Rb* loss in primary hepatocytes.

Cre, is a 38kDA product of the cyclization recombination (cre) gene of recombinase from the bacteriophage P1 [15]. It is a site-specific DNA recombinase that recognises a 34 bp site on the P1 genome[16]. This is known as the lox-p (locus of X-over P1) site. Cre efficiently catalyses the reciprocal DNA recombination between two lox-p sites[15]. The lox-p site itself consists of 13 base pair inverted repeats flanking an 8 base pair non-palindromic spacer region that gives the lox-p its directionality (Figure 1.1). The reaction is initiated by Cre binding specifically to the inserted repeats leading to the formation of region that consists of 4 Cre subunits and two lox-p sites in the same orientation. Cre catalyses the exchange between the pair of lox-p sites in the core spacer region by concerted cleavage and rejoining reactions[17].

In the following study the loss of *Rb* in hepatocytes was investigated using this cre-lox system. In this case two lox-p sites were inserted in introns either side of exon 19 of Rb. The mice bearing this genetic modification (Rb-floxed mice) were shown to behave the same as WT mice up until 14 months of age. Hepatocytes isolated from *Rb* floxed mice by perfusion were infected with an adenovirus expressing Cre. The addition of Cre recombines the 2 lox-p sites. This results in excision of the *Rb* site producing a protein that is missing 300 amino acids from its C-terminus and truncation of the Rb protein[18]. This has been shown to behave the same as a null allele and enables Rb specific functions to be assessed [14].

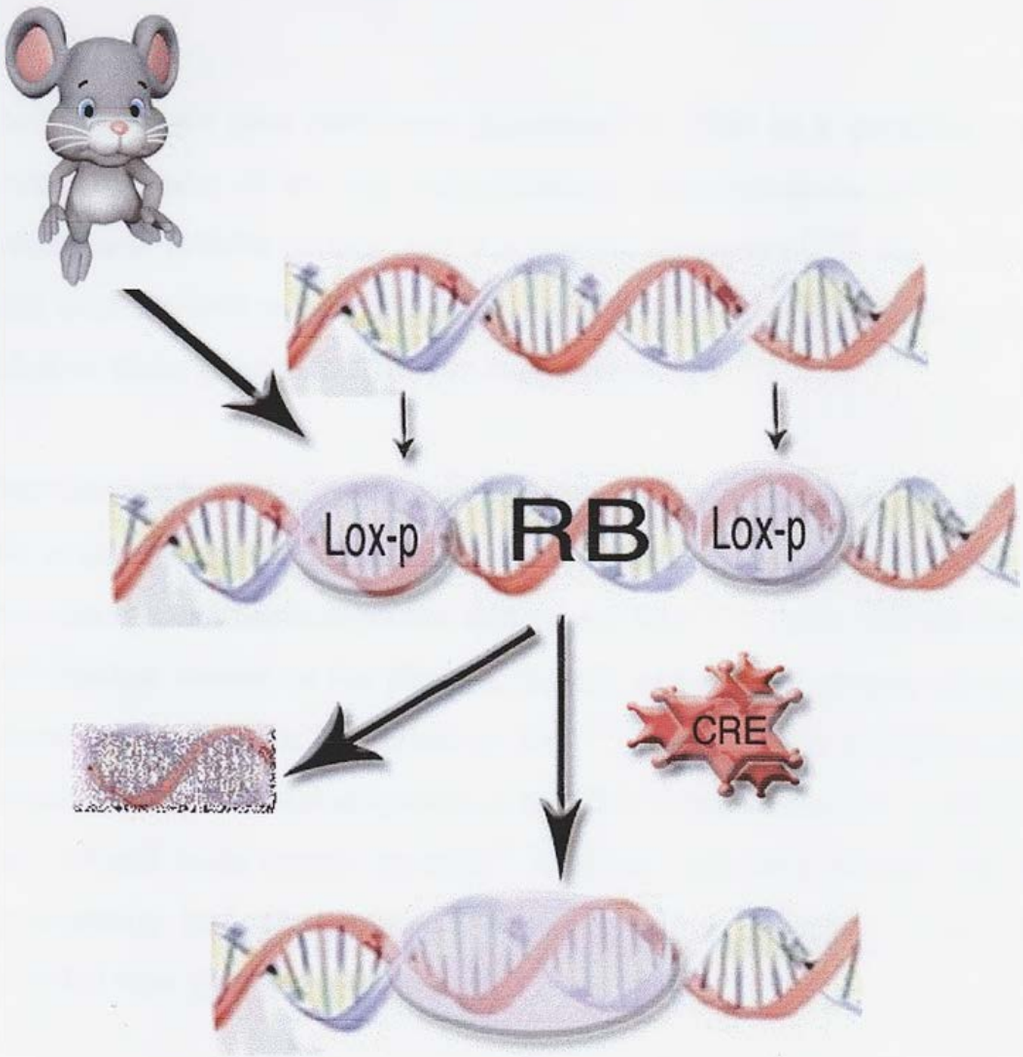


Figure 1.1: The Cre-lox system

The basic principle of the cre-lox targeting system is the insertion of specific lox-p sites around the gene of interest, followed by the introduction of an enzyme, Cre that recognises these sites. The enzyme binds to the DNA on these sites modifies it and recombines it resulting in the excision of the gene of interest.

1.3 Retinoblastoma protein (Rb)

Retinoblastoma gene (*Rb*) was discovered in 1986 as a germline mutation in an inherited cancer of the eye, retinoblastoma. Retinoblastoma protein (Rb) is a 9238 amino acid/100kDa protein and is a tumour suppressor[19, 20]. Rb is a nuclear protein that interacts with over a 100 other proteins although the physiological significance of all of these interactions has not been determined [21].

Previous studies using transgenic mice have given insights into the importance of the *Rb* gene. Knock out of *Rb* is embryonic lethal in mice on day 13.5 with defects in the nervous system, haematopoietic system and lens[13, 14]. Mice that are heterozygous for *Rb* develop tumors in the pituary, thyroid and adrenal glands, all of these tumors showing a loss of the WT allele of *Rb*[13, 22]. The presence of a placenta with WT Rb eliminates the aberrant apoptosis in the CNS found in the *Rb-/-* embryo however the lack of cell cycle control remains[23]. However Sage et al showed that the loss of *Rb* post-natally had more effects on cycle control in mouse embryonic fibroblasts (MEFs) than germline inheritance[24].

1.4 Rb function

Rb affects multiple cellular processes including transcription, differentiation, apoptosis and cell cycle. Regulation of transcription by Rb is pivotal for the role of Rb in managing the cell cycle. Rb controls the cell cycle through hypophosphorylated Rb binding to E2F family members and HDACS.

1.4.1 Regulation of transcription by Rb

Rb is a critical regulator of transcription through two main mechanisms: the regulation of the E2F transcription factors and the induction of methylation.

The regulation of E2F transcription factors

Rb is a member of the pocket-protein family, which also includes p107 and p130, which are regulators of E2F transcription factors (Figure 1.2). The largest region of homology between all three proteins is in their pocket domain, which they use for their interaction with E2F family of transcription factors and the products of viral infection [25, 26]. The expression of the pocket proteins varies: Rb is expressed in both proliferating and non-proliferating cells, p107 is found in proliferating cells associating with E2F during S-phase and p130 is found in quiescent cells [27-29]. Mutations are rarely found in p107 and p130 in cancer together with no increase in tumors in p107 and p130 null mice indicating that they do not function as tumour suppressors[30].

In the mouse, p107 and p130 show functional redundancy. Single null mice for p107 and p130 develop normally and exhibit no obvious adult phenotype. However double knock-out mice of p107 and p130 die peri-natally with severe skeletal abnormalities [31, 32]. p107 and p130 have a higher homology to each other than either has to Rb and preferentially bind different E2F transcription factors than Rb.

The E2F transcription family incorporates both activators and repressors of transcription. In mammalian cells, there are nine members of the family. E2F1-6 have an N-terminal DNA binding domain, dimerisation domain, as well as a marked box which is a conserved region involved in dimerisation and DNA bending. Excluding E2F6 they have a C-terminal transactivation domain, which contains the pocket protein binding region, reviewed by Dyson[33]. E2F7 and E2F8 are the most recent members of the family to be discovered. They both lack a transactivation domain, pocket protein binding domains and heterodimerisation domain. However they possess two DNA binding domains and bind to DNA in a DP independent manner possibly through homodimerising[34-38].

E2F1, -2, and -3a are activators of transcription, they posses a nuclear localisation sequence together with a cyclin A binding domain. Their expression is maximal in late G_1. These activators are bound to RB in G_0 and early G1 and upon

phosphorylation of Rb are released. They heterodimerise with a co-activator which is either DP1 or DP2 [39] and bind to E2F regulated promoters to turn on transcription of S-phase genes. Conditional gene targeting used to remove all three activator E2Fs demonstrated their importance for entry into S-phase and also how they exist in a positive feedback loop [40].

Rb represses the activity of E2F1-3 in three ways. Firstly it can bind directly to the activation domain of the activator E2Fs [41, 42]. Secondly the recruitment of Rb to the promoter blocks the assembly of the pre-initiation complexes[43]. Thirdly Rb uses a protein interaction domain distinct from E2F that is uses to modify chromatin structure[44, 45].

E2F-3b, E2F-4, E2F-5, E2F-6, E2F-8 and possibly E2F-7 are the repressor members of the family. E2F4 and E2F5 are the only two repressors that interact with the pocket proteins. E2F5 binds to p130[46] while E2F4 is able to bind to all 3 members[47-49]. E2F4 and E2F5 are expressed constitutively throughout the cell cycle. In G_0 and G_1 E2F4 and E2F5 are brought into the nucleus by binding to and forming transcriptional repressor complexes with the pocket-proteins, p107 and p130. Phosphorylation of p107 and p130 disrupts this binding. As E2F4 and E2F5 contain no intrinsic nuclear localisation sequence they are removed out into the cytoplasm enabling activating E2F complexes to bind to the DNA[33, 50, 51].

Prior to G_1 phase the repressor E2F4-p130 complex predominates especially in quiescent cells. In early G_1 this is replaced with E2F4-p107 and E2F4-RB. The recruitment of HDACs to E2F promoters is not dependent on Rb but requires p107 and p130[52]. In response to stress Rb has been found on E2F promoters and a possible explanation is that Rb was recruited there following p16 induction or Ras induced senescence[53, 54].

Two other members of the E2F family that are repressors of transcription are E2F3b and E2F6. E2F3b is encoded on the same locus as E2F3a but with different promoters. The two proteins are identical except for the N-terminal sequence: E2F3a

has one hundred and twenty two amino acids whereas E2F3b has six amino acids therefore lacking the cyclin A binding domain[55]. E2F3b is expressed constitutively throughout the cell cycle while E2F3a is expressed only at the G_1/S-phase transition. E2F3b represses transcription and reports show it to repress transcription of the tumour suppressor $p19^{ARF}$ in quiescent cells [56]. Unlike other members of the E2F family E2F6 lacks both a transactivation domain and pocket protein binding domain[57]. Recruitment of the polycomb group of proteins is how E2F6 is thought to induce repression[58]

Regulation of the E2F family is via a positive network loop with each other and also by posttranslational modifications. Phosphorylation on thr433 and ser403 in the transactivation domain by TFHII induces the degradation of E2F1 [59]. Free E2F is degraded in the ubiquitin system. The binding of the E2Fs to the pocket proteins increases their half-life but also prevents further accumulation as it blocks their synthesis[60].

At mid G_1 phase the repressor complexes on the promoters are replaced with E2F1 activator complexes (Figure 1.2). This is achieved by dissociation of HDAC from promoters with the appearance of histone acetyltransferases (HATs) aided by E2F [44]. The outcome is hyperactelyation of histones and induction of E2F dependent transcription. Acetylation of E2F itself by P/CAF on 3 lysine residues outsides its DNA binding domain increases E2F DNA binding, stabilises the protein and increases the transactivation activity of E2F[61, 62]. Early in S-phase E2F4 and Rb localise to foci that are sites of DNA synthesis.

Throughout the cell cycle and in combination with the pocket-protein family specific members of the E2F transcription family play an important role in the regulation of the cell cycle. This will be discussed in section 1.4.2.

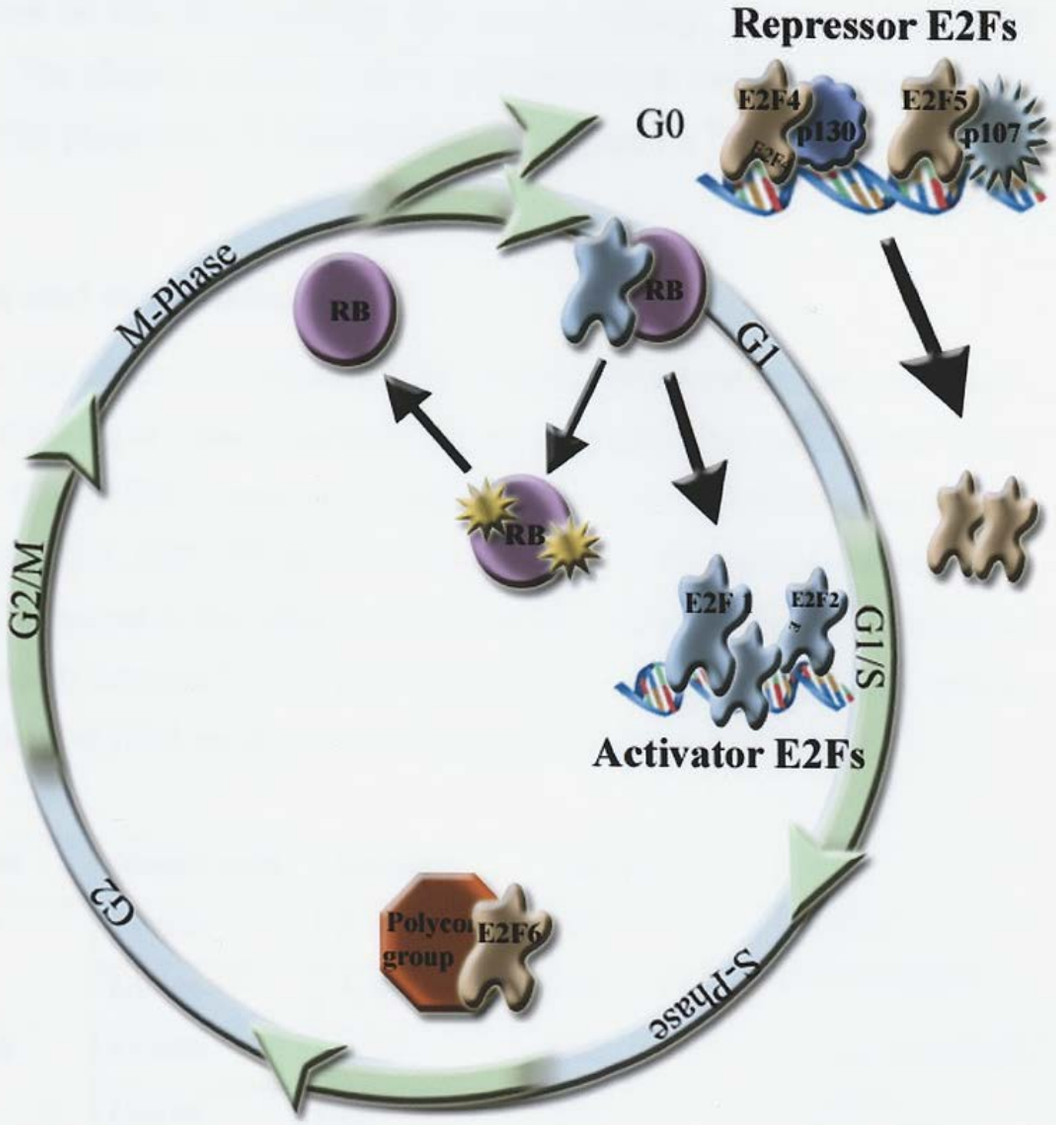


Figure 1.2: The Pocket protein family and E2F network

In G_0 phase of the cell cycle, E2F responsive genes are repressed by binding of E2F4/5 and p107/p130 complexes to promoter regions. During G_1 these complexes are phosphorylated alleviating their interactions. As E2F4 and E2F5 lack a nuclear localisation sequence these species are relocalised to the cytoplasm. At Mid-G1, upon phosphorylation of Rb by cyclin D/CDK4/6 E2F1 is released and binds to the DNA activating the transcription of S-phase genes. Rb is maintained in this hyperphosphorylated state until the end of M phase when it is dephosphorylated by the phosphatase PP1A.

E2F is not just important for the cell cycle and S-phase. It induces expression of genes involved in the DNA damage and repair pathway, apoptosis and DNA replication[63]. The phosphorylation of Rb is maintained until the end of mitosis when a member of the phosphatase 1A family dephosphorylates Rb [64].

Acetylation and methylation by Rb

Another way Rb affects transcription is by inducing deacetylation and methylation resulting in silencing of genes. The basic unit of chromatin is the nucleosome, which consists of 147bp of DNA wrapped around a protein core. The protein core consists of the histones H2A, H2B, H3 and H4. This structure of the nucleosome influences transcription as access to the DNA is influenced by post-translational modifications on the histone N-terminus[65]. The post-translational modification patterns indicate whether sections of DNA are in active transcription or silenced (Table 1.1).

Modification	**Amino acid**	**Number**	**Histone**	**State**
Acetylation	Lysine	9, 14,18, 23	H3	Active transcription
	Lysine	5, 8,12 16	H4	
Methylation	Lysine	9, 27	H3	Transcriptionally inactive chromatin
	Lysine	20	H4	
Phosphorylation	Serine	10	H3	Promotes acetylation lys14
Methylation	Lysine	9	H3	Interfere with phosphorylation on ser 10

Table 1.1: The pattern of modifications on the histone tails and the impact that it has on transcription of that site of DNA

The acetylation of lysine ε-amino group neutralises the charge and decreases the affinity of histones for the negatively charged DNA. This allows transcription factors and co-activators to bind to the DNA. The function of the histone deacetylases (HDACs) is to remove acetyl groups from the DNA preventing transcription. The recruitment of HDACS 1, 2 and 3 to gene promoters is crucial in the maintenance of

gene silencing by RB[66]. RB binds to HDAC 1 and HDAC 2 through their LxCxE motif but it cannot bind directly to HDAC3 [67]. Rb brings HDACs into the vicinity of the E2F responsive gene promoters preventing their acetylation and consequently the activation of their promoters[68].

Rb can execute long-term repression by removing acetyl groups from a histone in exchange for methyl groups[69]. This maintains a deacetylated status and thus histone methylation induces the silencing of proteins. It is chemically stable and when it was initially discovered was thought to be permanent. However the discovery of a histone demethylase, reversed this idea and it is now understood to be a more dynamic modification[70]. Two histone methyltransferases Rb interacts with are SUV39H1 and protein arginine methyltransferase 2 (PRMT2)[70, 71]. SUV39H1 is a lysine methyltransferase and attaches methyl groups to lysine 9 on histone 3. PRMT2 is an arginine methyltransferases. Suv39H1 does not bind directly to Rb but to HDAC1. RB forms a complex containing HDACS, SUV39H1 and Rb interacting proteins at the histone[72]. This results in deacetylation followed by methylation of the lysine. The interactions of RB with both PRMT2 and SUV39H1 can result in methylation of the E2F promoter[71, 72]. In response to cyclin-CDK phosphorylation Rb no longer binds SUV39H1 allowing transcription to proceed. Methylation has the capability to be lethal through silencing important genes. For example in HCC the overexpression of SMYD3, a histone methyltransferase has been observed demonstrating the impact the dysregulation of this system can have[73].

Methylation is the only known natural modification of DNA and occurs exclusively on a cytosine followed by a guanine. Methylation of the cytosine present in promoters of CpG islands permanently represses them. Due to the risk associated with CpG sites their frequency throughout the human genome is low. CpG stands for cytosine followed by guanine with p representing the phosphodiester bond between the two bases. However islands with a high frequency of CpG do arise consisting of small areas about 300-3000bp in length. They are normally present in the 5'end of an expressed gene and over 60% of promoters are found in CpG islands. Many CpG islands are not in the promoters of genes and their significance is not clear. This

methylation is transmitted through mitosis thus making it an epigenetic mechanism of inheritance[74]. There are three methyltransferases, responsible for this with two of them, DNA methyltransferase 3A (DNMT3A) and DNMT3B, being *de novo* methyltransferases while DNMT1 is in charge of maintenance[75]. Rb is known to complex with DNMT1 and the repression of genes by Rb is enhanced by DNMT1[76].

Rb binds and recruits BRG and Brm, two homologs to the SWI/SWN complex in yeast [77, 78]. The SWI/SWN complex is a chromatin remodelling complex. Chromatin remodelling is a non-covalent modification resulting in localised changes in DNA/histone contacts. It may also mobilise the nucleosomes on the chromatin fibre to change their relative spacing and positioning on the promoter. There are three known chromatin remodelling complexes with an ATP-dependent helicase at their core. Rb uses these complexes to inhibit both proliferation and E2F responsive genes. Rb brings them to the cyclin A promoter. BRG is required for Rb to induce cell cycle arrest[45].

1.4.2 Cell cycle regulation by Rb

There are four main stages of the cell cycle, Gap_1 (G_1), S-phase, Gap_2 (G_2) and mitosis. The G_0 phase of the cell cycle or senescence is a state in which the cells are not actively dividing and must be stimulated in order to enter G_1. During G1 the cell prepares for duplication of the DNA, which occurs during S-phase. The cell proceeds to mitosis, where the DNA will be segregated into two new daughter cells.

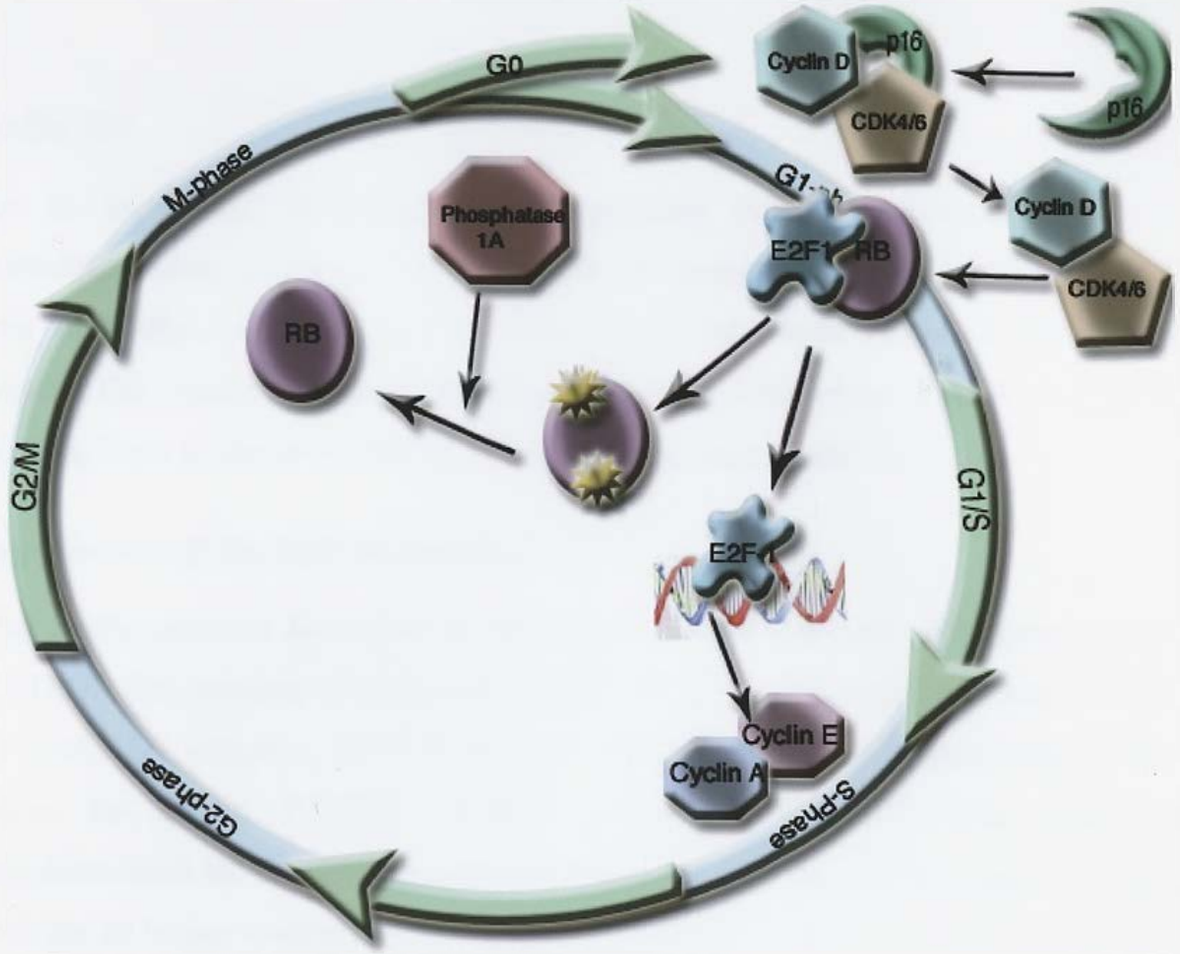


Figure 1.3: The Rb pathway

The CDK inhibitor p16 prevents cyclin D/CDK4/6 from phosphorylating Rb. Upon stimulation by the mitogens, cyclin D/CDK4/6 is activated and phosphorylates Rb. This disrupts the binding between RB and E2F enabling E2F to switch on the transcription of S-phase genes such as cyclin E and cyclin A. This phosphorylation of RB is maintained until S-phase when it is dephosphorylated by a phosphatase.

Cyclin D1

This is the cyclin associated with progression from the quiescent into the proliferative state. Cyclin D1 is responsible for progression through the restriction point thus after induction there is strict control over both cyclin D mRNA and protein. The cyclin D family members associate with either CDK4 or CDK6, allowing them to phosphorylate specific substrates such as Rb[79-81].

Regulation of the G1S transition

After production and dependent on cell type, cyclin D1 associates with either CDK4 or CDK6. This binding of cyclin D1 to the CDK is the first step in the activation of the cyclin D1 complex, for it to be fully active it must be phosphorylated. Once active the cyclin D1/CDK complex phosphorylates Rb[82]. The levels of phosphorylated Rb control the restriction point which is at mid-G_1 phase when the cells are no longer responsive to mitogenic signalling. Even if the signal is removed, the cells are still committed to a full round of replication. Thus one role for Cyclin D1/ CDK4/6 in the transition from G_1 to S-phase: is the phosphorylation of Rb[83].

In the liver, hepatocytes exist in the resting G_0 phase of the cell with less than 5% of the cells actively proliferating. Extra cellular signals, such as cytokines secreted as a consequence of viral hepatitis can fire up the cells to leave G_0 and enter G_1 phase of the cell cycle. Such signals activate RAS, which through map kinases (MAPKs), ERK1 and ERK 2 stimulate the transcription of Cyclin D1[84-86]. During G_1 as it is unstable Cyclin D1 is produced continuously, with an upregulation in transcription towards the end of G_1. Up to mid G_1 any alteration in extracellular signals halts this production. This enables the cells to assess their extracellular environment, noting any change and responding to it appropriately either proceeding with the cell cycle or arresting it[87].

During G_0 and early G_1 Rb is hypophosphorylated, enabling it to bind to chromatin modifying enzymes such as histone deacetylases [44]. This prevents acetylation and thus activation of transcription.

Co-ordination of Rb activities allows the sequential activation of the cyclins to occur. In its hypophosphorylated form Rb can form a complex with HDAC1 and BRG/BRM. Upon Rb phosphorylation in the C-terminus by cyclin D the interaction with HDACs are disrupted leading to a relief in the transcriptional repression of the cyclin E promoter. Once cyclin E has accumulated and is active it has the ability to phosphorylate both Rb and BRG. This disrupts their interaction allowing release of repression on the cyclin A and CDK2 promoters. This enables the ordered expression of cyclin A and CDK2[88, 89].

Cyclin E

The human gene for cyclin E produces several polypeptides with molecular weights between 39-52kDa. Cyclin E half-life is approximately 30 minutes with levels cyclin E maintained through degradation, transcription and post-translation modifications. Expression of cyclin E varies during the cell cycle with accumulation of mRNA and protein beginning during G_1, peaking during the G1/S-phase transition and is down regulated during G2/M[89, 90]. During G_1 the relief of repression by the Rb-HDAC complex on the cyclin E promoter is achieved by cyclin D phosphorylation of the Rb-HDAC complex[89].

Cyclin E associates with CDK2 and this complex is responsible for phosphorylating a number of proteins. As free cyclin E is degraded in the proteasome the binding of cyclin E to CDK2 protects it from degradation. The auto-phosphorylation of cyclin E/CDK2 on cyclin E is essential for its ubiquination by SCF at the end of S-phase [91, 92]. One protein cyclin E-CDK2 can phosphorylate is E2F and this modulates E2Fs activity forming a positive feedback loop[93]. Cyclin E has a nuclear localisation sequence (NLS) relying on importin-α and importin-β for transport into the nucleus.

However CDK2 lacks a NLS and is dependent of cyclin E for transport into the nucleus[94, 95].

The main function of Cyclin E/CDK2 is to induce S-phase entry and start DNA replication by the induction of S-phase genes. The cyclin E/CDK2 complex has the ability to phosphorylate BRG1, a member of the chromatin remodelling complex and inhibit its ability to induce growth arrest[88]. This inhibition of BRG1 activity is thought to maintain the chromatin in a transcription permissive state. At the beginning of DNA replication Cyclin E interacts with Cdc6 a component of the replication machinery this interaction is essential for the initiation of replication[96]. Alongside this function of the complex is co-ordination of centrosome duplication with DNA replication[97].

During G_1, NPM, a multifunctional nucleolar protein associates with the centrosome preventing the centrosomes duplication. Prior to the onset of DNA synthesis cyclin E/CDK2 phosphorylate NPM dissociating it from the centrosome allowing duplication. These processes of centrosome duplication and DNA synthesis are co-ordinated events at the G_1/S-phase transition any dysregulation in this synchronization leads to hyperamplification of the centrosomes and chromosomal instability. NPM reassociates with the spindle pole during mitosis ensuring the centrosome is only duplicated once during each cycle.[97]

Through destroying repressors, such as p27 cyclin E/CDK2 modulates its own activity. Phosphorylation of p27 targets it for destruction[98]. Low molecular weight forms of cyclin E formed by cleavage by the protease elastase that are tumour specific have been discovered[99]. These forms of cyclin E have a higher affinity for CDK2, are biologically more active and can stimulate the cell to progress through the cell cycle more efficiently than the full-length form. In HCC these forms of cyclin E are present and have been found overexpressed in 65% of cases[100].

Cyclin A

Cyclin A is crucial for S-phase during which 3.2 billion base pairs of DNA are replicated. During this stage of the cell cycle the DNA consists of replication factories scattered throughout the genome beginning to unwind the double helix[101]. The role of cyclin A during S-phase is to phosphorylate a number of components of the replication machinery.

Cyclin A is synthesised and destroyed after cyclin E but slightly earlier than cyclin B [102-104]. Cyclin A associates with two CDK's; CDK2 and CDK1 and functions in both S-phase and mitosis [105]. There are two forms of cyclin A embryonic and somatic: the embryonic form is only expressed in meiosis and very early embryos whereas cyclin A2 is present in proliferating somatic cells[106, 107].

The cyclin A2 promoter is repressed by p107 binding to E2F during G_0/G_1 [108, 109]. At S-phase entry after Rb phosphorylation by cyclin E/D-CDK, E2F is released and cyclin A2 transcription is activated. Cyclin E-CDK2 complexes can bind directly to E2F/p107 complexes on the Cyclin A2 promoter and activate cyclin A expression [110]. Cyclin A2 levels peak at G_2/M [111]. Interactions between cyclin A2 and E2F are reported to result in a cyclin A2-CDK2 phosphorylating E2F switching off E2F transcriptional activation of cyclin A. This would limit the transcription of cyclin A2 forming a negative feedback loop. In order to be fully active the cyclinA/CDK2 or cyclinA/CDK1 complexes need to be phosphorylated on a threonine residue in their active site. Conversely phosphorylation by WEE1 and MYT1 of CDK1 on thr14 and tyr15 inactivate the cyclin-CDK complex[112, 113].

Cyclin A is important during replication as illustrated by its ectopic expression driving mammalian cells into S-phase and once synthesised at the onset of S-phase it localises to sites of DNA synthesis. Replication is initiated by the binding of the origin recognition complex (ORC) to initiation sites on the DNA. Essential co-activators of the ORC complex include CDC6, CDT1 and the Minichromosome maintenance proteins, reviewed by Takeda and Dutta[114] . Cyclin A phosphorylates both CDC6 and the MCM complex. Cyclin A-CDK2 phosphorylates CDC6 after G_1

phase, results in it relocalised from the nucleus to the cytoplasm. This segregates it from the DNA[115, 116].MCM 2-7 complex has an intrinsic helicase activity that it uses to unwind the DNA (figure 1.4) Phosphorylation of MCM4 subunit of the MCM complex by cyclin A-CDK2 inactivates its helicase activity[117].

After the DNA is unwound at the replication origin the individual strands are stabilised by binding to the ssDNA binding protein replication protein A (RPA), which promotes further unwinding. RPA is of 3 subunits and coats ssDNA inducing the recruitment of DNA polymerase α to syntheses the RNA primer that is the pre-requisite for DNA synthesis. Cyclin A-CDK2 phosphorylates RPA, however the outcome of this phosphorylation is unknown[118, 119]. Cyclin A/CDK2 also phosphorylates DNA polymerase α inhibiting its primase activity[120].

During G_1 the levels of CDK activity are low allowing prereplication complexes to assemble. Prereplication complexes are formed through association of the origin recognition complex (ORC) with co-activators, which include CDC6, CDT1 and the minichromosome maintenance (MCM) proteins[114]. However during the transition to S-phase CDK levels increase inhibiting the formation of new origins of replication. To ensure the DNA is replicated once during each cell cycle a "licence for replication" is in operation. This was discovered fusing cells in G_1 and G_2 with S-phase nuclei The G_1 cell replicated the DNA, while the cell in G2 did not [121]. Loading of MCM2-7 onto the chromatin has since been discovered to be the critical factor. The authority responsible for regulating the loading of MCM2-7 is the level of CDK activity in the cell [122, 123] (Figure 1.4).

Cyclin A is also active during mitosis and its function may be to increase the half-life of cyclin B. Cyclin A phosphorylates CDH1, which prevents CDH1 binding to APC and thus the activation of APC^{CDH}. This activate APC^{CDH1} complex can target cyclin B for degradation[124].

The exact mechanism for cyclin A destruction is unknown however it is clear that the D-box, the same region that is used for cyclin B destruction is necessary. There is

evidence to suggest that an APC form targets cyclin A for destruction. However it is not clear whether it is a different APC to the one that targets cyclin B or the same one but cyclin A has different responsiveness to it [125, 126].

Regulation of G_2/M by Rb

Important proteins at this checkpoint include Rb, p53, Gadd45a, p21 and 14-3-3. Induction of this checkpoint by p53 is dependent on Rb. p53 switches on the transcription of p21, which through inhibiting cyclin E and cyclin A complexes converts Rb to its hypophosphorylated active form that is able to bind E2F[127]. Formation of the Rb-E2F complex inhibits transcription of cyclin B1 and CDK1 and thus initiation of mitosis in the presence of genotoxic stress[128, 129]. Other genes p53 switches on at this checkpoint include Gadd45a and 14-3-3 [130]. Gadd45a binds to the CDK1 portion of the cyclin B/CDK1 complex. This removes it from cyclin B1, leaving free cyclin B1 to be degraded[131-133]. The multifunctional protein, NPM is involved in the G_2/M checkpoint. It binds to Gadd45a and brings it into the nucleus where Gadd45a functions. This movement is critical for function of Gadd45a as impairment of this interaction attenuates the cell's response to Gadd45a[134].

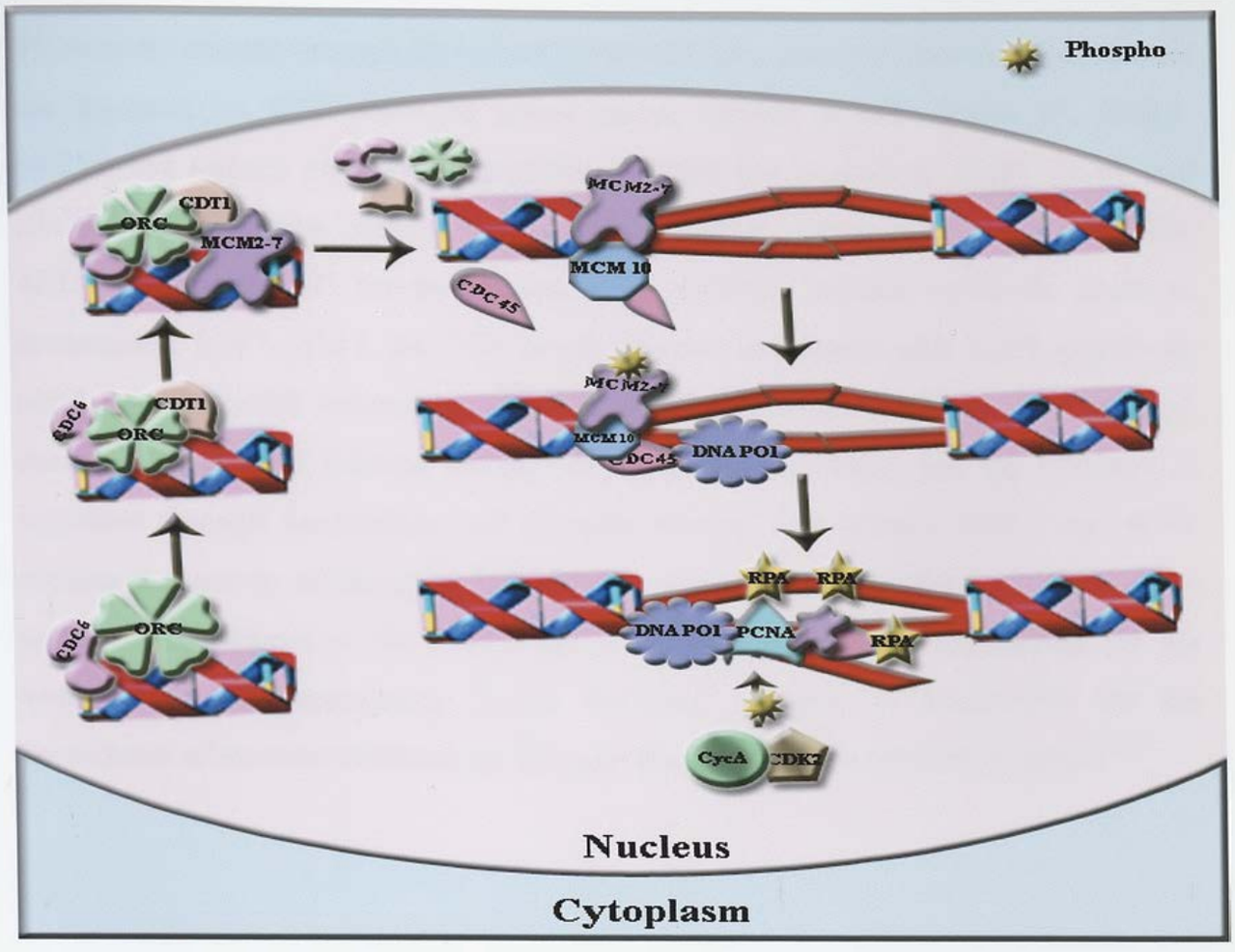


Figure 1.4 S-phase overview

The formation of the pre-replication complex begins when the origin recognition complex (ORC) binds to an origin of replication. This stimulates the binding of CDC6 and CDT1, which together with the ORC form the pre-replication complex. This complex promotes the loading of MCM2-7, which has an intrinsic helicase activity. Once MCM2-7 is loaded the pre-replication complex is dispensable. The binding of MCM-10 recruits CDC45 to the DNA, which in turn recruits DNA polymerase. The unwound single stranded DNA is stabilised by the presence of replication protein A (RPA) and CDC45. Cyclin A-CDK2 is known to phosphorylate components of the replication machinery.

Regulation of mitosis by Rb

Rb controls mitosis through its regulation of E2F (For detailed description of mitosis see appendix 1). E2F inducible genes during mitosis include cyclin B1, CDK1, cdc25a and mitotic checkpoint proteins (Section 1.4.5) such as Mad2, Bub1 and cdc20 [63, 135]. E2F also induces cyclin A transcription, which inhibits the APC. The APC targets cyclin B1 for destruction, thus inhibition enables cyclin B1 levels to accumulate. E2F1, E2F2 and E2F3a are positive regulators with E2F4 negatively regulating cyclin B1 transcription[136]. Cyclin B1 levels increase during G_2 and peak during mitosis. The binding partner of cyclin B1 is CDK1 and the complex is regulated through localisation and phosphorylation. The kinases WEE1 and MYT inhibits the activity of the cyclin B1/CDK1 complex, phosphorylated CDK1 on thr14 and tyr15. Members of the Cdc25 family of phosphatases are responsible for the activating dephosphorylation. Cyclin B/CDK1 complex is responsible for the breakdown of the nuclear envelope through phosphorylation of nuclear lamins [137].

1.4.3 Anti-apoptotic function of Rb

Combining the fact, that the *Rb-/-* mouse has extensive apoptosis[13, 14] together with the known role of Rb in differentiation leads to the hypothesis that in order to protect differentiating cells Rb inhibits apoptosis. Chimeric mice with both *Rb-/-* cells and WT cells show this role of Rb in the prevention of apoptosis to be non cell autonomous as is differentiation but not the aberrant cell cycles [138]. The mechanism of how Rb impedes apoptosis has not been fully elucidated although the loss of Rb induces both p53 mediated apoptosis and p53 independent apoptosis[139, 140]. E2F, the binding partner of Rb, can induce apoptosis independent of p53 via its function as a transcription factor. E2F1 induces the transcription of a number of known instigators of apoptosis including p73 and APAF1 [63, 141, 142]. Mice lacking both Rb and E2F1 and E2F3 survive longer than those with a loss of Rb alone supporting this role of E2F[143, 144]

1.4.4 Regulation of differentiation by Rb

The aberrant erthyropoiesis observed in *Rb-/-* embryos results from unrestrained activity of a protein called Id2 in macrophages[145]. Id2 belongs to the Id family that contains four proteins. The Id family are expressed widely during development. RB promotes macrophage differentiation by opposing the inhibitory function of Id2. The Id family inhibit the helix-loop-helix (HLH) family of transcription factors and their reactivation has been shown to contribute to malignancy[146]. Id2 is capable of interacting with hypophosphorylated Rb[147]. The role of Id2 in the aberrant erthyropoiesis is underscored by the loss of Id2 rescuing the embryonic lethality of loss of *Rb*, but these mice still die at birth with severe skeletal abnormalities [145, 147]. This loss of Id2 would lead to an increase in activity of the HLH factors contributing to defects in proliferation, differentiation and lack of development[148, 149]. $Rb^{+/-}$ mice develop pituary tumours. Comparing $Rb^{+/-}$ mice with and without Id2 revealed that $Rb^{+/-}$ mice lacking Id2 have fewer tumors. This infers that Id2 contributes to the transformation of the pituary tumour cells. Id2 induces VEGF, increase proliferation and through increasing the levels of cyclin E and cyclin A promotes the cell cycle [150]

.

1.4.5 Regulation of senescence by Rb

Senescence is a permanent form of cell cycle arrest with limited cellular proliferation. Maintenance of this state is dependent on an intact Rb pathway. Senescence is accompanied by marked changes in the chromatin structure. Rb recruits SUV39, the methyltransferase, heterochromatin protein 1(HP1) and histone methyltransferases to promoters. This results in the appearance of foci that have features of accumulated hypoacetylated histones, tri-methylated histones and HP1 binding. These accumulations are accompanied by a permanent repression of E2F responsive genes[54].

1.5 Regulation of Rb

Rb regulates many important cellular processes, such as transcription, progression of the cell cycle; differentiation, apoptosis and cellular senescence. Any adjustment to Rb or regulation of Rb impacts on these processes thus Rb is subjected to strict control, which is discussed in the following section.

1.5.1 Cyclins

Cyclins regulate the stages of the cell cycle together with their binding partners, with their serine/threonine kinases binding partners that are collectively known as the cyclin dependent kinases (CDKS). The production of cyclins oscillates during the cell cycle and is regulated by transcription and proteolysis. The cyclins are produced sequentially and once bound to the CDKs, the complexes themselves are regulated by phosphorylation. There are 11 members of the cyclin family. They all contain a cyclin box, which is a conserved stretch of hydrophobic amino acids. It contains an RxL motif, which they use for substrate specificity. They contain a PEST sequence at the end of the C-terminus that is used for degradation (For reviews see Sanchez and also Deshpande)[151, 152] (Figure 1.5).

The way in which cyclins exert control over Rb is through Rb phosphorylation via their CDK binding partners. In fact there are over 16 CDK phosphorylation sites in Rb governing the activity of Rb [153]. Rb is active in its hypophosphorylated state. In this state Rb can bind not only E2F but also HDAC. In fact Rb can form a trimeric complex with HDAC and BRG[89]. Phosphorylation of Rb in the C-terminus triggers a conformational change that allows phosphorylation of Ser567. This disrupts the pocket domain culminating in release of E2F [154]. The released E2F promotes transcription of S-phase genes, which includes cyclin E and A. Cyclin A and E exist in a feedback loop with Rb. Once cyclin E has accumulated and is active it has the ability to phosphorylate both Rb and BRG[88]. This disrupts their interaction allowing release of repression on the cyclin A and CDK2 promoter. This enables expression of cyclin A and CDK2.

1.5.2 Cyclin dependent kinase inhibitors (Cdki)

At the G1/S phase transition members of the INK4A (Inhibitors of the CDK4 kinases) family prevent RB phosphorylation and inhibit the cyclin D/ CDK complex. There are four members of this family $p16^{INK4A}$, $p15^{INK4b}$, $p18^{INK4C}$ and $p19^{INK4D}$ all having ankyrin repeats that can bind to the non-catalytic domains of CDK4/6 [155-158]. The binding of these inhibitors to CDK4/6 causes an allosteric change that alters the binding site for cyclin D and decreases its affinity for ATP[159].

Two other cyclin dependent kinase inhibitors are p21 and p27, which are members of Cip/Kip family of inhibitors. Their primary targets are cyclin E/CDK2 and cyclin A/CDK2. This prevents Rb phosphorylation and thus progression of the cell cycle. The p21 and p27 mechanism of inhibition of cyclinE/CDK2 and CyclinA/CDK2 is to form a ternary complex inhibiting the activity of the cyclin complex. In contrast to this formation of cyclin D/ CDK complex is assisted by p21 and p27 and also helps to ensure nuclear localisation of the complex as p21 and p27 bind to the nuclear export signal of cyclin D1. This binding of cyclin D/ CDK complex to members of the Cip/KIP family of inhibitors prevents these inhibitors interacting with cyclin E/CDK2, and inhibiting the complexes activity[160-162].

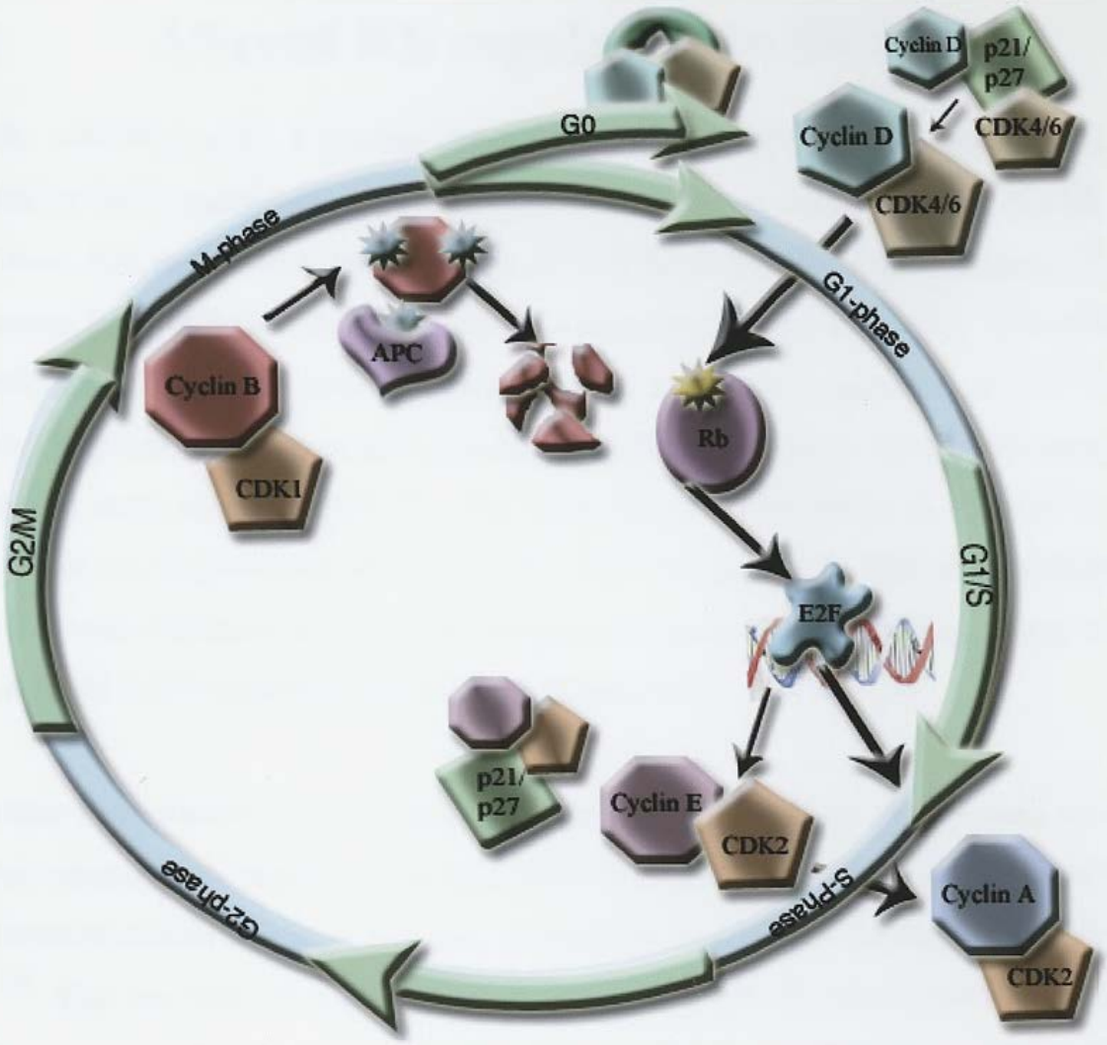


Figure 1.5: The Cyclin pathway

Upon stimulation by the mitogens, cyclin D transcription is initiated. The formation of the cyclin D/CDK4/6 complex is assisted by the cyclin dependent kinase inhibitors p21 and p27. Once formed the cyclin D/CDK4/6 complex phosphorylates Rb. This disrupts the binding between Rb and E2F enabling E2F to switch on the transcription of S-phase cyclins, cyclin A and cyclin E. Both cyclin A and E form complexes with CDK2. They are inhibited by the cyclin dependent kinase inhibitors (CDKI's) p21 and p27. Another member of the cyclin family cyclin B acts in mitosis. The presence of cyclin B prevents progression to anaphase and it is degraded by the anaphase promoting complex (APC) at the metaphase to anaphase transition

1.5.3 Altered Rb regulation in HCC

The CDK inhibitor p16, a known inhibitor of cyclin D1/ CDK4 complex is inactivated in HCC mainly by hypermethylation and loss of heterozygosity (LOH). Studies show that in between 16% to 91% of HCC have p16 hypermethylation, [163, 164] the lowest level of p16 hypermethylation is found in western countries. This p16 hypermethylation has been found associated with a loss of expression of p16 in HCC. Also hypermethylation of p16 was found in 32% of cirrhotic tissue, indicating it may be an early event in HCC[164]. The level of p16 methylation is affected by aetiology with the highest amount found with HCV induced HCC. This may explain why such a wide variation is observed between different studies[6]. In later stages of HCC p16 LOH is 51% and biallelic loss of p16 is 61%[165].

An increase in cyclin D1 expression is reported in HCC. Animal models such as a transgenic mouse with targeted overexpression of cyclin D1 to the liver developed HCC. Overexpression of cyclin D1 was maintained throughout development of the disease[166]. This increase of cyclin D1 could mimic hepatitis B virus related HCC as the virus can integrate into the cyclin D1 gene leading to amplification of the gene and the subsequent hyperproliferation of cells. In HCC amplification of cyclin D1 mRNA has been found to be as high as 87.5% [167].

1.6 The p53 connection

Like Rb p53 is also a tumour suppressor. The RB and p53 pathways are linked in at least two ways. Firstly p53 switches on p21 transcription. As p21 inhibits cyclin E/CDK2 and cyclin A/CDK2 both of which can phosphorylate Rb, leading to E2F release. Secondly E2F can induce $p19^{ARF}$ transcription, which antagonises MDM2 leading to p53 stabilisation. Virtually all human tumours have deregulated Rb or p53 pathways, with some tumours having both inactivated simultaneously.

p53 was discovered in 1979. In an unpertuRbed cell p53 is extremely labile functioning as exonuclease proof reading the DNA to detect any damage. This high

turnover of p53 is executed by MDM2, which ubiquinates p53 targeting it for degradation[168]. Unlike *Rb* null, p53 null mice are not embryo lethal; they survive until approximately six months of age when they get lymphomas. Upon a stress and dependent on the extent of the stress, numerous post-translational modifications, including phosphorylation and acetylation stabilise p53 and activate p53's transactivation activity. p53 forms a core through which a number of pathways converge making it vital in the decision making process of the cell, which is either halting the cell cycle or switching on apoptosis[169]. This regulation of p53 by post-translational modifications allows for rapid responses to changes in the surrounding environment. p53 activating MDM2 transcription enables levels of p53 to return to baseline post-repair of DNA damage

1.6.1 Alterations of p53 in HCC

Worldwide on average, there is a mutation of p53 in 30% of HCC. The DNA-binding domain of p53 is the single most frequent site of missense mutations in the gene leading to the stabilisation of the protein. A comparison of mutations in p53 with aetiology of HBV, HCV and alcohol all showed no significant difference between HCCs with differing aetiology[6]. The changes in p53 are thought to be a late event in carcinogenesis, thus it is not a prerequisite for malignant transformation.

A mutation known to contribute to but not sufficient for transforming cells is the transversion of an arginine to a serine at codon 249 of p53. This affects the transactivation function of p53. It is induced by the carcinogen aflatoxin, which is found on contaminated food products[170]. In fact a hepatitis B virus produced protein, Hbx, and aflatoxin has a synergistic effect on mutations in p53. The exact mechanism of how these two agents cooperate has not been fully defined, although Hbx protein is known to inhibit DNA repair by binding to DNA repair enzymes and to damaged DNA. Therefore damage that occurs through the action of aflatoxin on a background of HBV infection may not be repaired[171].

HCC associated with infection with HCV has a low percentage of mutated p53. However HCV core protein is capable of inhibiting the p53 promoter in both Hela and COS cells and interacts with various cellular pathways[172]. The non structural protein 3 (NS3), a DNA helicase produced as a result of HCV infections binds to and inactivates p53. A study using microarray and real-time PCR showed in HCV induced HCC cancers with mutant p53 had a different expression profile compared to those with WT p53. The genes included are involved in the cell cycle and cell proliferation, indicating that cells with mutant p53 had a higher malignancy potential than those with WT p53[173].

Also in the human liver cell line, HepG2, HBc and HBx, both produced as a result of HBV infection can inhibit the p53 promoter[174, 175]. HBx and p53 are known to interact with each other and counteract each other's effects.

1.6.2 Regulation of p53 stabilisation and activation

A regulator of p53 that forms a link between the Rb and p53 pathway is $p19^{ARF}$. E2F can induce transcription $p19^{ARF}$ while $p19^{ARF}$ through sequestering MDM2 stabilises p53. Other regulators of p53 include the kinases, acetylases and ligases that modify p53 as these all contribute to the stabilisation and activation of p53. Essentially the primary goal of these regulators is to release p53 from the constraints of MDM2, enabling it to act as a transcription factor (Figure 1.6). Dependent on the post-translational modification p53 switches on genes involved in DNA repair or apoptosis.

Phosphorylation of p53

The important role this post-translational modification plays in the regulation of p53 is illustrated be the presence of over 18 phosphoacceptor sites in p53. In response to DNA damage it is the first modification to occur on p53. The initial phosphorylation

of serine's 15 and 20 disrupts the interaction between MDM2 and p53, stabilising p53 while enabling further modifications to occur.[176], ATM and ATR, can induce these initial phosphorylations. Once stabilised further phosphorylations and modifications are required to activate p53. It appears the impact these phosphorylations have on p53 may be cell-type specific.

Dependent of the type of DNA damage either ATM or ATR or both are known to phosphorylate p53. ATM stimulates p53 phosphorylation itself or through Checkpoint kinase 2 (Chk2) on ser20 in response to ionising radiation (IR) [177]. The importance of this Chk2 phosphorylation is illustrated in CHK2-/- cells, as they fail to stabilise p53 in response to IR[178] In response to UV and stalled replication forks ATR phosphorylates p53 directly on ser20 while stimulating the activation of Checkpoint kinase 1 (Chk1), which can phosphorylate p53 on ser15 [179, 180].

The outcome of these phosphorylations was initially thought to disrupt the binding of p53 to MDM2. However observations using knock-in murine models have challenged this theory. Replacement of ser20 with alanine in embryonic stem (ES) cells, embryonic fibroblasts and thymocytes show that in response to DNA damage this phosphorylation is not required for p53 stabilisation[181]. A knock-in mouse of ser18 (human ser15) showed that it is required for maximal response to DNA damage but not necessary for acetylation of p53[182]. MDM2 binds to the N-terminal of p53, which contains within it a thr18. Phosphorylation of this residue has been shown to interrupt the binding with MDM2[183].

In response to double strand breaks DNA-PK phosphorylates serine 15. *In vitro* this has been shown to cause a change in the conformation in the N-terminus of p53. In response to UV and in conjunction with ATR, DNA-PK phosphorylates p53 on both serine 15 and 37 this dual phosphorylation stimulates the interaction with the TFIID transcription factor whereas phosphorylation of ser15 alone blocks binding of TFIID [184].

In the steady state of the cell, two residues in the C-terminus regulatory domain of p53 ser376 and ser378 are phosphorylated by protein kinase C. After DNA damage these two sites become dephosphorylated revealing a 14-3-3 protein-binding site, which leads to the stimulation of the site-specific DNA binding site[185].

Certain phosphorylations are important for the apoptotic function of p53. Phosphorylation of p53 on thr81 by JNK kinase, results in an increase in transactivation activity of p53 inducing p53 to switch on genes that are important in apoptosis.[186] High levels of DNA damage promote MAPK phosphorylation on ser33. This is necessary for p53 to induce expression of apoptotic target genes such as AIP1, BAX, PUMA and NOXA and also p21, which can arrest the cells cycle. After UV induced DNA damage phosphorylation of Ser46 in p53 is by both homeodomain interacting kinase (HIPK2) and MAPK [187-189] . Phosphorylation of ser46 by HIPK2 in a non-apoptotic DNA damage response manner co-operates with P/CAF to induce acetylation of p53 towards the p21 promoter. This illustrates the theory that dependent on the post-translational modifications the impact p53 has will be different.

The peptidyl-proply isomerase, Pin 1 interacts with a number of phosphoproteins through recognition of pser/pthr-pro motifs. Within p53 there are six Pin1 consensus motifs[190]. Pin1 has a WW domain for substrate interaction and an isomerase domain necessary to induce the conformational change of the target protein. Both these sites are essential for Pin1 activation of p53[191]. By using specific p53 mutant proteins it was found that ser33, ser 315 and thr81 in p53 are essential for pin1 binding. UV induced DNA damage induces phosphorylation at these residues by MAPK, CDC2 kinase and JNK [190, 191].

So, what is the effect of Pin1 binding to p53? The isomerase domain in Pin1 alters the conformation of p53. This altered conformation may let further post-translational modifications to occur, thus allowing p53 to bind more tightly to the DNA[191]. The co-transfection of p53 and Pin 1 increases p21 and Mdm2 expression. From studies of $pin1^{-/-}$ MEFs after UV damage, levels of p53 were found to be elevated longer

than in MEFs with the wild type protein, together with a lack of expression of the Mdm2 protein[190]. Further studies from Pin1$^{-/-}$ MEFS found the p53 induced apoptotic genes; BAX and DR5/killer were not upregulated [191].

Stimulus	Kinase	Site	Outcome
Ionising radiation UV UV	ATM ATR DNA-PK	Ser 15	Disrupts binding between p53 and MDM2
Ionising radiation UV	Checkpoint kinase 2 Checkpoint kinase 1	Ser 20	Disrupts binding between p53 and MDM2
	MAPK	Ser 33	
UV	ATR DNA-PK	Ser 37	In conjunction with ser 15 phos stimulates the interaction with the TFIID
Steady state	Protein kinase C	Ser 376/378	Masks s a 14-3-3 protein binding site
UV	MAPK HIPK2	Ser 46	Results in p53 inducing expression of apoptotic target genes
	TFIID	Thr 55	
UV/stress	Jun N-terminal kinase	Thr 81	

Table 1.2 Post-translational modifications of p53 by phosphorylation (For details see text).

Acetylation of p53

The post-translational modification acetylation was first discovered on histones in which it loosens the contact with DNA. It occurs on a wide plethora of transcription factors, including p53. The functional consequences of acetylation include an

increase in DNA binding, enhancement of stabilisation and changes in protein-protein interactions. Acetylation of p53 may hit "2 birds with one stone", not only is it thought to activate the transactivation function of the protein [192] but it may also prevent the ubiquination of p53 as both occur on lysine residues. Lysine residues in p53, Lys 320, 372, 373 382, 383 are all contained within the C-terminus. The C-terminus is thought to be a positive regulator of the transactivation function of p53. Acetylation of p53 is thought to activate the transactivation function by introducing a conformational change within the protein. Two mechanisms known to promote acetylation on p53 are phosphorylation of p53 at serine 15 or serine33/37 enhances the interaction between p53 and CBP/p300. Secondly, promyelocytic leukemia (PML) a tumour suppressor induces p53 acetylation through the formation of a trimeric complex with p53-PML-CBP complex.

The acetyltransferases p300 associated factor (PCAF), p300 and CREB binding protein are responsible for the acetylation of p53. The acetyltransferase P/CAF carries out the acetylation of lys320[193] with CBP and p300 responsible for acetylation of the rest of the lysine residues. Replacement of these four lysine residues 372, 373, 381 and 382 in p53 with alanine did not eliminate the ability of p53 to bind to the DNA and activate transcription. However single lysine substitutions did undergo MDM2 mediated ubiquination, the mutants with all four lysine residues substituted did not[194].

MDM2 binds to the N-terminus of p53, while acetylation occurs in the C-terminus. Thus MDM2, p53 and p300 have the ability to form a ternary complex. Mutation of all lysine residues to arginine in p53 prevents MDM2 ubiquination while MDM2 still retains the ability to bind to p53. This implies that the same lysine residues that are ubiquinated are also acetylated. Thus there appears to be competition between acetylation and ubiquination. However a report has shown that the mutation of six lysine residues to arginine had no effect on ubiquination but on transcriptional activation after DNA damage. This has been shown to be dependent on the levels of MDM2 within the cell with high amounts of MDM2 present causing degradation and low amounts inducing the stabilisation of p53[195, 196].

Crucial to the cell is the maintenance of p53 cellular homeostasis. A system must exist to aid in the efficient removal of p53 transactivation function post repair of the DNA damage. Using the HDAC inhibitor TSA an increase in the amount of p53 acetylation was observed, indicating that HDACS are also important in regulation of p53. Following on from this two deacetlyases were found to deacteylate p53 one is a component of the HDAC1 complex and the other deacetylase is sir2α. Sir2α is found in PML bodies, a conformational change is induced in Sir2α when it is bound to acetylated p53. This deacetylation can attenuate p53's transcriptional activity[197].

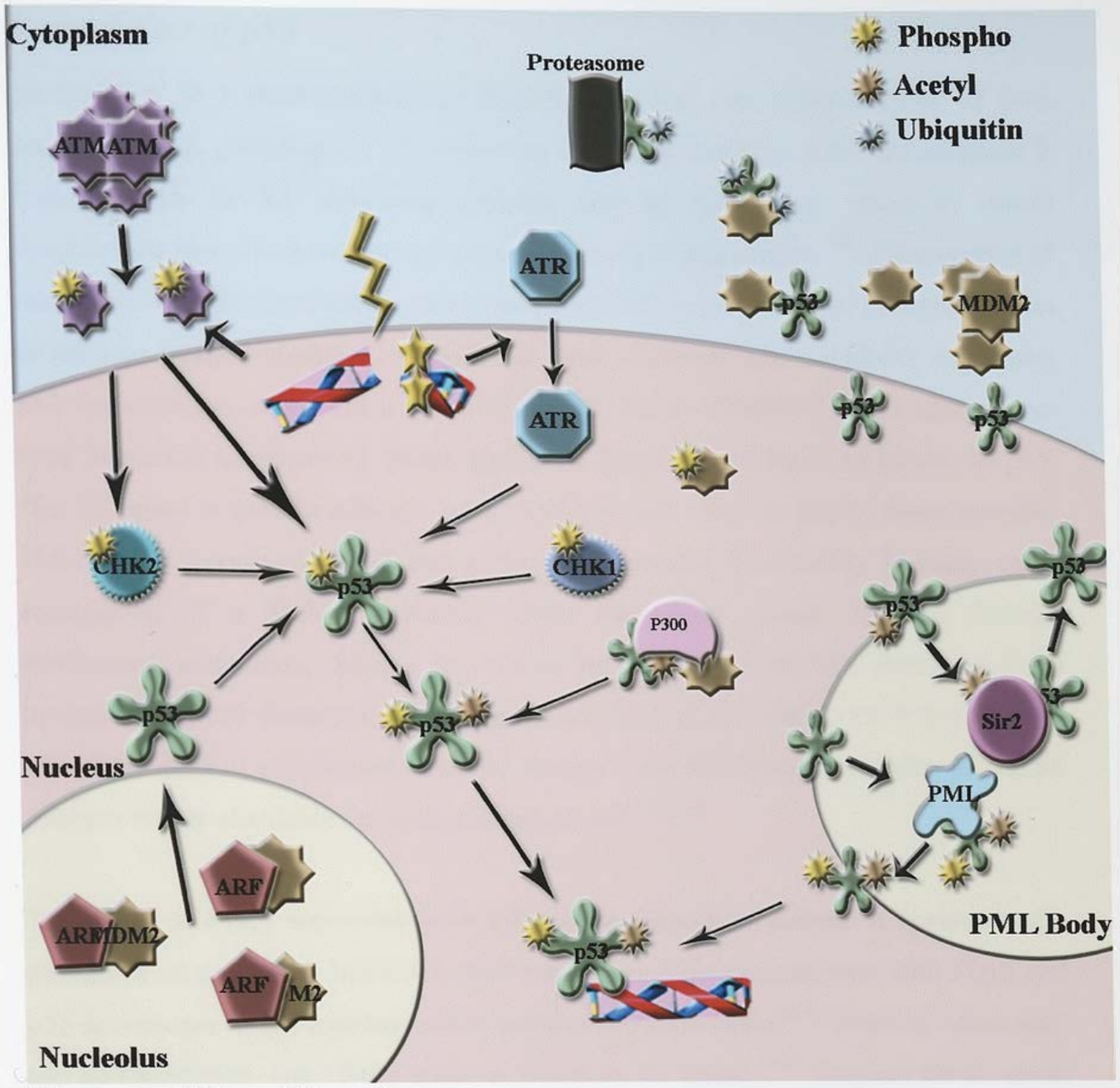


Figure 1.6 The p53 pathway

The tumour suppressor p53 is switched on in response to DNA damage, by a variety of methods. The DNA damage kinases ATM and ATR phosphorylate p53 itself, both activating their respective checkpoint kinases to phosphorylate p53 as well. The acetylation of p53 post-phosphorylation promotes the transactivation function. P53 may be acetylated by acetylases such as p300, P/CAF and CBP. P53 can also be moved into PML bodies and this is thought to bring it into close proximity with modifiers that promoter further post-translational modifications. In response to hyperproliferation the sequestration of MDM2 by $p19^{ARF}$ in the nucleolus, stabilises p53.

Sumoylation of p53

Sumoylation is a post-translational modification that has characteristics of both acetylation and ubiquination all occurring on lysine residues. Like ubiquination it requires both an E1 activating enzyme and an E3 ligase. However unlike ubiquination sumoylation does not target proteins for degradation [198]. Charteristics of acetylation of p53 observed in sumoylation include requirement of phosphorylation of residues in the N-terminus of p53 and both positively and negatively regulating p53. Sumoylation is dependent on the phosphorylation of ser20. Two E3 ligases have been identified as attaching **S**mall **U**biquitin **Mo**difier (SUMO) molecules to p53. One E3 ligase is protein inhibitor of STAT1 (PIAS), which is highly tissue specific. The other is Topoisomerase I and p53-binding protein (TOPORS). In many cases conjugation of a SUMO molecule alters the target protein function through biochemical activation, changes in cellular localisation or through protection from proteolysis. In p53 Sumoylation has been identified on Lys 386 in the N-terminus of p53. Other sites of attachment exist but remain to be identified, as ablation of lys386 does not totally eliminate the sumoylation on p53 [198, 199].

The effect of PIAS sumoylation of p53 is the subject of debate. It appears to be dependent on cell type. In HI299, MEFs and Tera cells cotransfected with PIAS and p53 an increase in the transactivation activity of p53 is found[199]; however when they are co-transfected into Hela cells a decrease is found [198] Reports show when TOPORS sumoylates p53, there is an increase in stabilisation and transcriptional activity of p53 [200].

The presence of both $p19^{ARF}$ and MDM2 increases the sumoylation of p53. The nucleolar sequence of $p19^{ARF}$ is critical for this $p19^{ARF}$ binds to MDM2 in the C-terminus at a site distinct from $p19^{ARF}$ inhibiting the ubiquination of p53. The binding of p53 to MDM2 is essential for the increase in sumoylation. In fact the three proteins are thought to form a trimeric complex with $p19^{ARF}$ as the linker. The function of stimulating the sumoylation of p53 by MDM2 and $p19^{ARF}$ has not yet been elucidated, although $p19^{ARF}$ is known to stimulate sumoylation independent of p53 [201].

Other proteins on the p53 pathway are sumoylated and the outcome of this effects p53. MDM2, the negative regulator of p53 is sumoylated by both RanBP2 and PIAS. RanBP2 is a nucleoporin protein that does not contain a ring finger like domain. As RanBP2 is found at the nuclear pore complex it may sumoylate MDM2 on entry into the nucleus. The localisation of MDM2 is critical for it to be sumoylated and once inside the nucleus it is further sumoylated by PIAS1. The consequence of sumoylation on MDM2 is not fully understood but it is thought to prevent self-ubiquination of MDM2 resulting in an increase in stability and further degradation of p53[168].

A critical protein in the formation of nuclear bodies is PML. Nuclear bodies are cell cycle regulated matrix associated subnuclear multi-protein complex structures that appear as punctate foci in the interphase nuclei [202]. The presence of p53 in them is totally dependent on the presence of PML. Sumoylation of the tumour suppressor PML at 3 lysine residues is a prerequisite for movement of it into these nuclear bodies. PML binds through this C-terminus to p53 and p53 binds through its central core domain to PML. Many different isoforms of PML exist and p53 specifically interacts with the splice variant PML3, which has an extended C-terminus [203]. The interaction between p53 and PML can be detected at a basal level within cells [202]. PML associates and brings into these nuclear bodies other proteins such as sp100, DAXX and the transcriptional coactivator CBP. Post-translational modifications such as phosphorylation and acetylation appear to occur and are regulated within these structures. The purpose of p53 within these nuclear bodies may be to bring it into close contact with transcriptional activators such as CBP. When p53 is localised into these structures the transactivation function of p53 is increased severalfold [204].

Murine double minute 2 (MDM2)

MDM2 was first identified in spontaneously transformed BALB/C 3T3 cells. The gene was located on small acentromeric extrachromosomal nuclear bodies known as double minutes that were only retained if they provided a growth advantage[205, 206]. MDM2 is an oncogene; it is overexpressed in approximately 7% of all tumours and

in one third of all human sarcomas[207]. Loss of MDM2 is embryo lethal, rescued by a combined loss of p53[208]. Overexpression of MDM2 leads to an inactivity of p53. Although mutations in both p53 and MDM2 would appear redundant patients who have a mutation in both have a poorer prognosis indicating that MDM2 does have functions that are independent of p53.

The MDM2 gene consists of 12 exons with two promoters one of which can be switched on by p53. There are two forms of the WT protein p90 and p76; the p76 version lacks part of the p53-binding domain. The mRNA transcripts are identical apart from an untranslated region on the 5' end of the P2 promoter. Transcripts from promoter 1 lack exon 2 while transcripts from promoter 2 lack exon 1 however proteins derived from both promoters are identical as translation begins in exon 3. The translation of the p2 promoter has also been found to be more efficient in human tumors[209]. At the mRNA level over forty isoforms of MDM2 have been identified. The expression and composition of these isoforms as proteins has yet to be fully defined. They are expressed in both tumors and normal cells. Splice variants transfected into cells and shown not to bind to p53 were still found to be oncogenic in vivo, indicating that MDM2 has functions separate of p53 maintenance and these isoforms of MDM2 may contribute to oncogenesis[210].

One of the main MDM2 functions is as an E3 ligase, which is an active part of the ubiquitin pathway. The ubiquitin pathway consists of three enzymes, E1, E2 and E3. Ubiquitin is a 76 amino acid protein that is activated upon binding to an E1 enzyme, once activated it is transferred to the E3 ligase via the E2. The E3 ligase conjugates the ubiquitin to the target protein and is responsible for substrate specificity. The ring finger domain of MDM2 contains the E3 ligase activity. MDM2 monoubiquinates p53 as well as polyubiquinating itself targeting itself for degradation. In contrast to polyubiquination, which targets proteins for degradation, monoubiquination has various outcomes such as receptor endocytosis, virus budding, transcription, DNA repairs and caspase recruitment in apoptosis[211, 212]. Therefore in conjugation with MDM2 other proteins must aid in the polyubiquination of p53 [213].

In response to mitogenic and cytokine signalling, a phosphorylation cascade ensues beginning with the activation of the second messenger PIP_3; this draws the kinase AKT to the plasma membrane where it is phosphorylated [214]. AKT phosphorylates MDM2 on ser 166 and 186, which is obligatory for the translocation of the Mdm2 from the cytoplasm into the nucleus [215]. PTEN, a phosphatase, dephosphorylates PIP_3, preventing the cascade [216], thus blocking the nuclear entry of Mdm2 segregating Mdm2 from p53 [217].

Acetylation of MDM2 increases the stability of p53. Both MDM2 and p53 bind to the first zinc finger domain of p300. MDM2 mutants that retain the ability to bind to p53 but are incapable of p300 binding are defective in p53 mediated degradation. These p53 mutants incapable of p300 binding escape MDM2 ubiquination[196].

In actively dividing cells, a member of the MDM2 family, MDMX stabilises p53 [218]. MDMX stabilises p53 by preventing its nuclear export in two ways. Firstly it binds to ubiquinated p53 in the nucleus and sequesters it, preventing its degradation by MDM2 in the cytoplasm. In fact, MDMX also stabilises MDM2 by preventing its polyubiquination. The three proteins, MDM2, p53 and MDMX can form a trimeric complex. The presence of MDMX in this complex, lacking a nuclear export signal may be the reason for the retention of p53 in the nucleus [219]. Although MDMX stabilises p53, the suppression of p53 transactivation function, induced by MDM2 is maintained. In the presence of $p19^{ARF}$, MDMX localises into the nucleolus and loses the ability to stabilise p53 and MDM2 [219]. This may be due to the formation of an $p19^{ARF}$ -MDMX complex resulting in less of both $p19^{ARF}$ and MDMX free to bind to MDM2, resulting in a more rapid degradation of p53 and MDM2

p19 Alternative reading frame ($p19^{ARF}$)

Two tumour suppressors $p19^{ARF}$ ($p14^{ARF}$ in humans) and $p16^{INK4A}$ are located on the CDKN2, illustrating the compact organisation of the genome. $p19^{ARF}$, referred to as ARF in the following section, and $p16^{INK4A}$ share a common exon 2. The start site of

p16 is in exon 1α and ARF is in exon1β. As their start sites are read in a different reading frame their primary amino acid sequence is not structurally similar [220].

ARF is not constitutively expressed; rather it is induced in response to hyperproliferation. The transcription factors c-myc[221], E2F[222], oncogenic RAS [223, 224] or virus E1A[225] rapidly switch on the expression of ARF. ARF localises to the nucleolus, a dynamic structure whose main function is the production of ribosomes. The nucleolus consists of three regions the nuclear organising region, the pars fibrosa, containing filaments of newly transcribed ribosomal RNA and the pars granulosa containing the ribosomal RNA together with protein ready to be transported out of the nucleus to the cytoplasm for ribosome assembly. The presence of ARF in the nucleolus inhibits ribosomal RNA processing[226] essentially shutting down the production of ribosomes and consequently protein construction. This impacts the cell cycle as it relies on the constant production of proteins for progression.

ARF is most widely known for stabilising p53; however transgenic mice show that this is not the only function of ARF. p53 null mice get lymphomas [227]with ARF null mice developing both fibrosarcomas and lymphomas. These observations suggest that ARF has functions independent of p53[228], this is supported by a finding that sencescence of p53-/- cells is ARF dependent.

The activation of p53 is via post-translational modifications. ARF stabilises p53 by interacting with MDM2, the exact mechanism for ARF mediated p53 stabilisation is not fully defined but three proposals have been put forward (figure 1.7). ARF shuts down protein production through inhibiting ribosome biogenesis but this is not necessary for stabilisation and activation of p53. This illustrates the neat organisation of the tumour suppressor network.

One way ARF has been shown to stabilise p53 is by sequestering MDM2 in the nucleolus[229] (Figure 1.7). This segregates MDM2 and p53, preventing MDM2 induced degradation of p53. This enables other kinases and acetylases to modify p53.

Another mechanism is forming a ternary complex between all three proteins. ARF has distinct sites for MDM2 and p53. Support for the formation of this complex comes from increases in p53 sumoylation are dependent on the presence of both MDM2 and ARF in the nucleolus [201]. These increases in sumoylation could be competing with ubiquitination as both occur on the same lysine residues. This would lead to an increase in stabilisation of p53. Another way is ARF binding to MDM2 in the nucleoplasm with a consequential stabilisation of p53[230]. The report showed the majority of ARF was nucleolar with a small portion found in the nucleoplasm. This was deemed sufficient to bind to MDM2. Tshe physiological significance of this is undefined as firstly ARF was induced using IPTG (isopropyl thiogalactoside). Secondly this was in cells that do not normally express ARF. Therefore the high excess of ARF present in the cells may have enabled it to function in areas where it normally does not.[230]

ARF is a relatively stable protein with a half-life of about 6 hours. Following polyubiquination it is degraded in the proteasome. As there is only one lysine residue in mouse ARF with none present in human ARF polyubiquination does not occur on lysine residues, but on arginine residues. The nucleolar protein nucleophosmin (NPM) extends the half-life of ARF from 6-10 hours, although ubiquination of ARF is still evident[231]. In additons the interaction between ARF and NPM can induce the degradation of NPM although this is dependent on conditions. NPM binds to nucleic acids in the presence of ARF. ARF binds NPM using residues 1-14[232, 233]and NPM binds to ARF via its oligomerization domain [232, 233] .This may inhibit the formation of the oligomer of NPM while the monomer form of NPM may be less stable. The interactions of ARF with NPM are closely tied to the function of ARF in ribosomal processing. Through inhibiting $p19^{ARF}$'s ability to attenuate ribosomal RNA processing NPM could promote S-phase thereby allowing ribosomes to be produced and thus proteins required to enable the cell to enter s-phase[234].

A recently discovery of an ARF p53 independent function is the inhibition of NF-κB. Through an unknown mechanism ARF stimulates ATR, which activates Chk1 leading to phosphorylation on thr505 of NF-κB. This phosphorylation of NF-κB

leads to a downregulation in the transactivation function of NF-κB [235, 236]. The reason why ARF may downregulate NF-κB could be because it antagonises[237] the function of p53, thereby diluting any affect that ARF may have. Another p53 independent function of ARF is sumoylation, although ARF does sumoylate p53, the presence of p53 is not a requirement for ARF induced sumoylation to occur. ARF appears to induce sumoylation of proteins it interacts with the exact outcome of this is undefined[237, 238].

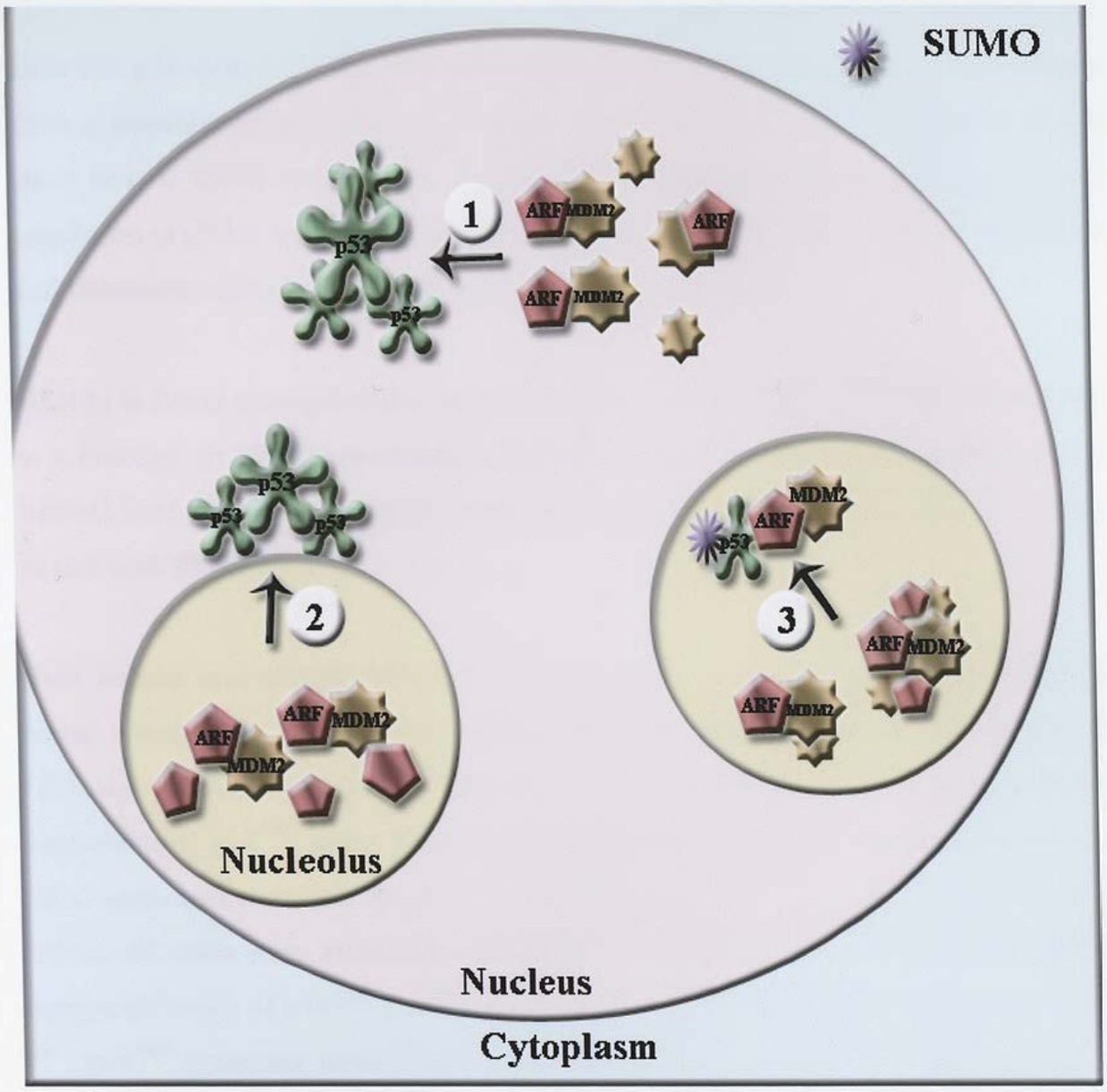


Figure 1.7: Three mechanism of ARF stabilisation of p53

ARF has been postulated to stabilise p53 by three methods. (1) ARF binds to MDM2 in the nucleoplasm and moving it away from p53. (2) ARF sequesters MDM2 in the nucleolus. This prevents p53 and MDM2 interacting. (3) ARF, MDM2 and p53 form a trimeric complex; this has been shown previously to induce sumoylation of p53. (For more details see text)

1.6.3 Uncontrolled p53 regulation in HCC

Like Rb, p53 is an important tumour suppressor. At least 50% of all human tumours have a mutation of p53 and it is thought those tumours without a mutation in p53 itself have a mutation in a p53 regulator. This emphasises how important proper regulation of p53 is to the cells. MDM2 and $p19^{ARF}$ are two important p53 regulators and alterations of both MDM2 and $p19^{ARF}$ are found in HCC.

MDM2 is found up regulated in approximately 25% of HCC [239, 240]. This would lead to a decrease in p53 levels present. As both mutation in p53 and overexpression of MDM2 have similar outcomes it is not surprising that a combination of both is found in less than 4% of HCC[240].

Both human and mouse ARF ($p14^{ARF}$ and $p19^{ARF}$) are situated on the CDKN2A locus, which is the second most mutated in human cancers, second only to p53. In HCC the most common $p14^{ARF}$ alterations are hypermethylation and upregulation in expression of $p14^{ARF}$ gene. A report by Tannapfel et al showed as many as 84% of HCC cases had increases in $p14^{ARF}$ mRNA expression[237]. In a study by Ito et al in which, all cases were associated with HBV or HCV this rose to 93%. Both studies compared levels of $p14^{ARF}$ mRNA expression in HCC to adjacent non-tumour tissue [241]. $p14^{ARF}$ promoter methylation found in HCC varies. Cases of HCC arising in patients with haemochromatosis and aflatoxin showed hypermethylation of $p14^{ARF}$ promoter to be in between 29-46% [237, 242]. In contrast with this there are reports of low levels of methylation, 9% [243] or no methylation of $p14^{ARF}$ promoter in cases associated with HBV and HCV[241]. This evidence suggests alterations of $p14^{ARF}$ in HCC is dependent on aetiology and appears to be an important event in the development of HCC

1.6.4 Intra S-phase checkpoint

Incorporation of checkpoints after each cell cycle stage protects cells as they prevent cycle progression in the presence of DNA injury. S-phase is instigated by the

presence of cyclins A and E (section 1.4.2), two genes whose transcription is E2F induced. Upon phosphorylation Rb releases E2F and RB loss has shown to increase DNA damage[244].

Ataxia telangiectasia mutated (ATM) and ATM RAD3 related protein (ATR) belong to a family of kinases, the phosphatidylinosital-3-kinase related kinases (PIKK). ATM and ATR are activated upon DNA damage and initiate a signalling cascade resulting in p53 activation and repair of damaged DNA. Their conservation through evolution illustrates their importance of these proteins as homologs of both ATR and ATM are found in both budding and fission yeast [245]. Survival of cells with impaired ATM and ATR is compromised, as they are defective in eliciting a response to DNA damage.

In response to DNA damage E2F family members can induce ATM transcription, resulting in Chk2 phosphorylation and p53 activation, culminating in apoptosis. Phosphorylation of E2F1 alone by ATM/ATR inhibits its degradation [246]. Phosphorylation of E2F1 by cyclin A/CDK2 at ser375 increases the binding affinity of E2F for Rb[247].

Up until recently ATR and ATM were thought to act independently in response to distinct signals. ATM responded to IR and double strand breaks and ATR activated in response to single stranded DNA and stalled replication forks. It is now apparent that they co-operate with each other to respond to certain signals in a controlled cell cycle responsive manner.[248]

In an unstimulated cell, ATM exists as a homodimer with the kinase domains of each subunit facing each other. In response to simulation there is an intermolecular phosphorylation resulting in the disruption of the dimer and the resulting monomers can phosphorylate their substrates[249] . In fact ATM may not be activated in response to DSB but in response to chromatin remodelling. The interacting partners of ATM are also highly conserved and compose the MRN complex. This consists of Meiotic recombination 11(Mre11), RAD50 and Nijmegen break syndrome 1(Nbs1). These proteins are bound together in a structure that suggests it may have a role in tethering broken chromosomes together. After DNA damage ATM phosphorylates Nbs1 in a

conserved domain within the C-terminus of Nbs1. This is essential for bringing ATM to the DNA enabling it to phosphorylate its substrates at the site of damage e.g. chk2. mutation of this domain impairs the response of the cells to IR[250]. In fact there is conserved motif in Nbs1, ATRIP and Ku80, the site being essential for bringing ATM, ATR and DNA-PK to sites of DNA damage [250].

In contrast to ATM, ATR is activated in response to ssDNA and stalled replication forks. ATR and its primary substrate Chk1 are essential, loss of both is embryonic lethal[251]. Even in the absence of damage ATR protein has been found recruited to chromatin during S-phase and G2. The reason for the presence of ATR at replication forks is not clear although it may be when the DNA is replicating fragile sites which are more susceptible to mutations [252].

In response to DNA damage the kinase activity of ATR is not increased. It is relocalised to sites of DNA damage bringing it into close proximity to its substrates such as Chk1. ATR is continually bound to the ATR interacting protein (ATRIP), which can interact with replication protein A (RPA). In an unstressed cell RPA coats ssDNA when replication origins fire. ATRIP interacts with RPA on the site of ssDNA and recruits along with it ATR and thus this brings ATR into close proximity with it subtrates allowing it to phosphorylate them[253].

The function of ATR at stalled replication forks is dependent upon the presence of claspin and ATRIP. Claspin is recruited to replication origins as they fire and they migrate to replication forks.

A recent report shows not only ATM but both ATM and ATR are required for a sustained and effective response to IR induced DNA double strand breaks. Previously it was thought that ATM alone phosphorylated chk1 and chk2. In response to IR ATM acts upstream of ATR, together with Mre11. These double strand breaks (DSB) stimulate Mre11 to activate its intrinsic nuclease activity. This converts the DSB into ssDNA, promoting binding of RPA and the subsequent activation of the ATR pathway. This mirrors the pathway found in budding yeast in

which the homolog of ATR, mec1 requires the Mre11 homolog to respond to DSB. This activation of ATR downstream of ATM is cell cycle dependent only happening in S and G_2 phases of the cell cycle whereas ATM is activated throughout the cell cycle. This leads to speculation that there may be other factors involved in activation of ATR in such a cell cycle specific way[248].

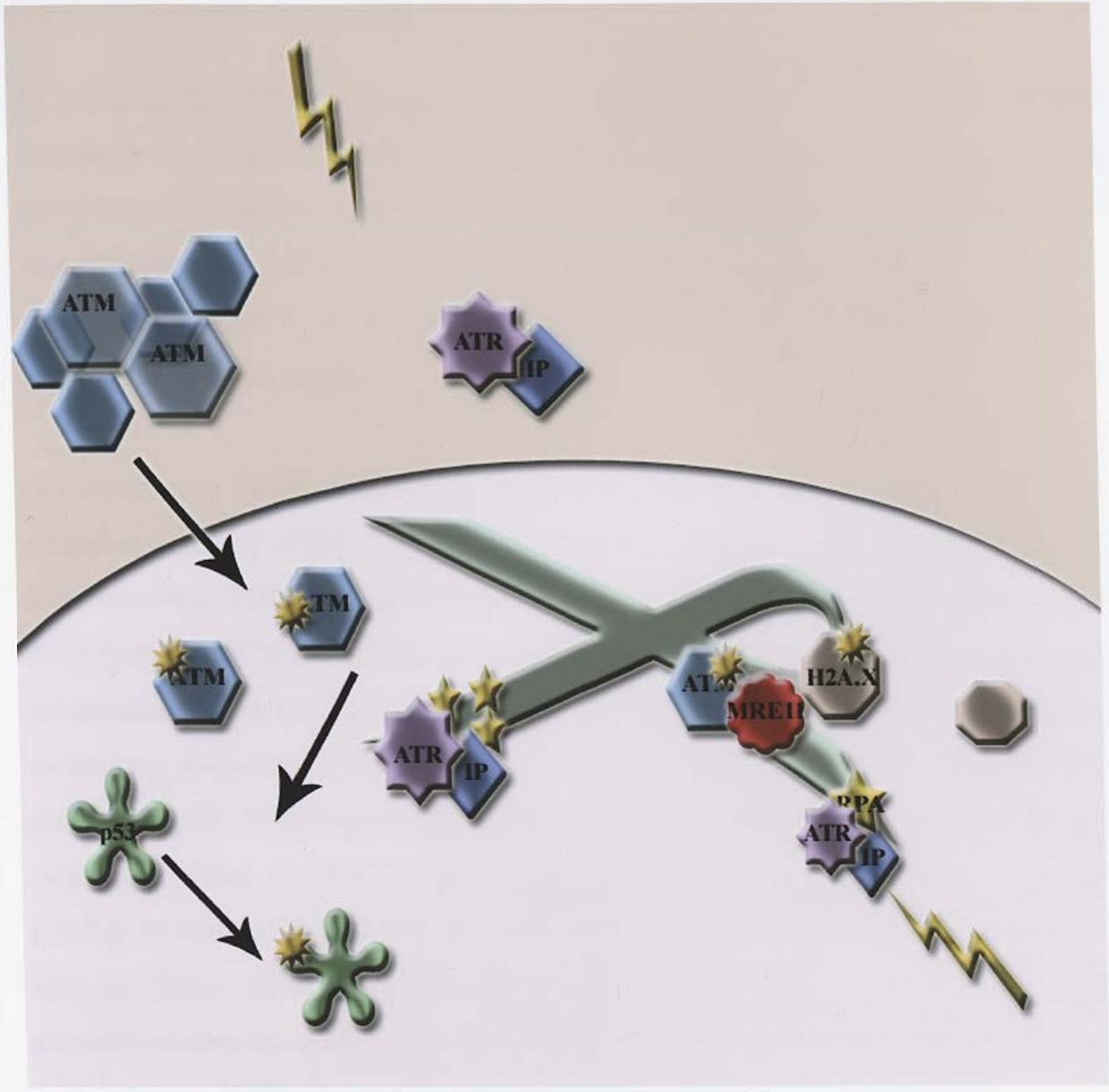


Figure 1.8: The ATM and ATR pathway in response to DNA damage

In an unstressed cell ATM exists as homodimer in response to DNA damage there is an intermolecular phosphorylation resulting in a disruption of the dimmer. The dimer is active and stimulates checkpoint kinase 2. The damage response kinase ATR exists in a complex with ATR interacting protein (ATRIP). Upon DNA damage single stranded DNA becomes coated with replication protein A (RPA). Binding of ATRIP to RPA bringing alongside ATR. Recently it has come to light that in response to double strand breaks ATM binds in the presence of Mre11. Mre11 has a nuclease

activity and converts the double stranded DNA into single strands. RPA binds and brings ATR.

In response to damage, RAD17 is phosphorylated by ATR[254]. It has sequence homology to replication protein C (RPC) and acts in a similar manner to RPC, promoting the loading of the PCNA related complex RAD9-RAD1-HUS1 (9-1-1) complex onto the DNA [255-257]. The function of this RAD17 and 9-1-1 complex is unknown although it is thought to induce the replication of DNA that is more appropriate to DNA damage [258].

In response to DNA damage the molecular chaperone nucleophosmin (NPM) is phosphorylated by ATR on ser125 [234]. This same residue is phosphorylated by CK2 and stimulates NPM to release bound histones. This NPM phosphorylation reduces the affinity of NPM for its denatured substrates[259]. NPM can bind both ATR and p53 simultaneously. In response to low doses of UV NPM binds to the p53 N-terminus preventing phosphorylation on ser15. This inhibits the activity and transactivation activity of p53. With higher UV doses this NPM effect on p53 is lost[234]. This dose responsive effect of NPM on p53 may prevent premature activation of p53. NPM binding to both ATR and p53 may prevent further p53 stabilisation. In tumor cells, such as HCC, NPM overexpression could lead to inactivation of p53[260]. NPM phosphorylation by ATR may induce NPM to release p53, mimicking what occurs with histones. NPM also has the ability to bind to MDM2 stabilising p53[261].

1.6.5 The mitotic checkpoint

Rb imposes on mitosis through inhibiting E2F, which switches on transcription of cyclin B1 and MAD2, which are two critical regulators of mitosis (Appendix 1). Phosphorylation by cyclin B/CDK1 and binding to securin inhibits separase activity. Activated separase cleaves the cohesion that links the sister chromatids. The anaphase promoting complex (APC), which is controlled by MAD2 tags securin and cyclin B with ubiquitin selecting them for degradation in the 26S proteasome. This

turnover of the anaphase and cytokinesis inhibitors, cyclin B1 and securin, enables progression to anaphase initiating the end of mitosis[262]. Cdc20 availability is the limiting factor for APC activation during mitosis. Cdc20 binds to both the APC and APC substrates through its C-terminus. Modification of cdc20's N-terminus controls its activity. This checkpoint prevents the activation of the APC[262, 263].

The mitotic checkpoint also known as the spindle assembly checkpoint is activated at every unattached kinetochore during the metaphase to anaphase transition. In prophase the centrosomes duplicate and form poles at either end of the cell (Figure 1.9). During metaphase the centrosomes produces oligomers of tubulin that connect with the kinetochores on the sister chromatids (Figure 1.9). When both poles are attached to the sister chromatids via their tubulin fibers a tension is created at the kinetochore. Microtubule attachments that fail to provoke tension are severed by aurora kinase B thus producing unattached kinetochores. These activate the mitotic checkpoint [264, 265]. An unattached kinetochore is attached to a microtubule motor containing centromere protein E. Centromere protein E activates the kinase BubR1[266]. The kinase activity of BUbR1 recruits Mad1. This allows Mad1 to form a landing pad for Mad2 at the kinetochore[267]. This stimulates the binding of Mad2 to cdc20, sequestering cdc20 away from the APC (Figure 1.9)[268].

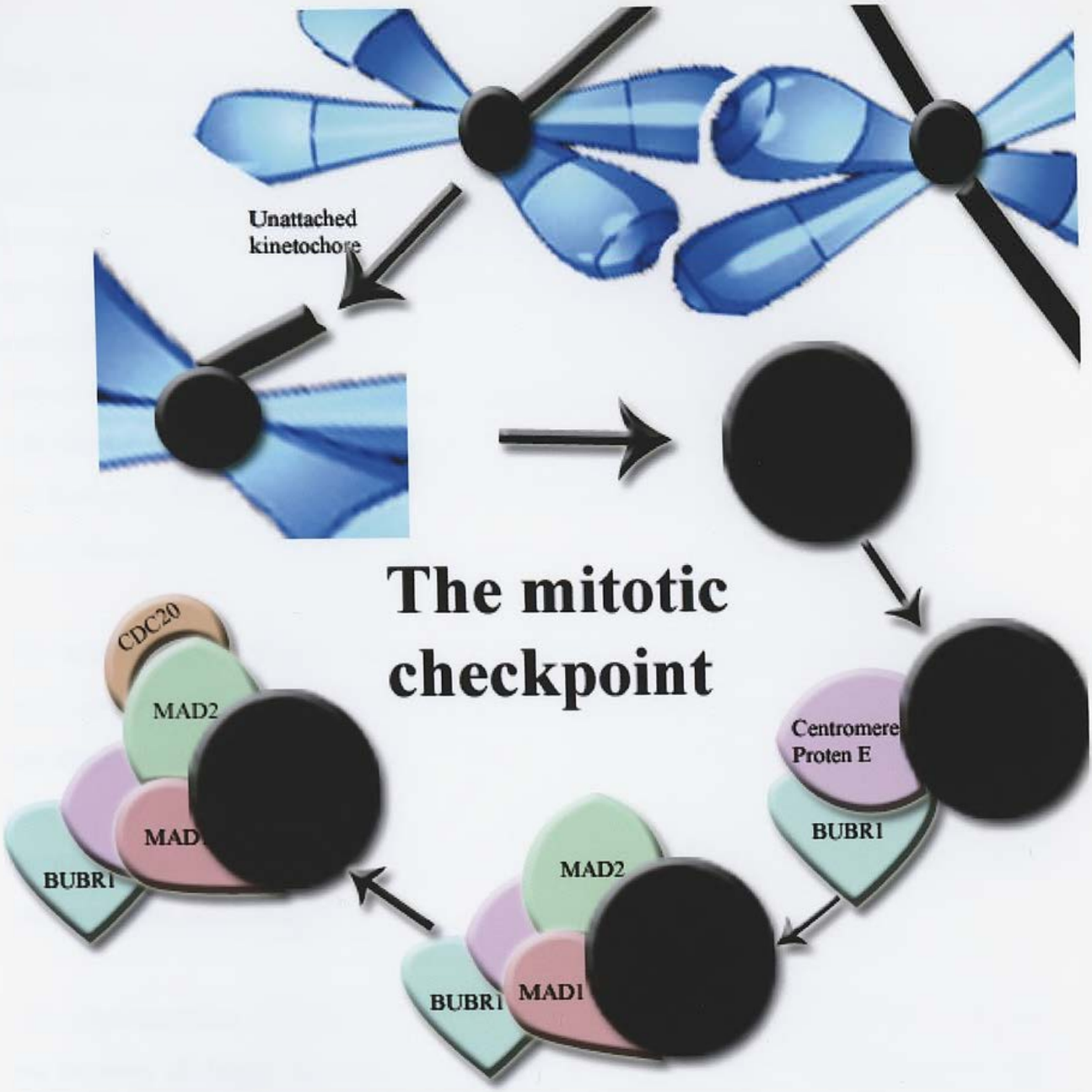


Figure 1.9: The mitotic checkpoint

The mitotic checkpoint is activated in response to unattached kinetochores. It begins with centromere protein E stimulating the kinase activity of BUBR1. The activity of BUBR1 recruits Mad1, which forms a landing pad for Mad2 to bind. The binding of Mad2 allows Mad2 to bind to cdc20. This sequesters cdc20 away form the APC, preventing its activation and thus progression to anaphase.

Until recently how the binding of Mad1 to Mad2 stimulated the binding of Mad2 to cdc20 was undefined. Three pieces of evidence were known. Firstly, prior to activation of the checkpoint Mad2 is in an inactive form that cannot bind to cdc20. Secondly, both Mad1 and cdc20 bind to the same region in Mad2, therefore it was not through a change in conformation of Mad2. Thirdly the dimerisation of Mad2 is essential. NMR and X-ray crystallography resolved the structure of Mad2 together with a Mad1:Mad2 complex. This shows Mad2 binds Mad1 in the same way as a seat belt binds a passenger, indicating that Mad2 could only bind Mad1 or cdc20 and not both proteins simultaneously[269 268]. Combining this evidence enabled a model to be out forward.

The model suggested there are two conformations of Mad2, open and closed. An open conformation consists of Mad2 with nothing bound an empty seat per se, that can bind substrates. The binding of Mad1 results in a closed conformation. If the binding of two Mad2 closed conformations were energetically unfavourable therefore the Mad2:Mad1 complex would only bind to another open Mad2 conformation, activating it[269-271].

The oligomeristion of Mad2 explains how this Mad2: Mad1 complex could stimulate the binding of Mad2 to cdc20. Mad2 dimerises only if the conformations of the Mad2 proteins are different. One Mad2 is in the open conformation and one in the closed. At the unattached kinetochore, Mad1 is there binds to Mad2 forming a Mad1:Mad2 closed complex. An open Mad2 binds stimulating cdc20 to bind to this open conformation Mad2, creating a closed Mad2:cdc20 complex. This would dissociate from the other closed conformation, thus creating an inhibitory complex. This shows Mad1 as a launching tool for the creation of the Mad2:cdc20 complex. This model has yet to be proven, but does help to explain certain facts such as the two types of mad2 seen at the unattached kinetochore, one having a high turnover (in the o-conformation waiting to bind cdc20) and another with a slow (most likely bound to mad1). It also helps to explain how Mad1 could form the platform that establishes the association between Mad2 and cdc20 [267].

1.7 Aims and hypothesis

Rb plays an important role in regulation of the cell cycle, apoptosis and differentiation. As Rb loss of function is found in a high proportion of liver cancers, it is important to understand what happens to hepatocytes when *Rb* is lost. The aim of this work was to understand how *Rb* loss could contribute to the development of liver cancer. Three hypotheses were put forward:

- The hypothesis was upon loss of *Rb* that $p19^{ARF}$ stabilised p53
    - The aim was to elucidate the mechanism leading to the transient stabilisation of p53 in *Rb-/-* hepatocytes.

- The hypothesis was an increase in ROS induced DNA damage in *Rb-/-* hepatocytes.
    - The aim was to determine if there was an increase in DNA damage and to establish the pathway leading to an increase in DNA damage in *Rb-/-* hepatcytes.

- The hypothesis was dysregulation of both cyclins and checkpoint proteins leads to the phenotype of abnormal nuclei.
    - The aim was to analyse the state of cell cycle control.

Chapter 2:

Materials and methods

2.1 Hepatocyte culture

Primary hepatocytes are obtained by a two-step retrograde perfusion[272]. The perfusion apparatus was sterilised with 70% ethanol and rinsed with dH_2O. The collagenase, 25mg (Sigma c-1538) was diluted in 120mls digestion medium (Table 2.1.1) containing 20ng/ml DNASE 1 (Roche cat no. 128493). The mouse was given a lethal dose (300µl) of the anaesthetic sagatal and the peritoneal cavity was opened. The intestines were moved to one side to expose the hepatic portal vein and a loose ligature was placed around the inferior vena cava. An incision was made in the right atrium of the heart and a fine bore canula (OD 1mm, ID 0.5mm) was inserted into the thoracic inferior vena cava and secured by the ligature. Oxygenated perfusion medium (Table 2.1.1) enters into the liver at a flow rate of 8.4mls per minute. The hepatic portal vein was cut and the liver was perfused for 5 minutes, followed by digestion medium for a further 10 minutes. Once the liver had digested fully it was removed, added to a dish containing a small amount of plating medium and gently brushed to disaggregate the hepatocytes. The hepatocytes were washed through a 250µM sieve into an ice cold jar.

The suspension was transferred to an ice cold falcon tube and pelleted by centrifugation at 50g for 5 minutes at 4°C. The supernatant containing debris and non-parenchymal cells was removed and the pelleted hepatocytes were resuspended gently in 8mls of plating medium (Table 2.1.1) plus 5.25mls of percoll to further purify the hepatocytes population. The hepatocytes were spun at 50g for 10minutes at 4°C, this resulted in dead cells, debris and non-hepatocytes floating in the percoll

layer while the murine hepatocytes pelleted. The supernatant was removed and the pelleted hepatocytes were resuspended in 5mls of ice-cold plating medium.

Cell viability was determined using the trypan blue exclusion method. 20μl of the cell suspension was added to 40μl trypan blue (Sigma) and 40μl PBS. A drop of this solution was added to a haemocytometer and both the stained (dead) and unstained (live) cells were counted in five $1mm^2$ squares on the haemocytometer. Typically, approximately 20 to 30 millions cells at 80-95% viability were obtained.

At the time of plating the adenoviral infection was done. The cells were plated at a density of $0.5Million/cm^2$ on 2 well slides, 4 well slides, 24 well plates and $10mm^2$ dishes in plating medium containing or not adenovirus at a multiplicity of infection (MOI) of 10. Controls use empty adenovirus DL70 (Virapur) or no virus as indicated; Rb deletion is achieved using Cre adenovirus (Virapur).

The cells were allowed to attach for 2 hours, following this the medium is changed for serum free Chee's medium-arginine free (Table 2.1.1), with a medium change every 24 hours. The medium containing the virus was disposed of in pre-sept containing beakers and the safety cabinet where the work was carried out was UV-irradiated overnight.

Medium	Type	Supplier	Supplements
Perfusion	Liver perfusion	GiBCO/Invitrogen(17701-038)	50ng/ml Gentamicin
Digestion	L15 medium	Sigma(L5520)	50ng/ml Gentamicin, 4mM L-Glutamine, 3mM NaOH, 0.14mM Dexamethasone, 1.7mM Insulin, 40mM Hepes,
Plating	DMEM	Sigma(D6421)	50ng/ml Gentamicin, 4mM L-Glutamine, 3mM NaOH, 0.14mM Dexamethasone, 1.7mM Insulin
Culture	Chee's (Arginine free)	GiBCO/Invitrogen(special order)	50ng/ml Gentamicin, 4mM L-Glutamine, 3mM NaOH, 0.14mM Dexamethasone, 12.5ng/ml EGF, 1% Insulin-transferrin-selenium

Table 2.1.1: The medium and supplements used for the culture of primary hepatocytes.

2.2 Immunoblotting

2.2.1 Preparation of samples

To prepare the cell pellet a $10mm^2$ dish containing approximately 1.7 million cells is washed in sterile PBS. In a total volume of 6mls ice cold PBS the cells are scraped using a sterile cell scraper and spun at 400g for 5 minutes. The cell pellet is snap frozen on dry ice and stored at -70°C until use.

The cell pellet is lysed according to the protein of interest, for proteins in the nucleus, cytoplasm and nucleolus (ARF), a Hepes buffer was used and for proteins bound to the DNA (H2A.X) an acidic buffer was used.

For ARF, the cells are lysed in lysis buffer (50mM Hepes pH 7.5, 150mM NaCl, 1mM EDTA, 2.5mM EGTA, 0.1% Tween 20) with phosphatase inhibitors; 10mM β-glycerophosphate, 4mM Sodium fluoride, 100μM sodium orthovandate and 10μl sigma protease inhibitor cocktail per 1ml of lysis buffer. The cell lysate is sonicated for 2 X 7sec on ice, setting 5 with the output power at 12-14% and incubated for 30 minutes on ice. This is spun for 2 minutes at 9,500g at 4°C. The supernatant is stored at -70°C until use[273].

In the case of H2A.X the lysis buffer used is 10mM Hepes pH 7.9, 1.5mM $MgCl_2$ and 10mM KCl with the protease inhibitor 1.5mM PMSF and 0.5mM DTT a reducing agent. Approximately 7 volumes of lysis buffer is added to the cell pellet on ice and incubated on ice for 30 minutes. The cells are spun for 5 minutes at 9,500g at 4°C and 0.2mls of the supernatant is dialysed against 0.1M acetic acid for 2 hours at 4°C, with further dialysis against distilled water overnight. The sample is collected; protein quantified and run on SDS-PAGE.

2.2.2 Immunoprecipitation

The rabbit trueblot^{tm} kit (ebioscience) was used. This involves using beads coated in rabbit IgG and a specific secondary that has a lower affinity for reduced 55kDa heavy and 23kDa light chains of the immunoprecipitating antibody preventing interference of the heavy and light chains of the antibody.

For each immunprecipitation 500µg of protein was used. By preclearing the sample, removal of non-specific binding proteins to the beads was done, 50µl of rabbit IgG beads was added to the sample, incubated on ice for 30minutes, spun and the supernatant was transferred to a new eppendorf. Antigen precipitation was done by adding the antibody (5µl for ARF) to the sample and incubating on ice for one hour. Beads coated with rabbit IgG were added, and the sample was incubated for a further two hours on a rocker. The sample was spun, supernatant removed and the beads were washed 3 times in lysis buffer (See section 2.2.1).

2.2.3 Quantification of protein

The Bio-rad assay, based on the Bradford method was used for the quantification of protein. The assay was done according to the manufacturers instructions. Briefly a standard curve was created using 1-10µg of protein. A 1/50 dilution of the sample was done in triplicate. The plate was incubated for 10minutes and read at 590nm on a plate reader.

As the SDS from the lysis buffer interfered with the Bradford assay, when appropriate, the Lowry assay was used. This was done according to manufactures instructions. Briefly a standard curve was created using 1-10µg of protein. A 1/2 dilution of the sample was done in triplicate. The reagents added and the plate was incubated for 15 minutes and read at 630nm on a plate reader.

2.2.4 Protein electrophoresis

SDS gels were prepared according with the constituents as described in table 2.2.4.1 and immediately placed in the assembled bio-rad™ apparatus. The liquid was poured up to approximately 1cm below the top of the small glass plate. dH_2O was immediately placed on top to remove air bubbles from the gel. The gel was allowed to polymerise and the water was removed. After polymerisation the stacking gel was prepared (table 2.2.4.1) and overlayed on top of the separating gel. The comb was inserted and the gel was allowed to polymerise. Depending on the protein studied 50-200µg of protein was mixed with 5X loading buffer (0.33M Tris-HCL (Sigma), pH 6.8, 50mM EDTA (Sigma), 10% w/v SDS, 50% Glycerol, Bromophenol blue dye and dH_2O) or laemmli buffer for immunoprecipitation. The protein was denatured by heating it to 100°C for 5mins, it was immediately placing on ice and pulse spun. The sample was loaded onto a 10%, 12% or precast gradient SDS gel as indicated in the text, the SDS gel used varying with the size of the protein. Using electrode buffer (0.01M TRIS (Sigma), 0.2M Glycine (Sigma), 0.1% SDS (Sigma) and dH_2O) the SDS gels were run at 100V with for approximately 2 hours at 4°C.

Separating gel			***Stacking gel***	
Percentage gel	***10%***	***12%***		
dH_2O	4.05mls	3.35mls	dH_2O	6.1mls
Tris-HCL pH8.8	2.5mls	2.5mls	Tris-HCL pH6.8	2.5mls
10% SDS	100µl	100µl	10% SDS	100µl
Acrylamide	3.3mls	2mls	Acrylamide	1.3mls
10% Ammonium persulphate	50µl	50µl	10% Ammonium persulphate	50µl
Temed	5µl	5µl	Temed	10µl

Table 2.2.4.1 Constiuents of Sodium dodecyl (SDS) gels used.

To transfer the protein from the gel to the PVDF membrane ; ECL™ Hybond P™ (Amersham) was used, the membrane was soaked in 100% methanol for 30 seconds, washed in milipore dH_2O for 10 minutes and placed in transfer buffer (10mM TRIS, 0.7M Glycine, 20% Methanol (fisher), 0.1% SDS and dH_2O) together with two fiber pads and two pieces of filter paper. Protein was transferred to the membrane via electrophoresis at a constant voltage of 45V overnight at 4°C in transfer buffer with constant stirring.

2.2.5 Detection

PVDF membranes were washed once in TBS-Tween (TBST) (10mM Tris-HCL, 150mM NaCl (Sigma), 0.1% Tween 20, pH 7.4) and stained with Ponceau S solution to check for transfer. Following blocking the membranes were incubated with the specific primary antibody (table 1.2). The blot was washed 3 times with TBST for 10 minutes and incubated with the specific secondary, donkey anti-rabbit HRP (Amersham) or goat anti-mouse(Dako) for 45 minutes in 5% Marvel TBST at room temperature with agitation. The blot was washed a further 3 times with TBST, followed by one final wash with TBS.

Protein of Interest	Species and Isotype *Manufacturer* *(cat no.)*	Antibody Incubation			
		Conc.	Time	Diluent	Temp
$p19^{ARF}$	Rabbit polyclonal *Abcam(Ab-80)*	0.1µg/ml	2 Hours	TBST	Room Temp
p53 *CM5*	Rabbit polyclonal *(Gift from T. Hupp)*	1/1,500	O/N	5%Marvel TBST	4°C
NPM	Rabbit polyclonal *Abcam (15440)*	1/1,000	2 hours	TBST	Room temp
MDM2(Ab-2) *Clone:* *2A10*	Mouse monoclonal IgG_{2A} *Calbiochem (OP115)*	0.1µg/ml	2 hours	5% Marvel TBST	Room temp
MDM2(Ab-3) *Clone:* 4B11	Mouse monoclonal IgG_{2A} *Calbiochem (OP143)*	0.1µg/ml	2 Hours	5% Marvel TBST	Room temp
H2A.X Clone JBW301	Mouse monoclonal IgG_1 *Upstate*	7.15µl/5mls	2Hours	5% Marvel TBST	37°C
MnSOD	Sheep polyclonal *Calbiochem(574596)*	1/1,000	2 Hours	5% Marvel TBST	Room temp
Phospho-p53 (serine 15)	Rabbit polyclonal *Cell signalling(9284)*	1/500	O/N	5% Marvel TBST	4°C
Chk1	Rabbit polyclonal *Cell signalling(2345)*	1/1,000	O/N	5% Marvel TBST	4°C
Phospho-Chk1	Rabbit polyclonal *Cell signalling(2344)*	1/1,000	O/N	5% Marvel TBST	4°C

(serine 317)					
Chk2	Rabbit polyclonal *Cell signalling(2662)*	1/1,000	O/N	5% Marvel TBST	4°C
ATR	Rabbit polyclonal *Abcam(Ab 10312)*	1/10,000	2 Hours	5% marvel TBST	Room temp
p27	Rabbit polyclonal *Abcam (Ab 6547)*	1/2000	1.5 hours	5% Marvel TBST	Room temp
Cyclin A	Rabbit polyclonal *Abcam (AB 7916)*	1/100	2 hours	TBS-Tween 20	Room temp
Cyclin E	Rabbit polyclonal *Abcam (Ab 7959)*	1/100	2 Hours	TBS-Tween 20	Room temp
Cyclin B	Rabbit polyclonal *Abcam (Ab 2949)*	1/100	2 Hours	TBS-Tween 20	Room temp
Gadd45a	Rabbit polyclonal *Chemicon (AB3863)*	1/1,000	2 Hours	5% marvel TBST	Room temp
CDC25A	Rabbit polyclonal *Cell signalling(3652)*	1/1,000	O/N	5% Marvel TBST	4°C
Mad2	Goat polyclonal *Abcam (Ab 13615)*	1/1,000	2 Hours	5% marvel TBST	Room temp
ß-actin	Rabbit polyclonal *Abcam(Ab 8227)*	1/1,000	Overnight	5% Marvel TBST	4°C

Table 2.2: The antibodies used for immunoblotting and the conditions in which they were incubated with the membrane.

The detection was performed using the ECL™ plus chemiluminescent detection system (Amersham). The reagents are mixed according to the manufactures instructions. The membrane was placed on a glass plate, protein upwards and the mixed reagent pippeted onto the surface. This was incubated for 5 minutes at room temperature. The blot was exposed with ECL™ hyperfilm (Amersham) or imaged using the versadoc 4000 (Bio-rad).

2.3 Immunofluorescence

Cells were grown on 2 well chamber slides (Nunc). At the required timepoint the cells were fixed in 50% Acetone/50% methanol for 3 minutes. Removed and allowed to air dry. These were then stored at -70°C until use.

The slides were removed from the freezer allowed to thaw and washed 3 times in PBS. They were blocked in blocking solution for 10 minutes and incubated in primary antibody (table 3 for blocking solutions and time for incubation). The slides were washed in PBS and with the specific secondary antibody (Table 2.3.1) for 30 minutes diluted 1/200 in blocking solution. After 3 further washes in PBS, they were incubated with To-Pro 3 dye diluted 1/1000 in PBS. The slides were rinsed briefly in PBS, allowed to air dry and mounted using Mowiol.

Where required, an amplification step was performed using an avidin-biotin method. After blocking, the slides were treated with 3% H_2O_2 for 10 minutes to block endogenous biotin. They were incubated with an avidin and a biotin blocking solution each for 15 minutes with 2 washes of PBS inbetween. Post-blocking they were washed 3 times and incubated with primary antibody, a rabbit polyclonal to ARF (Abcam) diluted in blocking buffer 1/20 for 1 hour at room temperature. After 3 washes the slides were incubated for 30 minutes with a secondary antibody, swine anti-rabbit biotinylated antibody diluted 1/400 in blocking solution. They were washed and incubated with the strepavidin conjugated fluoresence diluted 1/200 in blocking solution for 30 minutes at room temperature. They were counterstained with To-Pro 3 dye and mounted with Mowiol as before.

Table 2.3.1: The antibodies, isotypes and conditions used for immunofluorescence (On following page).

Protein of Interest	Blocking solution	Antibody Incubation				Secondary antibody
		Isotype	Conc	Time	Temp	
$p19^{ARF}$	Normal swine serum PBS Tween 20	Rabbit polyclonal *Abcam(Ab 80)*	1/20	1hour	Room Temp	Swine anti-rabbit biotinylated
p53 *Clone:PAB421*	Normal goat serum PBS Tween 20	Mouse monoclonal IgG_{2A} *Calbiochem(Ab1)*	1/100	O/N	4°C	Goat anti-mouse IgG_{2A}
Nucleolin	Normal goat serum PBS Tween 20	Rabbit polyclonal *Abcam(Ab16940)*	1/100	1Hour	Room temp	Goat anti-rabbit
H2A.X *Clone: JBW301*	Normal goat serum PBS Tween 20	Mouse monoclonal IgG_{2A} *Upstate(05-636)*	1/100	1Hour	Room Temp	Goat anti-mouse IgG_{2A}
Gadd45a	Normal goat serum PBS Tween 20	Rabbit polyclonal *Chemicon (AB3863)*	1/100	1Hour	4°C	Goat anti-rabbit
MDM2 (AB-2) *Clone: 2A10*	Normal goat serum PBS Tween 20	Mouse monoclonal IgG_{2A} *Calbiochem(OP115)*	1/50	1Hour	Room Temp	Goat anti-mouse IgG_{2A}

When double immunofluorescence was performed for colocalisation studies, both antibodies were used as in a single immunofluorescence. As there is an increased chance of non-specific binding there was an increase in the amount of controls done (Table 2.3.4).

First set	**Second set**	**Expected outcome/ Reason**
Primary 1/secondary 1	Primary 2/secondary 2	Positive- to ensure that doing the immuno either way has no effect
Primary 2/secondary 2	Primary 1/secondary 1	
Primary 1/secondary 2		Negative- to ensure that both the primary and the secondary are not binding non-specifically.
Primary2/secondary 1		
Secondary 1	Secondary 2	Negative-no non-specific binding of the secondary antibodies to anything in the cell
Secondary 2	Secondary 1	

Table 2.3.4: The controls for double immunofluorescence and the reasons why they were done.

2.4 RNA

2.4.1 RNA extraction

RNA was extracted from a $10mm^2$ dish that contained approximately 1.7million to 2 million cells. This yielded approximately 0.5μg/μl to 1.1μg/μl of RNA each time. The cells were scraped in a total of 6mls of ice cold PBS using a sterile cell scraper and spun at 400g for 5 minutes.

The RNA was extracted using a kit (Qiagen mini kit), based on the binding of the RNA to a silica gel membrane. The cells were lysed in a strongly denaturing guanidine isothiocyanante and β-mercaptoethanol containing buffer that immediately inactivates RNAases allowing for isolation of total RNA. Dependent on the size of the pellet between 600μl to 1.2mls of this buffer was added, the tube vortexed and incubated at room temperature for a short time in order to completely lyse the pellet. Following lysis the pellet was homogenised in a QIAshredder™ column.

Once homogenised, 70% ethanol was added to the sample to aid the binding of the RNA to the membrane, the sample mixed and placed onto a column containing the membrane. The column was spun and this step was repeated. Afterwards the membrane containing the RNA was rinsed twice to wash away contaminants. To dry the membrane containing the RNA it spuned for 2 minutes at 8,000g. The RNA was eluted from the column by adding 30μl of RNAse-free water twice. The amount of RNA obtained was quantified using a spectrophotometer and the absoRbance was measured at 260nm and 280nm, 260nm giving the concentration and the ratio between 260nm and 280nm giving the purity of the RNA (which was always between 1.9 and 2.1). The RNA was stored at -70°C until use.

2.4.2 Reverse-transcription PCR

Reverse transcription was done for detection of the levels of mRNA in the cells. The cDNA produced was used for PCR and real-time PCR. RNA was extracted according to the method above. 3μg of RNA was used in each reaction and made up to 11μl using DEPC water. Oligo (dt), 1μl, was added to the tube and mixed gently. The sample was heated to 70°C for 10 minutes, chilled immediately on ice and pulse spun. For each reaction mixture 4μl of 5x synthesis buffer, 0.5mM dNTP, 0.01M DTT and 10U/μl of MMLV enzyme, final concentration, was added. The tube was mixed, pulse spun and incubated at room temperature for 10 minutes. The optimal temperature for the activity of the enzyme is 37°C, the tube was heated to this for 60 minutes and the reaction terminated by heating the tube to 90°C for 10 minutes. The tube was placed on ice for 10 minutes and pulse spun. In order to degrade any single stranded DNA and RNA that remained 1μl of RNase H was added and the tube was heated to 37°C for 20 minutes.

2.4.3 Real-time RT-PCR

The assay by design system (Applied Biosystems) was used. In this method two primers and a taqman probe is used. The probe contains a 5' end that has a reporter fluorogenic dye and a quencher dye at the 3' end. The probe anneals to the target sequence of the cDNA and as the primer is extended the nuclease activity of the taq polymerase cleaves the probe, resulting in removal of the reporter signal from the template leading to an increase in fluorescence reporter signal as it is removed from the quencher. The cleavage of the reporters from the probes with each cycle results in an increase in fluorescence intensity that is proportional to the amount of amplicon produced. The cDNA used was prepared by reverse transcription as above.

The house- keeping genes used were GAPDH and TATA binding protein. A standard curve for ARF, GAPDH and TATA binding protein was performed each time the reaction was done. Prior to the first run a standard curve for ARF was done to

determine at what dilution an optimal signal was obtained which was 1/20. The dilutions for the standard curve were 1/10, 1/20, 1/40, 1/60, 1/120. Each well in a 96 well reaction plate contained 16.2µl of cDNA dilution together with 18µl of PCR mix and 1.8µl of the assay by design mix. The PCR mix contains the taq and the assay by design mix contains the primers together with the taqman probe. In total there was 36µl, which was transferred to a 382 well plate with 10µl of the sample added to each well in triplicate. To prevent evaporation of the sample during the run, the samples were pulse spun and overlayed with a plate sealer.

The real-time PCR reactions were run on an ABI PRISM 7900HT Sequence Detection System. The reaction cycle controlling, fluorescence detection, data acquisition and analysis were done through ABI PRISM SDS 2.1 program. Each real-time PCR run consisted of three stages: stage 1, 56°C 2 min; stage 2, 95°C 10 min; stage 3, 95°C 0.15 min and 60°C 1 min, cycled 40 times.

2.5 DNA

2.5.1 DNA extraction

Dependent on the end use of the DNA two different methods of DNA extraction were used. The DNeasy kit from Qiagen™ was used for PCR (Section 2.8) and the DNA damage kit (Section 2.9). This method is based on the binding of the DNA to a silica gel membrane. For the measurement of 8-oxo-dG sites (Section 2.10) the DNA was extracted using the sodium iodide method[274]. When DNA extractions were done to check for the recombination of Rb, a 6mm^2 dish containing approximately 0.5million cells was used. Whereas for 8-oxo-DG and the DNA damage kit a larger quantity of DNA was required so 10mm^2 dish containing approximately 1.7 million cells was used. The cells were washed, scraped in sterile PBS and spun at 400g for 5 minutes. The supernatant was removed and the pellet was stored at -20°C until required for use.

For the DNeasy kit the pellet was allowed to thaw and resuspended in 200µl of PBS. The cells were lysed by adding proteinase K together with a guandium hydrochloride containing buffer, followed by vortexing and heating the tube to 70°C for 10 minutes. Ethanol was added to precipitate the DNA and the sample was transferred to a column containing the membrane. The column was spun allowing the DNA to bind to the membrane, which was washed twice with high salt containing buffers. Elution buffer was added onto the membrane, spinning the column and repeating this step once. The DNA was stored at 4°C short term and -20°C long term.

For the sodium iodide method the DNA was extracted according to the manufacturers instructions. Briefly the cell pellet was lysed in a non-ionic surfactant, polyoxyethylene oxyphenyl ether buffer and spun at 10,000g for 20 seconds at 4°C. The resulting supernatant contains cellular macromolecules such as RNA and is removed. The pellet was suspended in 200µl of an enzyme solution for 1 hour at 37°C. This enzyme solution contains a protease the digests the proteins into polypeptides and SDS that expands the DNA liberating it from nucleus protection. The addition of 0.3mls of NAI dissolves the polypeptides and other biological molecules. The DNA was precipitated by addition of 0.5mls of isopropyl alcohol. The solution was spun at 10,000g for 10minutes. The supernatant was removed and the pellet was washed and vacuum dried. RNase and DNase free water was added and to calculate the concentration the absoRbance was measured at 260 and 280nm.

2.5.2 PCR

PCR reactions were carried out in 0.5ml thin-walled eppendorf tubes in a standard thermocycler (Hybaid and eppendorf). All reagents were obtained from invitrogen. A standard Taq polymerase (Invitrogen) was used. In the case of the hybaid machine all reactions were overlaid with paraffin oil. PCR products were visualised on agarose gel; 1.5% for p53, p21, ARF and β-actin) and 1.8% for Rb, agarose diluted in syber safe™ an alternative for ethidium bromide which has reduced mutagenicity. The gel was imaged using the UV transluminater facility of the versadoc 4000(Bio-rad).

Gene	Primer	Primer sequence	Product size
p53	Exon 6 Intron 7 NEO	GTGGTGGTACCTTATGAGCC CAAAGAGCGTTGGGCATGTG CATCGCCTTCTATCGCCTTC	642bp wt 510bp deleted
RB^{275}	212 18	GAAAGGAAAGTCAGGGACATTGGG GGCGTGTGCCATCAATG	680bp WT 748bp floxed 300bpdeleted
ARF	Forward Reverse	AGGGATCCTTGGTCACTGTGAGGATTC GCAAAGCTTGAGGCCGGATTTAGCTCTGCTC	500kb
β-actin	Forward Reverse	TTCTTTGCAGCTCCTTCGTTGCCG TGGATGGCTGCGTACATGGCTGGG	500kb

Table 2.8.1: The PCR primers and the expected product sizes with these primers.

Gene	Melting	Denaturation	Annealing	Elongation	Cycles
p53	94°C 5min	94°C 1min	62°C 1min	72°C 1 min	35
RB	94°C 5min	94°C 1min	58°C 1min	72°C 1 min	35
p19^{ARF}	94°C 3min	95°C 1min	65°C 45secs	72°C 2min	38
β-actin	94°C 3min	94°C 1min	60°C 1min	72°C 1 min	20

Table 2.8.2: The cycling conditions for the nominated genes and the specific primers from table 5

2.5.3 DNA Damage Kit (Biovision)

The purpose of this assay was to quantify apurinic and apyrimindinic sites (AP sites) in hepatocyte DNA. The method is based on a probe that reacts with the aldehyde groups in the apurinic and apyrimndic sites in the DNA. This probe contains a biotin group and is coupled to a strepavidin HRP, which can be read on a spectrophotometer. A standard curve is created using DNA with known amounts of AP sites and is prepared by diluting the top stock of 40 ARP sites with TE buffer.

From a $10mm^2$ dish, DNA was extracted and quantified on a spectrophotometer by reading it at 280nm and made up to a concentration of 0.1μg/μl. The DNA was tagged with the aldehyde reactive probe (ARP) by incubating 0.5μg of the DNA with 5μl of ARP for 1 hour at 37°C. The tagged DNA was resuspended in Tris-EDTA buffer containing glycogen, the glycogen added to aid precipitation of the DNA. In order to precipitate the AT-tagged DNA, ethanol was added, the sample placed at -20°C for 10minutes and spun at 12,000g for a further 10 minutes. The pellet was washed 3 times in 70% ethanol and diluted in 1ml of TE buffer. Into a well of a 96 well plate, 60μl of standards or the DNA to be tested was added in triplicate. 100μl of DNA binding solution was added to each well, the plate was kept at room temperature overnight to allow the tagged DNA to bind to the plate surface. The plate was washed 5 times with wash buffer, 100μl of the HRP-strepavidin solution was added and the plate was shaken for 1 hour at room temperature. The plate was washed again 5 times with wash buffer. 100μl of the HRP developer (H_2O_2) was added to the plate and incubated at 37°C for 1 hour. The optical density was measured at 650nm in the spectrophotometer.

2.5.4 8-oxo-dG Measurement

The levels of 8-oxo-dG were measured using an Elisa kit according to the manufacturers instructions. A plate pre-coated with a monoclonal antibody to 8-oxo-dG was incubated with 50μl of either samples, DNA extracted from WT and *Rb-/-* hepatocytes using the sodium iodide method or 8-oxo-DG standards, ranging from

0.125ng/ml to 10ng/ml. Also 50µl of mouse monoclonal to 8-oxo-DG was added and the plate was incubated overnight at 4°C. Afterwards the contents were poured off and the plates were washed three times with 250µl of PBS. A 100µl of a HRP conjugated anti-mouse antibody was added for one hour at room temperature. The wells were washed again followed by addition of a 100µl of chromatic enzyme substrate solution for 15 minutes in the dark. The reaction was terminated by addition of 100µl of 1M phosphoric acid. The absoRbance was read at 450nm.

2.6 Reactive oxygen species (ROS) measurement

2.6.1 CM-H_2DCFDA measurement of ROS

5-(and 6-)chloromethyl-2',7'-dichlorodihydrofluorescein diacetate (CM-H_2DCFDA) was used to measure the amount of ROS in the cells. For the assay the cells were plated onto 24 well plates with a seeding density of 0.13 million/ml and cultured until the indicated time.

CM-H_2DCFDA is a cell permeable diacetate ester. Upon entry into the cells the acetate groups are cleaved by intracellular esterases and the thiol reactive chloro-methyl groups reacts with intracellular glutathione and thiols leading to its retention in the cells. Upon reaction with ROS it fluoresces green.

A 100µM top stock solution was made by adding 1 ml of DMSO to 50µg of CM-H_2DCFDA This was diluted to a 10µM working solution in HBSS. The cells were washed 3 times in 1X HBSS and 500µl of the diluted CM-H_2DCFDA solution was added to each well. The amount of fluorescence was measured over one hour on a Fluoroskan (Thermo lifesciences) at 485nm and 510nm with readings taken every 3 minutes. The control was Dimethylsufoxide (DMSO) alone added at the same

concentration as the CM-H_2DCFDA. The amount of fluorescence was normalised to the amount of protein.

2.6.2 Dihydroethidium (DHE) measurement of superoxide anion

Dihydroethidium was used to measure the amount of superoxide anion in the hepatocytes. As with the CM-H_2DCFDA assay the cells were plated onto 24 well plates with a seeding density of 0.13 million/ml and cultured until the indicated time.

Upon reaction with ROS Dihydroethdium is oxidised to ethidium and intercalates with the cell's DNA fluorescing red. In the DHE assay, a top stock solution of 31mM was made. This was diluted to a 100μM working solution with serum free Chee's medium and 500μl of this working solution was added directly onto each well after washing once in HBSS. The cells were placed back into the incubator for 4 hours, after which they were removed washed 3 times in Hank's balanced salt solution (HBSS) and read on the fluorimeter at 480nm and 567nm. The control was DMSO alone added at the same concentration as DHE. The amount of fluorescence was normalised to the amount of protein.

Results for both assays were corrected for the amount of protein in each well. To this aim, after the fluorescence reading, the cells were freeze-thawed and 100μl of lysis buffer (1.5M Tris-HCL pH 7.5 and 0.1% SDS) heated to 100°C was added. The samples were scraped using a cell scraper and placed immediately on ice. Once lysed, the Lowry protein assay was done to quantify the amount of protein.

2.7 Preparation of mouse embryonic fibroblasts (MEFS)

The mother was culled by cervical dislocation on day 13.5 of pregnancy. The intestines were moved to one side and the womb containing the embryos was exposed. The womb was removed by cutting at either end, placed in a Petri dish containing PBS and opened. The embryos were removed from the womb with a forceps with each one placed separately into a Petri dish. There was approximately 6 embryos per animal. The yolk sac was removed and the embryo was culled by decapitation. The heart and liver could clearly be identified and were removed. The remaining tissue was chopped up using a scalpel and transferred to a 30ml tube containing 2.5% trypsin (DIFCO) in 5mls. The universal was placed at 37°C for 30minutes on a roller. Once digestion was completed, the universal was filled with Glasgow MEM medium and spun at 266g for 5 minutes. The digest was transferred to a Petri dish containing Glasgow MEM medium supplemented with 1.0mM sodium pryuvate, 0.1mM non-essential amino acids and 5% fetal calf serum final concentration. The cells were allowed to settle, fed and left until confluent in Glasgow MEM medium.

Chapter 3:

A mechanism for transient p53 stabilisation in *Rb-/-* hepatocytes.

3.1 Introduction

Previous work in the group had shown Rb loss leads to a transient p53 stabilisation in primary hepatocytes[276]. The hypothesis was that upon *Rb* loss $p19^{ARF}$ stabilises p53. The aim of this chapter was investigate this hypothesis to determine the mechanism leading to this transient p53 stabilisation in primary hepatocytes.

The transcription factor p53 was discovered in 1979, since then there has been an explosion of work on this tumour suppressor[277]. The role of p53 in the cell is to form the core of a signalling network. Upstream of p53 the damage is sensed and conduction of the signal to p53 is normally in the form of post-translational modifications. This enables p53 to provide a rapid response to a DNA damaging event. These post-translational modifications stabilise p53, an extremely labile protein, and switch on its function as a transcription factor. Regulation of p53 is the primary function of MDM2, which is itself an oncogene[168]. In order for p53 to be stabilised and activated the union between MDM2 and p53 needs to be disrupted (as discussed in section 1.1.1). Dependent on degree of insult, p53 switches on either DNA repair or apoptosis, which pathway is selected is normally determined through post-translational modifications (See section 1.6.2)

$p19^{ARF}$ forms a link between the RB and p53 pathways as $p19^{ARF}$ stabilises p53 and $p19^{ARF}$ transcription is induced by $E2F^{222}$. The exact mechanism of how $p19^{ARF}$ stabilises p53 is not fully defined it is thought that $p19^{ARF}$ sequesters MDM2 in the

nucleolus leaving p53 to act in the nucleoplasm[229, 278, 279]. $p19^{ARF}$ is normally switched on in response to hyperproliferation and not a DNA damaging event. Normally $p19^{ARF}$ resides in the nucleolus but there are reports of it functioning in the nucleoplasm[230].

A $p19^{ARF}$ binding partner in the nucleolus is the NPM. NPM is a multifunctional nucleolar phosphoprotein, existing as a hexamer[280, 281]. It has roles in ribosome biogenesis, centrosome duplication, is a molecular chaperone and is also a marker of cellular proliferation[280]. NPM is found on chromosome 5 and NPM loss is embryonic lethal on day 9.5[282]. The NPM gene shows haploinsufficiency as MEFS derived from $NPM^{+/-}$ mice were immortalised after a number of passages and had an increase in aneuploidy. It is found mutated in 35% of acute myeloid leukaemias and the mRNA is increased to over 50 times its normal level in liver cancer. Interaction between NPM and $p19^{ARF}$ inhibits the ability of $p19^{ARF}$ to retard rRNA processing, which may be one way in which NPM would promotes cells to re-enter the cell cycle [226]. This interaction also extends the half-life of $p19^{ARF}$ [231]. Also NPM has been reported to set the threshold for the p53 response to UV linking it to both p53 and $p19^{ARF}$[234].

RB negatively regulates the transcription factor E2F. An increase in E2F activity is observed upon loss of Rb[283]. If this active E2F switched on transcription of $p19^{ARF}$, $p19^{ARF}$ could sequester MDM2 in the nucleolus with the resulting observed stabilisation of p53.

3.2 Results

3.2.1 A transient stabilisation of p53 following deletion of Rb by cre recombinase

Previous work in the lab showed in *Rb-/-* hepatocytes there is a transient stabilisation of p53[283]. To confirm these results the level of p53 expression in *Rb-/-* hepatocytes was evaluated using immunofluoresence (Figure 3.2.1). The stabilisation of p53 begins at 48 hours post-plating, peaks at 72 hours and decreases again at 96 hours in *Rb-/-* compared to WT hepatocytes, which show a basal level of p53 at all timepoints tested as observed in Sheahan et al[283]. In addition it reveals the localisation of p53, p53 is both a nuclear and cytoplasmic protein(Figure 3.2.1). At 48 and 72 hours post-plating p53 (Red) is found in the nucleus (Blue). However at 96 hours p53 was found in the nucleolus.

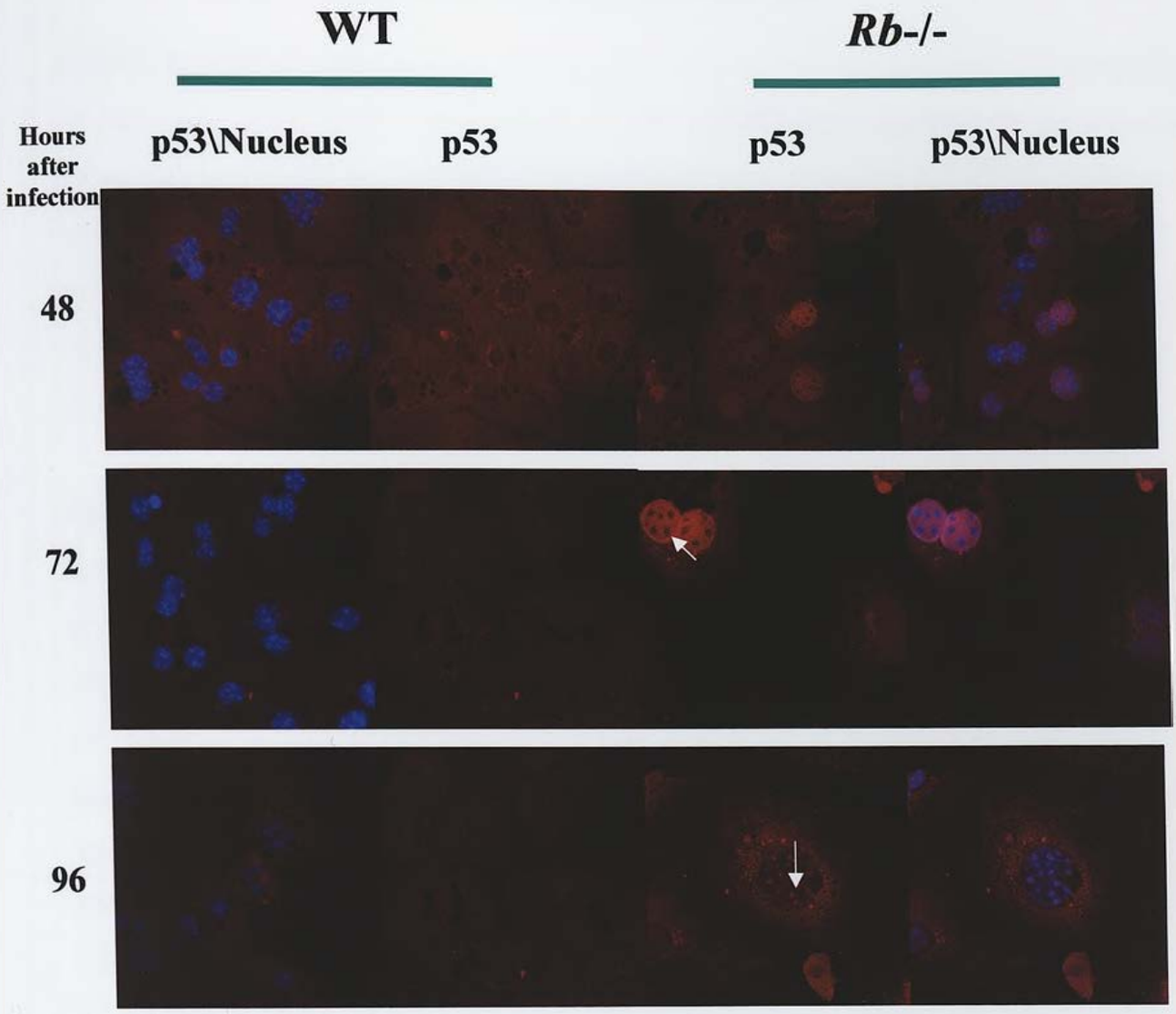


Figure 3.2.1: Increase in p53 expression in *Rb-/-* hepatocytes.

Immunofluoresence showing p53 (Red) expression and localisation in WT and *Rb-/-* cells at 48, 72 and 96 hours post-plating after infection with adenovirus control (WT) or adenovirus cre (*Rb-/-*). The mouse monoclonal antibody PAB421 (1:100) against p53 followed by a goat anti-mouse 542-fluor conjugated (1:200) secondary antibody was used. The nucleus (Blue) was stained with TO-PRO3. The arrows indicate p53 positivity at 72 hours in the nucleus and 96 hours in the nucleolus. The images were captured using a Zeiss Axiovert confocal microscope. The experiment was repeated three times with consistent results.

3.2.2 MDM2 expression and localisation in WT and *Rb-/-* hepatocytes.

MDM2 is crucial in the maintenance of p53 levels as it is the negative regulator of p53. Therefore to unravel the mechanism of p53 stabilisation, analysis of the expression levels and localisation of MDM2 were required. Many isoforms of MDM2 are known to exist and in the hepatocytes three isoforms of MDM2 were investigated, p90, p76 and p57. Two monoclonal antibodies available in the laboratory were used; clone 2A10 (Ab-2) binds to p90, p76 and p57 in hepatocytes while clone 4B11 (Ab-3) binds only to p57 in hepatocytes (Figure 3.2.3).

Clone 2A10 showed differences in the expression levels of p90 and p76 isoforms between WT and *Rb-/-*hepatocytes. The expression of the MDM2 isoform; p90 peaked at 72 hours this is the same timepoint as p53 expression peaks suggesting it was not the p90 isoform of MDM2 that is regulating p53. The p76 isoform reported not to bind to p53 however a peak in expression was observed at 72 hours and it could be acting as a dominant negative to stabilise $p53^{284}$ (Figure 3.2.4A). Clone 4B11, showed the levels of the p57 isoform of MDM2 increasing at 48 hours in *Rb-/-* cells, decreasing at 72 hours in *Rb-/-*compared to WT and increasing again at 96 hours in *Rb-/-* cells compared to WT Clone 2A10 showed the expression of the p57 isoform to increase with time (Figure 3.2.3A and 3.2.4A). This is contrary to the pattern of p53 expression, which peaks at 72 hours and decreases at 96 hours (Figure 3.2.1A). Previous reports have shown $p19^{ARF}$ binding to MDM2 in the nucleolus. This segregates MDM2 from p53 preventing MDM2 targeting p53 for degradation. The localisation of MDM2 is an indicator of whether $p19^{ARF}$ is binding to MDM2. Immunofluorescence using clone 2A10 showed MDM2 localising into the nucleolus (Figure 3.2.5). In *Rb-/-* hepatocytes at 48 hours, MDM2 was in the cytoplasm moving to the nucleolus at 72 hours and remaining there at 96 hours. However at 120 hours MDM2 was no longer found in the nucleolus. In WT hepatocytes it remained in the cytoplasm at all timepoints tested.

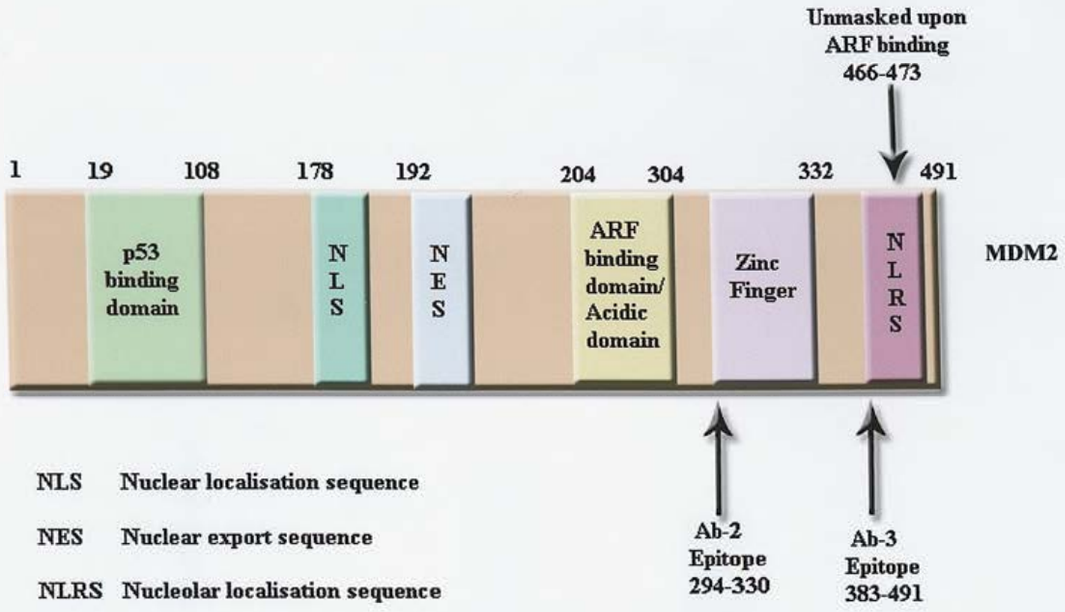


Figure 3.2.2: Structure of MDM2 protein

MDM2 protein structure and the regions in MDM2 where antibodies clone 2A10 (Ab-2) and clone 4B11 (Ab-3) bind.

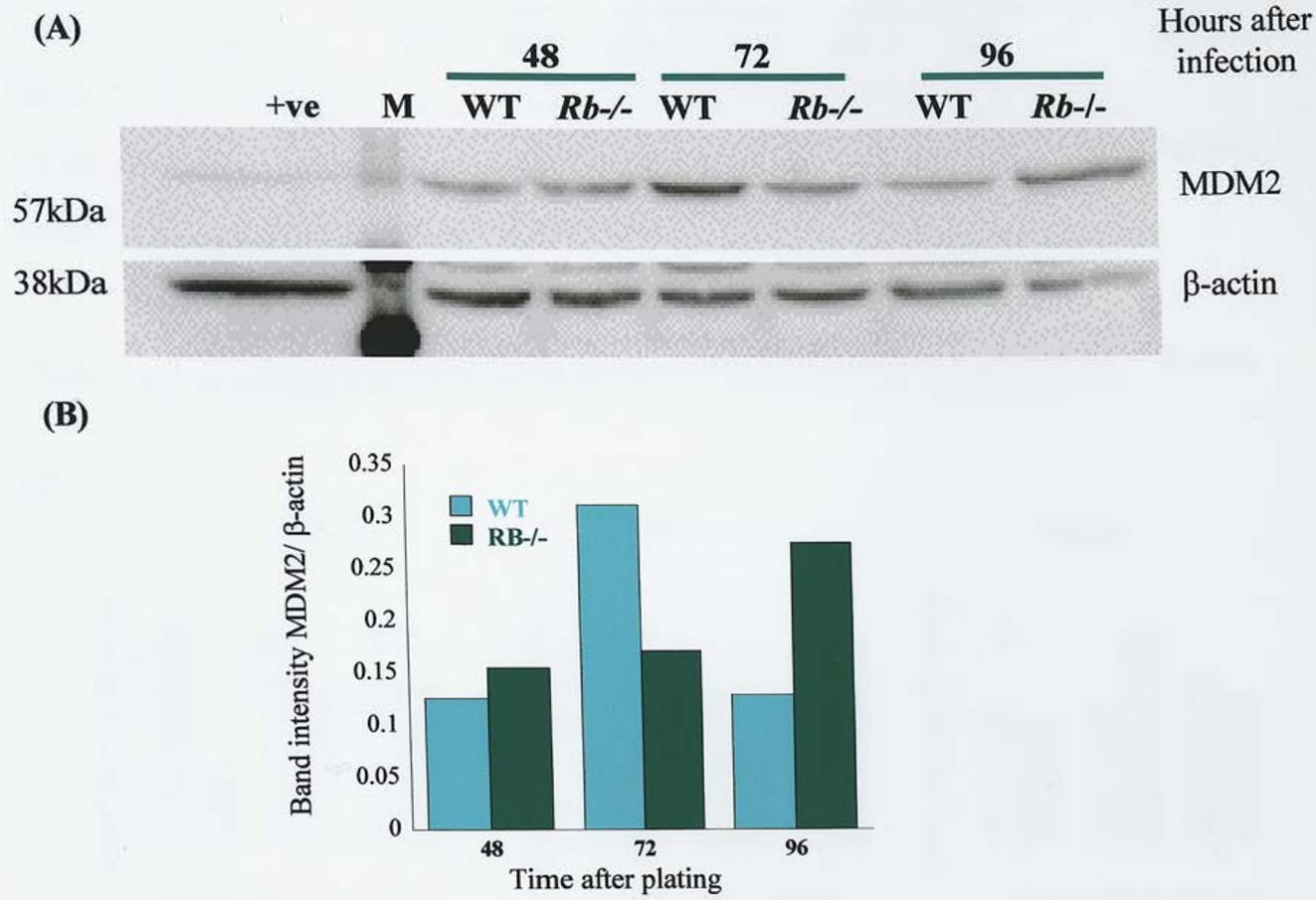
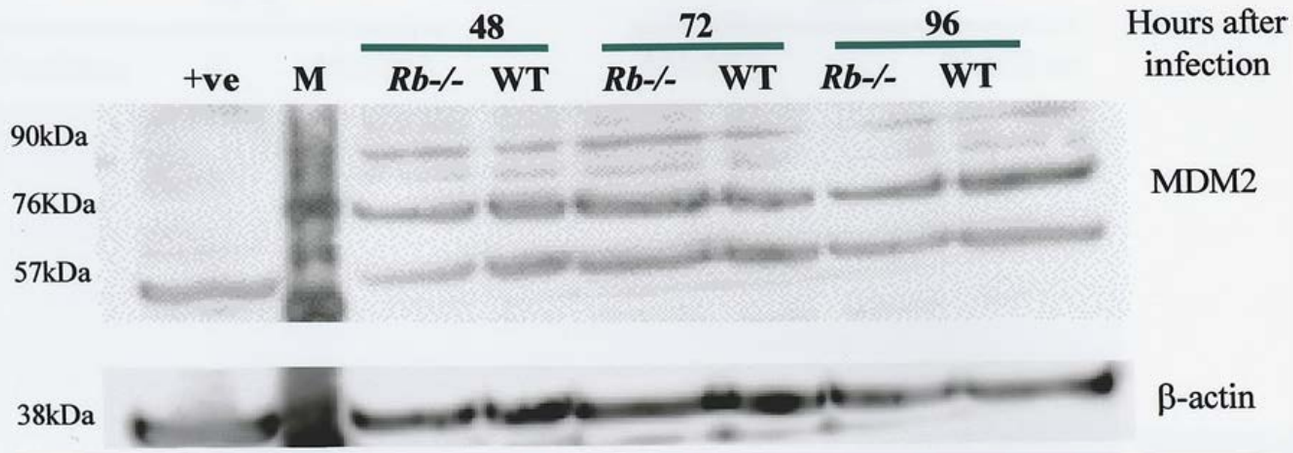


Figure 3.2.3: MDM2 isoform p57 expression in WT and Rb-/- hepatocytes

(A) Immunoblot showing the expression of the p57 isoform of MDM2 at 48, 72 and 96 hours post-plating in WT and *Rb-/-* hepatocytes. 50μg of total cell lysate was run on a 10% SDS gel with A549 cells used as a positive control. The gel was transferred to a PVDF membrane, which was probed with a mouse monoclonal 4B11 (1:1,000) (Calbiochem Ab-3) against MDM2 and a Goat anti-mouse HRP linked (1:2,000) (Dako) secondary antibody. β-actin was used as the loading control. M represents molecular weight markers. (B) A graph illustrating analysis of p57 isoform of MDM2 bands normalised to β-actin done using the quantity one™ (Bio-rad) software. The experiment was repeated three times with consistent results.

(A)



(B)

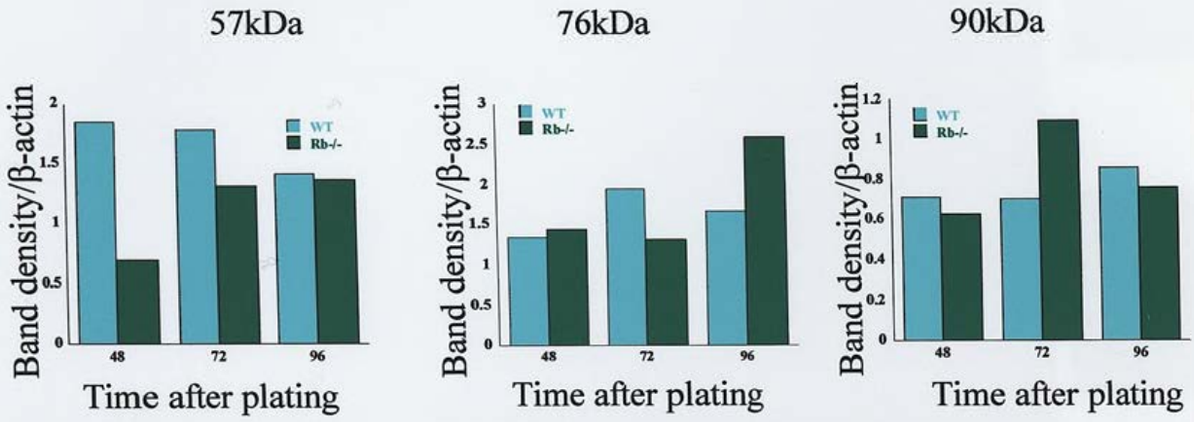


Figure 3.2.4: Expression of isoforms of MDM2 in *Rb-/-* and WT hepatocytes.

Western blotting, , showing the expression of p90, p76 and p57 isoforms in WT and *Rb-/-* hepatocytes at 48, 72 and 96 hours post-plating. 50µg of total cell lysate was loaded per lane on a 10% SDS gel, A549 cells were used as the positive control and transferred to a PVDF membrane. Using the mouse monoclonal 2A10 (1:1,000) the membrane was probed followed by goat anti-mouse HRP conjugated secondary (1:2000). β-actin was used as the loading control with M representing molecular weight markers (B) Graphs showing the densitometry of p57, p76 and the p90 isoform of MDM2 normalised to β-actin done using the quantity one™ (Bio-rad) software.. This was repeated three times with consistent results.

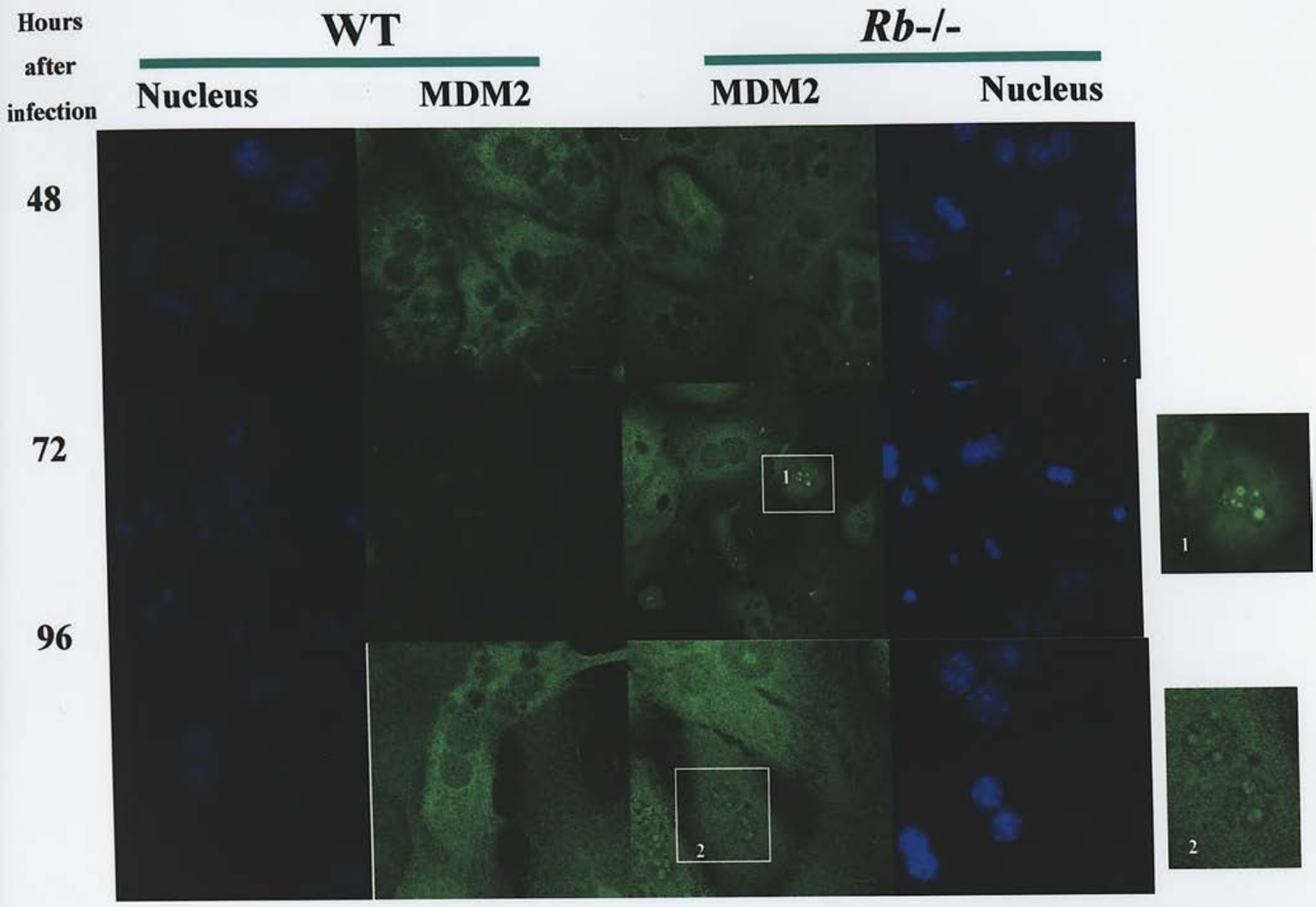


Figure 3.2.5: MDM2 localises into the nucleolus in Rb-/-hepatocytes.

Immunofluorescence showing MDM2 (green) localisation at 48, 72 and 96 hours post-plating in WT and *Rb-/-* hepatocytes. The mouse monoclonal clone 2A10 antibody (1/50) against MDM2 followed by a goat anti-mouse 488 fluor conjugated secondary antibody (1:200) was used. The nucleus was stained with To-PRO3 (blue). The numbered boxes indicate the areas enlarged. Images were captured using a Zeiss Axiovert confocal microscope. The experiment was repeated with consistent results.

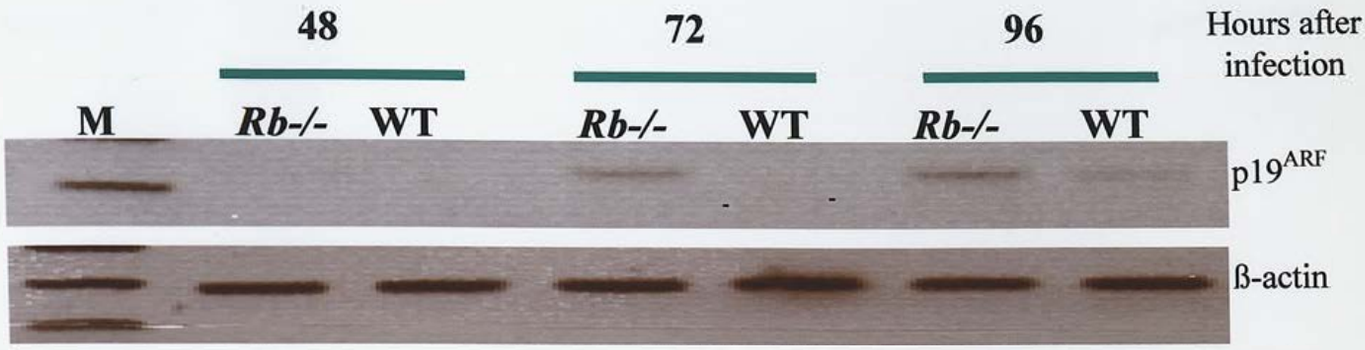
3.2.3 $p19^{ARF}$ is overexpressed in *Rb-/-* hepatocytes compared to WT

Previous reports show that E2F1 activity increases with *Rb* removal [283]. MDM2 localisation in the nucleolus combined with $p19^{ARF}$ being a known E2F responsive gene determined the next stage was to examine $p19^{ARF}$ expression. $p19^{ARF}$ RNA levels were analysed using reverse transcription PCR (RTPCR) and real-time RTPCR. RTPCR shows negligible $p19^{ARF}$ expression in WT hepatocytes whereas *Rb-/-*hepatocytes show $p19^{ARF}$ expression at 48 hours, increasing up to 72 hours with a slight decrease seen at 96 hours (Figure 3.2.6A). Real-time RTPCR was used to quantify these results showing that $p19^{ARF}$ expression in *Rb-/-* hepatocytes is up to 8-12 times higher than in WT at all timepoints tested (Figure 3.2.6 B and C).

$p19^{ARF}$ protein expression was analysed by western blotting and immunofluorescence. The results consolidate the $p19^{ARF}$ RNA data, in *Rb-/-* hepatocytes, expression of $p19^{ARF}$ was found as early as 30 hours post-plating, by immunofluorescence with western blotting showing $p19^{ARF}$ expression at 48 hours, increasing further at 72 hours and it maintains this increase at 96 hours, where the protein begins to dimerise (Figure 3.2.7A).

$p19^{ARF}$ is a known nucleolar protein and this is considered to be where it functions effectively. Immunofluorescence was done to confirm $p19^{ARF}$ localisation in the nucleolus. (Figure 3.2.8A). In *Rb-/-* hepatocytes $p19^{ARF}$ localises exclusively in the nucleolus at all timepoints tested (Figure 3.2.8A). $p19^{ARF}$ was not expressed in WT hepatocytes at any timepoint. Also immunofluorescence was done to a specific nucleolus marker nucleolin to ensure that the area of the hepatocyte $p19^{ARF}$ resides is the nucleolus (Figure 3.2.8A). The expression of $p19^{ARF}$ was roughly quantified by manual counting of immunofluorescence with over 80% of the cells positive at 48 hours, 72 and 96 hours (Figure 3.2.7B). Interestingly the levels of $p19^{ARF}$ did not decrease after 96 hours in conjunction with the levels of p53.

(A)



(B)

Real-Time PCR results

Time	*Rb-/-*	WT	Ratio
48 Hours	0.08	0.01	7.8
72 Hours	0.139	0.011	12.5
96 Hours	0.214	0.023	9.2

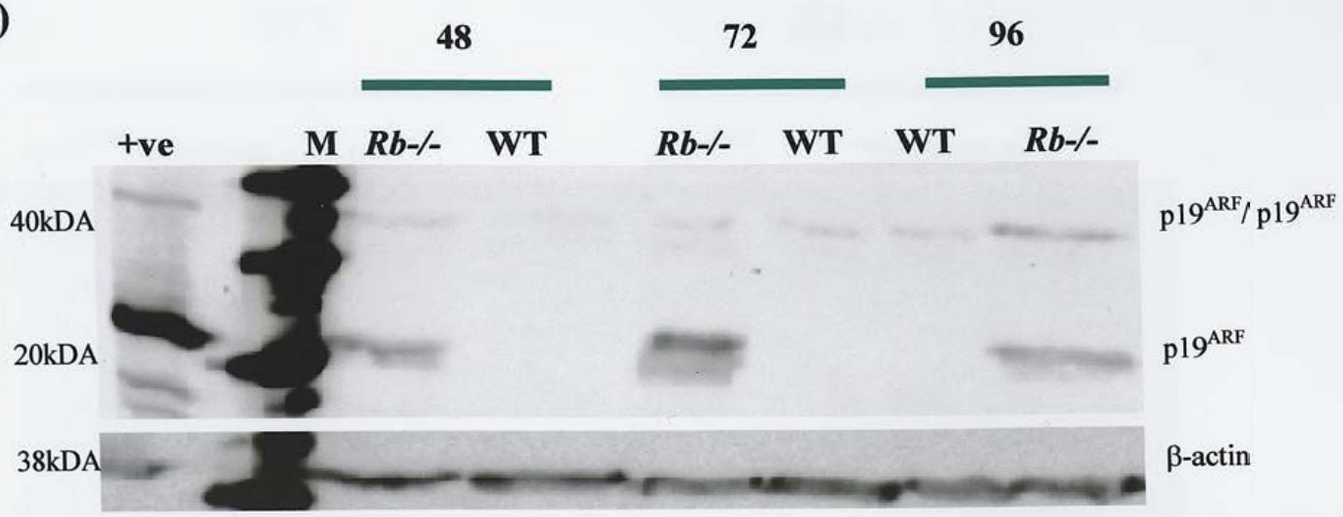
(C)



Figure 3.2.6: $p19^{ARF}$ mRNA is expressed in *Rb-/-* hepatocytes.

(A) Reverse transcription PCR showing $p19^{ARF}$ mRNA expression in WT and *Rb-/-* hepatocytes using $p19^{ARF}$ specific primers at 48, 72 and 96 hours post-plating. β-actin was used as a loading control. M represents molecular weight markers. (B) Real-time PCR measurement of $p19^{ARF}$ mRNA in WT and *Rb-/-* hepatocytes using the taqman method. The table shows the ratio of $p19^{ARF}$ mRNA expression in *Rb-/-* hepatocytes compared to WT after normalising to TATA-binding protein and GAPDH, which were used as the housekeeping genes (See materials and methods section 2.4.3). (C) This graph shows the average ratio of $p19^{ARF}$ mRNA expression in *Rb-/-* hepatocytes compared to WT from two different real-time PCR reactions at the same times as in (A) and (B). These experiments were repeated with consistent results.

(A)



(B)

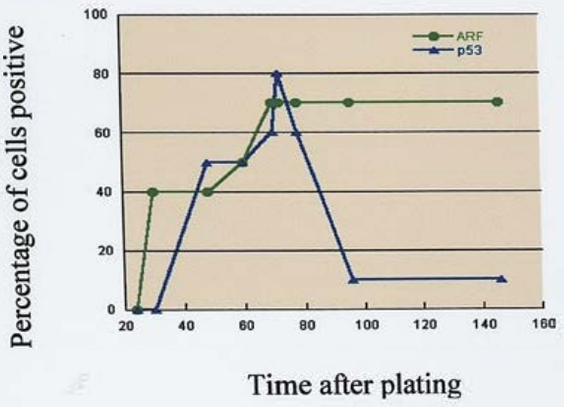


Figure 3.2.7: p19^{ARF} protein is expressed in Rb-/- hepatocytes

Immunoblot showing p19^{ARF} expression in WT and *Rb-/-* hepatocytes at 48, 72 and 96 hours post plating. 200μg of total cell lysate was loaded per lane with mouse embryonic fibroblasts (MEFS) used as the positive control. A 12% SDS gel was run, transferred to a PVDF membrane and probed with a rabbit polyclonal to p19^{ARF} (1:1000) (Abcam), followed by a donkey anti-rabbit HRP conjugated secondary (1:2000) (Amersham). The loading control used was β-actin. M represents molecular weight markers. (B) Quantification of p19^{ARF} and p53 positive cells in WT and *Rb-/-* hepatocytes from from 24 through to 120 hours. Positive cells were counted from immunofluorescence slides after staining for p53 with the mouse monoclonal Pab421 (1:100) and the same rabbit polyclonal against p19^{ARF} used in (A). The experiments were repeated with consistent results.

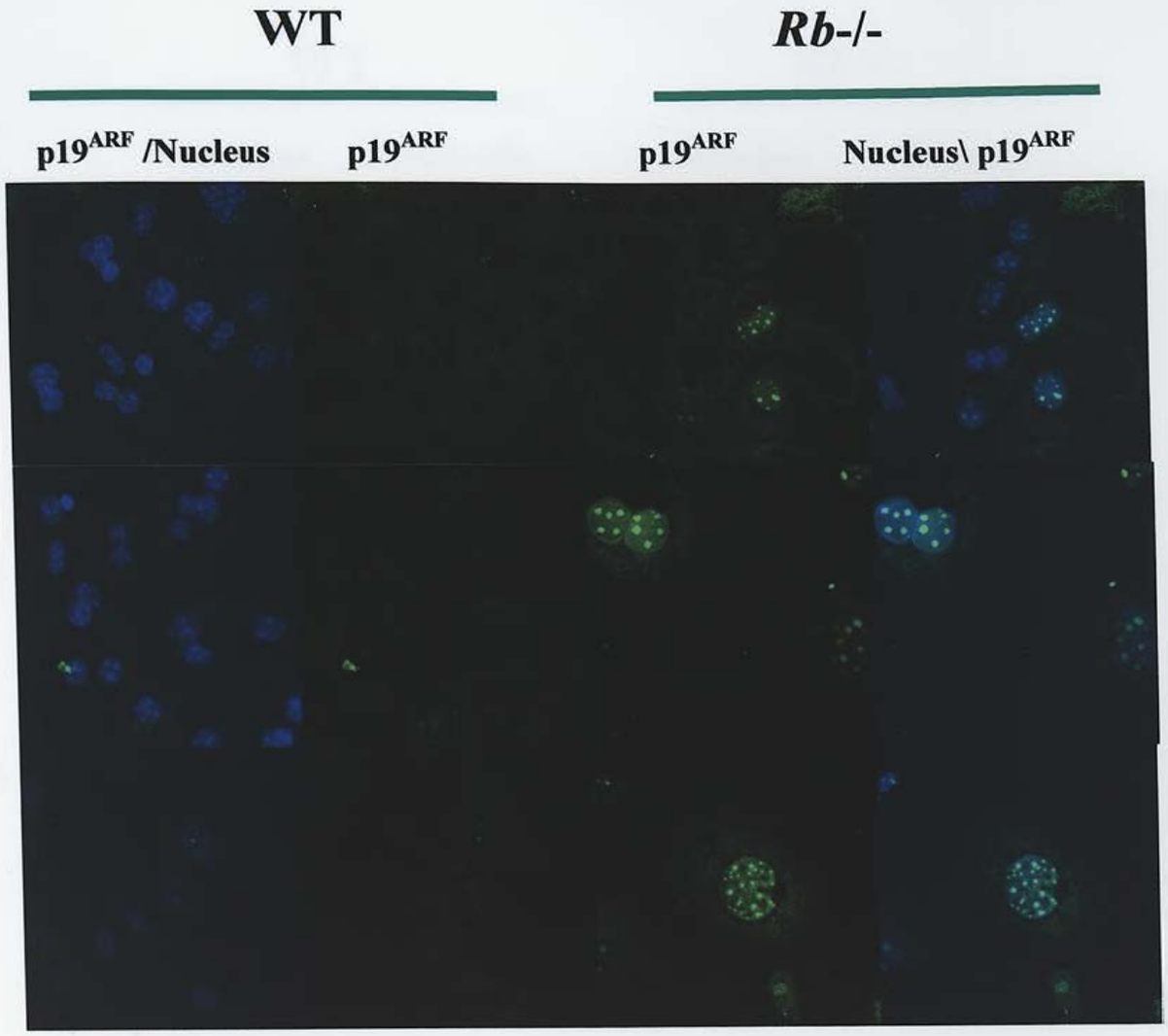


Figure 3.2.8: $p19^{ARF}$ localises in the nucleolus in *Rb-/-* hepatocytes.

Immunofluorescence to show localisation of $p19^{ARF}$ in WT and *Rb-/-* hepatocytes nucleolus at 48, 72 and 96 hours post-plating. Staining for $p19^{ARF}$ (Green) was done with a rabbit polyclonal (1:20) followed by a swine anti-rabbit biotinylated (1:400) and strepavidin 488-fluor conjugated (1:200) antibodies. TO-PRO3 was used to label the nucleus (Blue). Images were captured using a Zeiss Axiovert confocal microscope. The experiment was repeated three times with consistent results.

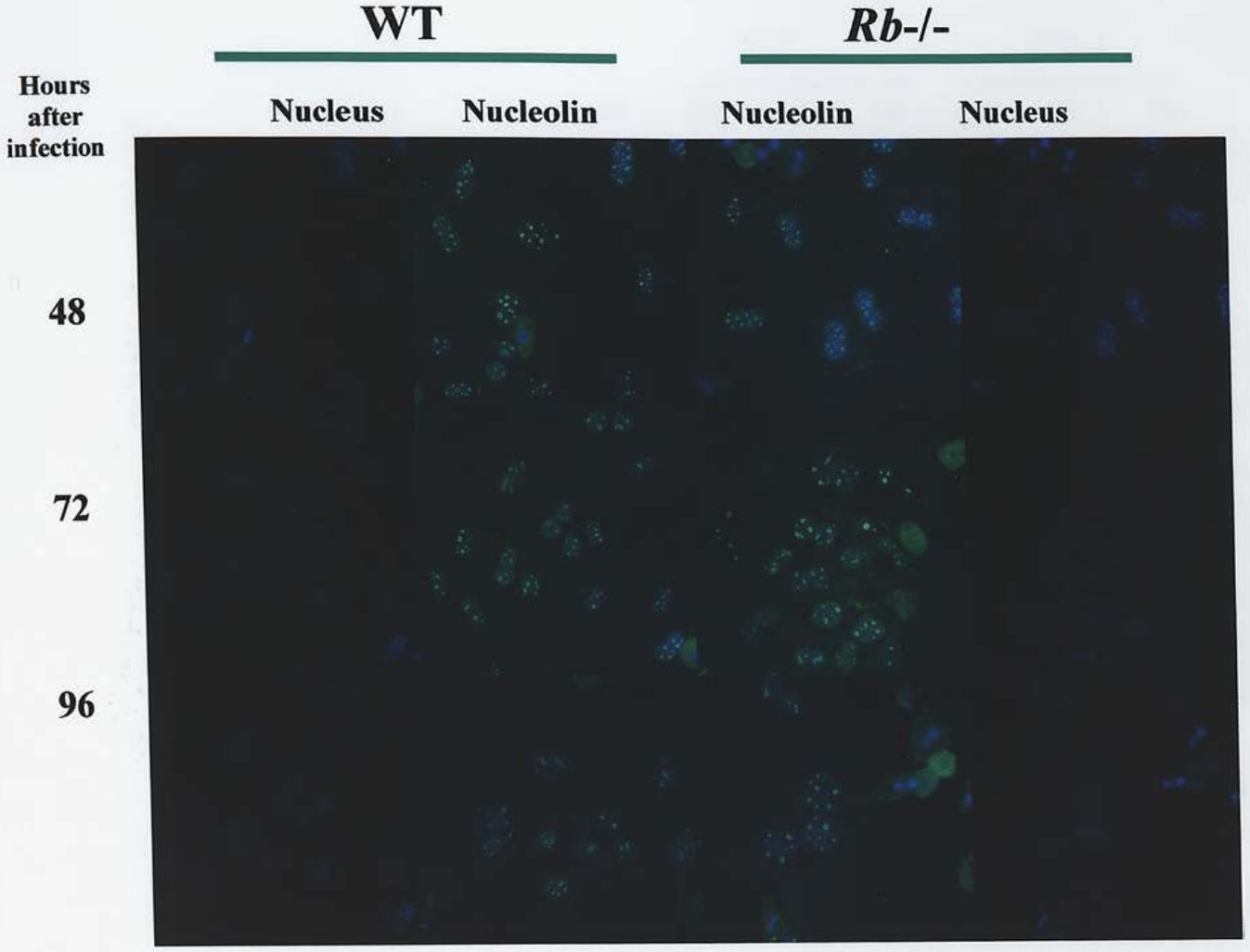
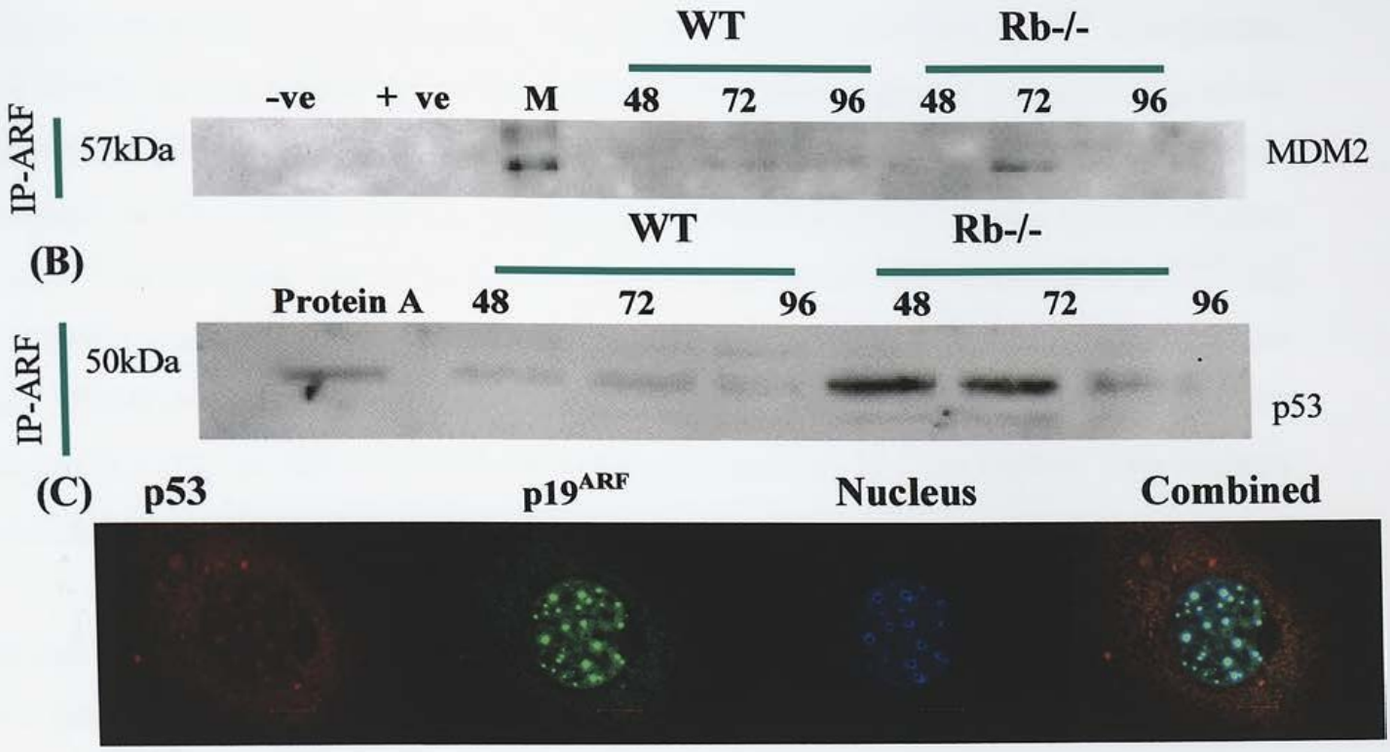


Figure 3.2.9: Identification of the nucleolus using nucleolin, a nucleolus specific marker.

Immunofluorescence to identify the nucleolus, using the specific marker; nucleolin (Green). The primary used was a rabbit polyclonal to nucleolin (1:100) followed by a goat anti-rabbit 488-fluor conjugated (1:200) (Molecular probes) secondary antibody. The nucleus (Blue) was labelled with TO-PRO3. Images were captured using a Zeiss Axiovert confocal microscope. The experiment was repeated three times with consistent results.



Time post-plating	% p53 with $p19^{ARF}$	% $p19^{ARF}$ with p53
99 hours	25	90

Figure 3.2.10: $p19^{ARF}$, MDM2 and p53 binding in WT and *Rb-/-* cells

(A) Immunoblot that shows binding between MDM2 and $p19^{ARF}$. In both WT and Rb- hepatocytes a rabbit polyclonal to $p19^{ARF}$ was used for immunoprecipitation. The precipitates were immunoblotted for MDM2 using clone 2A10 at 48, 72 and 96 hours post-plating. The negative control was protein A incubated with cell lysate without antibody and the positive control was MEFs. (B) $p19^{ARF}$ was immunoprecipitated from WT and *Rb-/-* hepatocytes as in (A) and immunoblotted for p53 using the rabbit polyclonal CM5, the negative control was the same as in A. (C) Immunofluorescence for both p53 (Red) and $p19^{ARF}$ (Green) using the clone PAB421 for p53 and a rabbit polyclonal to $p19^{ARF}$. To-pro 3 was used to stain the nucleus (Blue). Heugans deconvolution software was used to calculate the % of $p19^{ARF}$ binding to p53 at 99 hours post-plating

3.2.4 Interactions of $p19^{ARF}$, MDM2 and p53

The previous results illustrate in *Rb-/-* hepatocytes, p53 is stabilised, $p19^{ARF}$ is expressed and MDM2 is found localised to the nucleoli. To obtain a greater understanding of the mechanism of p53 stabilisation, the interactions between $p19^{ARF}$, p53 and MDM2 were analysed. In *Rb-/-* hepatocytes, immunoprecipitation for $p19^{ARF}$ shows MDM2 binding to $p19^{ARF}$ at 72 hours. This was the only timepoint at which MDM2 bound to $p19^{ARF}$ and no binding was observed in WT hepatocytes. This consolidates the immunofluorescence data MDM2 is present in the nucleolus (Figure 3.2.5) and binding to $p19^{ARF}$ at 72 hours (Figure 3.2.10), the time at which the stabilised levels of p53 are highest. This strongly implies that $p19^{ARF}$ binding to MDM2 leads to p53 stabilisation.

However, in *Rb-/-* hepatocytes p53 binding to $p19^{ARF}$ was observed at 48 and 72 hours, but not at 96 hours (Figure 3.2.10B), this was not seen at any timepoint in the WT hepatocytes. The binding of p53 to $p19^{ARF}$ at the early timepoints combined with the colocalisation of 25% of p53 with $p19^{ARF}$ and 90% of $p19^{ARF}$ with p53 (Figure 3.2.10C), implies that $p19^{ARF}$ binding to p53 may be targeting it to the nucleolus

3.2.5 Nucleophosmin expression in WT and *Rb-/-* hepatocytes

The high level of $p19^{ARF}$ expression, together with expression and localisation of MDM2 explain the peak of p53 at 72 hours. Thus, the levels of p53 should remain high alongside $p19^{ARF}$ levels, although in *Rb-/-* hepatocytes this is not the case. The levels of p53 (Figure 3.2.1A) decrease at 96 hours, but $p19^{ARF}$ remains consistently high, (Figure 3.2.7A). The reason for this was investigated. A protein previously identified to compete with binding of MDM2 to $p19^{ARF}$ is nucleophosmin (NPM)[285] NPM is a nucleolar phosphoprotein and a marker of cellular proliferation, which can induce dimerisation of proteins.

In *Rb-/-*hepatocytes the levels of NPM increase from 48 hours post-plating through to 96 hours where they peak, WT cells show a similar pattern. However at both 72 and 96 hours there is an increase in expression of NPM in *Rb-/-* hepatocytes compared to WT hepatocytes (Figure 3.2.11). To determine if NPM was competing with MDM2 for binding to $p19^{ARF}$ co-immunoprecipitation was done, in *Rb-/-* hepatocytes $p19^{ARF}$ binds to NPM at 72 hours increasing further at 96 hours, no binding above background was observed in WT hepatocytes at any timepoint (Figure 3.2.12A).

There has been a report of the human form of $p19^{ARF}$, p14 forming a dimer in response to reactive oxygen species. It showed MDM2 having less affinity for the dimer form over the monomer form[286]. The Immunoprecipitation for NPM, together with the probe for $p19^{ARF}$ showed that the dimer form of $p19^{ARF}$ binding to NPM at 96 hours (Figure 3.2.12B), but not any other timepoint. This indicates that either the dimer may be formed as a result of $p19^{ARF}$ binding to NPM or the dimerisation of $p19^{ARF}$ increases the affinity of $p19^{ARF}$ for NPM over that of MDM2.

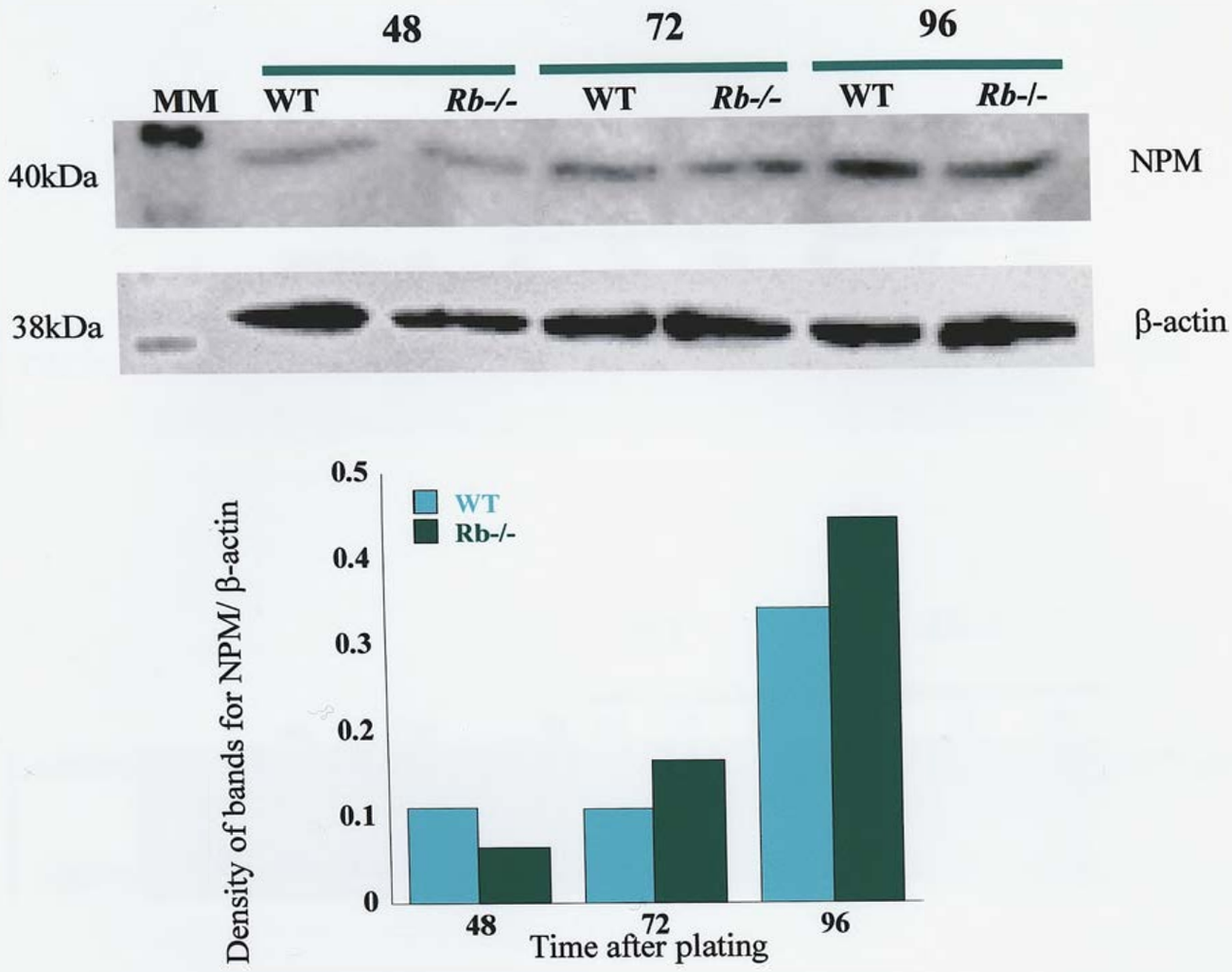


Figure 3.2.11: The expression of NPM in WT and *Rb-/-* hepatocytes

Western blot illustrating NPM expression of in WT and *Rb-/-* hepatocytes. 50μg of protein was loaded per lane, run on a 10% SDS gel and transferred to a PVDF membrane. The membrane was probed with a rabbit polyclonal to NPM (1:1,000) (Abcam) followed by a donkey anti-rabbit HRP conjugated (1:2,000) (Amersham) secondary antibody. β-actin was used as the loading control. The graph shows the results of the anaylsis of the bands demonstrated in the immunoblot shown in this figure by densitometry. Each bar on the graph represents the density of a NPM band divided by the density of an β-actin band. This was repeated three times with three different animals with consistent results. MM represents molecular weight markers.

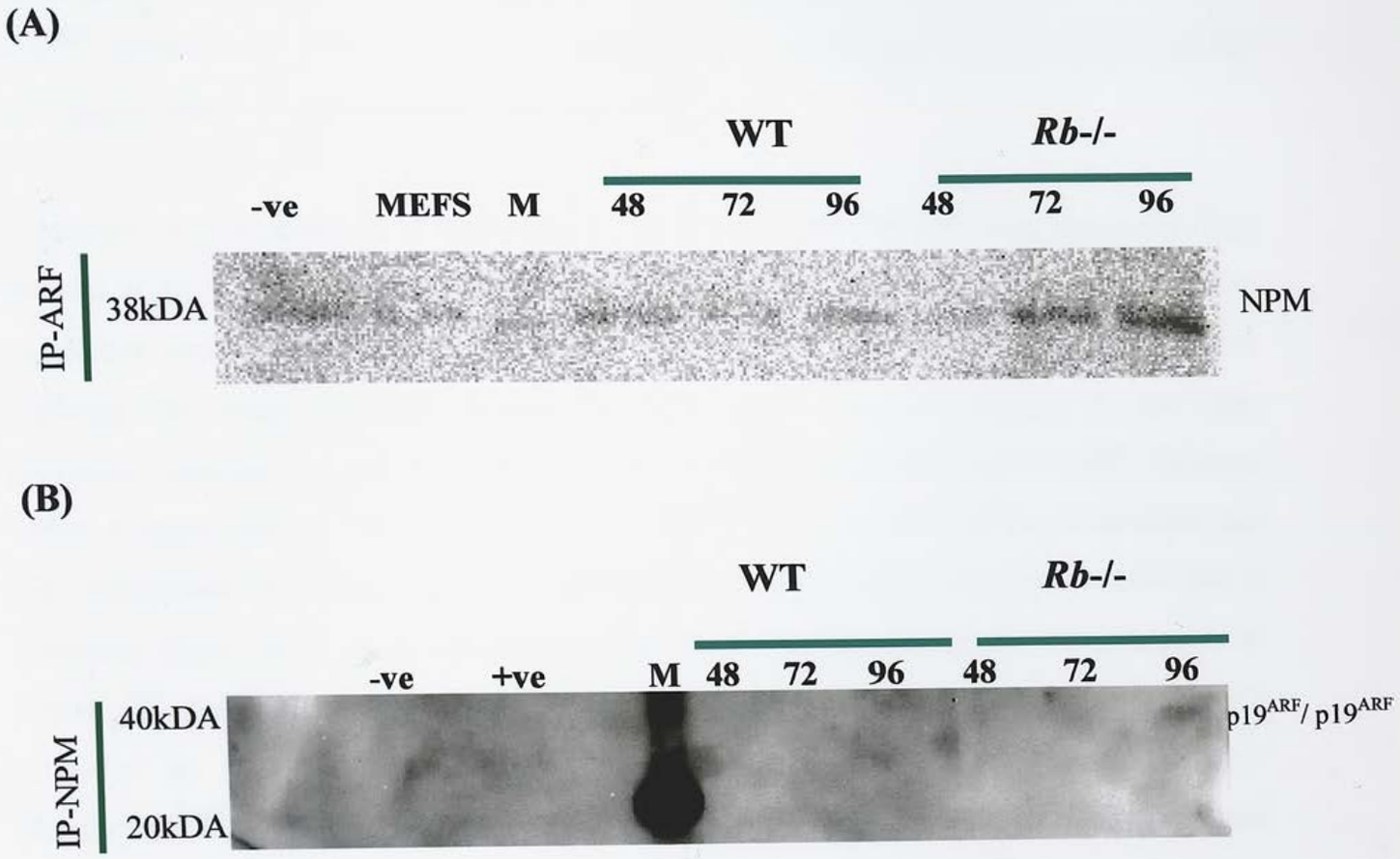


Figure 3.2.12: The binding of NPM and $p19^{ARF}$ in WT and *Rb-/-* hepatocytes

(A) Immunoblot showing the binding of $p19^{ARF}$ to NPM in *Rb-/-*hepatocytes. $p19^{ARF}$ was immunoprecipitated from WT and *Rb-/-* hepatocytes at 48, 72 and 96 hours post-plating and probed with a rabbit polyclonal to NPM. (B) NPM was immunoprecipitated from WT and *Rb-/-*hepatocytes at 48, 72 and 96 hours post-plating and the membrane was probed with a rabbit polyclonal to $p19^{ARF}$. In both (A) and (B) the negative control (-ve) used was beads alone, the positive control used (+ve) was mouse embryonic fibroblasts (MEFS) and M stands for molecular weight markers.

3.3 Discussion

This work expands on a previous finding of the group that there is a transient stabilisation of p53 in *Rb-/-* hepatocytes [283]. The hypothesis was that upon loss of *Rb* $p19^{ARF}$ stabilised p53. The aim of this chapter was to investigate this hypothesis as the mechanism that could be leading to p53 stabilisation.

Expression and localisation of the negative regulator of p53, MDM2 was examined. This showed in *Rb-/-* hepatocytes expression of the p57 isoform of MDM2 is opposite to the expression pattern of p53. This indicates it may be this isoform that is regulating p53. Although the exact domains present in this isoform are not defined it has been previously reported to bind to p53[287]. Cellular location of the different MDM2 isoforms varies, a report showed the p57 isoform of MDM2 to be exclusively in the nucleus and also upregulated in tumour cells [288]. The MDM2 p2 promoter is induced by p53 and is translated eight times more efficiently than the transcripts from the p1 promoter of MDM2 [289]. It has been suggested transcription of the p57 isoform is induced on the p2 promoter by p53 this would match p57 expression patterns observed in *Rb-/-* hepatocytes [288]. Expression of this isoform is not as a result of apoptosis as the isoforms of MDM2 induced by apoptosis are p68 and p28 [290].

In *Rb-/* -hepatocytes MDM2 localises to the nucleolus at 72 and 96 hours post-plating. The presence of MDM2 in the nucleolus, indicated $p19^{ARF}$ was playing a role. $p19^{ARF}$, through sequestering MDM2 obstructs the MDM2 and p53 complex [230]. The region of the cell where this interaction occurs is the subject of debate, some groups have reported it in the nucleoplasm [230] but the majority have reported it to occur in the nucleolus[229, 273]. Thus $p19^{ARF}$ expression was analysed at both mRNA and protein level. $p19^{ARF}$ was expressed in *Rb-/-* hepatocytes with negligible expression found in WT cells. Also localisation of both $p19^{ARF}$ and the nucleolus specific marker nucleolin confirmed

$p19^{ARF}$ was in the nucleolus. As both $p19^{ARF}$ and MDM2 were in the same region of the cell, binding of $p19^{ARF}$ to MDM2 was analysed. It was found at only 72 hours and it was the p57 isoform that bound to $p19^{ARF}$. This coincides with maximal stabilisation of p53, which binding of $p19^{ARF}$ to MDM2 is reported to do[229, 230].

Also $p19^{ARF}$ bound p53 at 48 and 72 hours. No binding was detected at 96 hours but p53 was found in the nucleolus. The binding of $p19^{ARF}$ to p53 may move p53 to the nucleolus. The objective of this could be to bring p53 into close proximity with effectors such as ATR, enabling post-translational modifications on p53 to occur. Binding of $p19^{ARF}$ and p53 along with MDM2 in the nucleolus is known to induce sumoylation of p53, although the outcome of this sumoylation is not known. In certain cases p53 sumoylation is reported to increase its stability[199, 200]. However if p53 was being sumoylated by $p19^{ARF}$ reports show it should be present in the nucleolus and binding to $p19^{ARF}$ at all timepoints tested. At 96 hours $p19^{ARF}$ no longer binds to MDM2 or p53, the levels of p53 decline with the expression of $p19^{ARF}$ remaining constant (Figure 3.3.2)

A known nucleolar protein and binding partner of $p19^{ARF}$ is NPM. In *Rb-/-* hepatocytes examination of NPM expression revealed it to increase with time. This was also observed in the WT cells. At 96 hours post-plating expression of p53 decreases while expression of $p19^{ARF}$ is sustained in *Rb-/-* hepatocytes. NPM binding to $p19^{ARF}$ augments the half-life of $p19^{ARF}$, the mechanism is not fully defined although it is not through preventing the ubiquination [231] . Analysis of NPM and $p19^{ARF}$ binding found it occurring at 72 hours and increasing further at 96 hours. This may explain why the increase in $p19^{ARF}$ is maintained, together with the increase in activity of E2F. Binding was only observed between MDM2 and $p19^{ARF}$ at 72 hours and not 96 hours. This implies $p19^{ARF}$ binding to NPM may prevent binding to MDM2. Both NPM and MDM2 bind to the same region of $p19^{ARF}$ [285] and are reported to compete for binding to $p19^{ARF}$. The dimer form of $p19^{ARF}$ has less affinity for MDM2 [286] and it appears to bind to NPM in *Rb-/-*hepatocytes. This suggests dimerisation of $p19^{ARF}$ could promote NPM binding while expelling MDM2. The observed decrease in p53 at 96 hours is consistent with

these results (Figure 3.3B). NPM promotes S-phase, the binding of NPM to $p19^{ARF}$ would prevent any further stabilisation of p53 allowing the cell to re-enter the cell cycle.

In summary, the evidence presented herein to support the hypothesis that $p19^{ARF}$ is important in regulating p53 in *Rb-/-* hepatocytes is $p19^{ARF}$ is upregulated and at the time of the peak of p53 stabilisation both MDM2 and $p19^{ARF}$ are found in the nucleolus and bind together. In addition, when $p19^{ARF}$ binds NPM there is a decrease in p53 expression. The suggested pathway is *Rb* loss increases E2F1 activity with an outcome of $p19^{ARF}$ upregulation. The $p19^{ARF}$ produced binds to and sequesters MDM2 in the nucleolus alleviating p53 from MDM2 mediated degradation resulting in an upregulation in p53 stabilisation in the nucleus (Figure 3.3A). However at 96 hours post-plating, $p19^{ARF}$ dimerises resulting in $p19^{ARF}$ binding to NPM and MDM2 expulsion from $p19^{ARF}$. This liberated MDM2 targets p53 for degradation resulting in a decrease in p53 levels (Figure 3.3B). In conclusion this evidence presented supports the hypothesis that the upregulation of $p19^{ARF}$ in *Rb-/-* hepatocytes contributes to a transient stabilisation of p53.

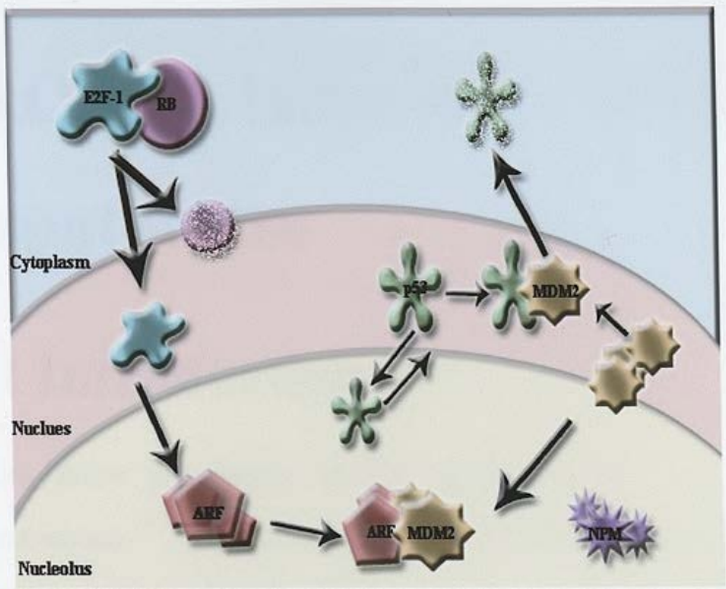


Figure 3.3.A:

Pathway part 1-72 hours

Upon Rb loss, E2F1 is released and enters the nucleus where it turns of $p19^{ARF}$ transcription. $p19^{ARF}$ expression peaks and it binds MDM2. This moves MDM2 from the nucleoplasm to the nucleolus. This prevents MDM2 and p53 binding enabling p53 stabilisation. (For more detail see text).

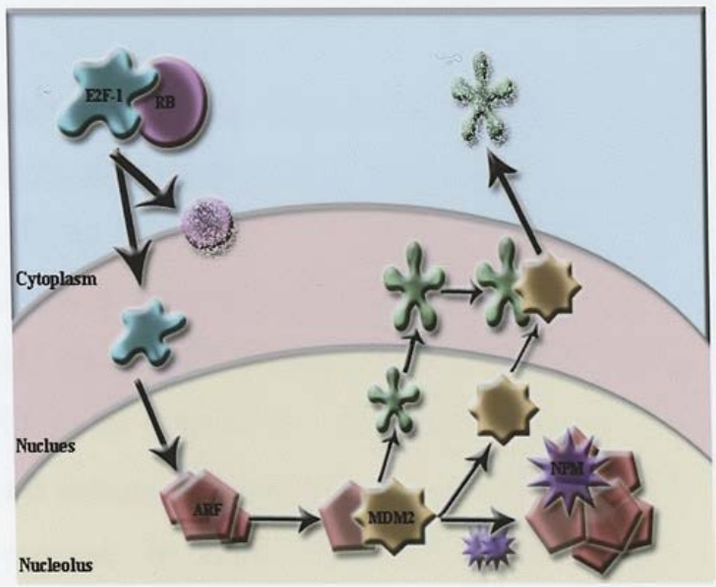


Figure 3.3.B:

Pathway part 2-96 hours

Between 72 and 96 hours $p19^{ARF}$ dimerises. As MDM2 has less affinity for the $p19^{ARF}$ dimers, this allows NPM to bind $p19^{ARF}$. MDM2 is released and binds to p53 targeting it for degradation. (For more detail see text).

Chapter 4:

Rb loss leads to reactive oxygen species (ROS) induced DNA damage in hepatocytes

4.1 Introduction

Work done previously in the group showed an increase in E2F activity in *Rb-/-* hepatocytes [283]. Reports in the literature link an increase in E2F activity to elevated ROS levels and DNA damage [291, 292]. The aim of this chapter was to investigate the hypothesis that *Rb* loss produces an increase in ROS induced DNA damage. Also to establish the pathway creating this increase in ROS induced DNA damage.

As stated previously there is an upregulation of $p19^{ARF}$ in *Rb-/-* hepatocytes (Figure 3.2.6) A p53 independent function of $p19^{ARF}$ is inhibiting the transactivation activity of NF-κB via ATR. $p19^{ARF}$ activates ATR, however the exact mechanism of how $p19^{ARF}$ does this is currently unknown. Activated ATR phosphorylates Checkpoint kinase 1 (Chk1) on ser 317 inducing its activity. This activated Chk1 phosphorylates NF-κB on thr505 in its C-terminus, which downregulates NF-κB's transactivation activity[235]. As NF-κB instigates production of MnSOD, any decrease in NF-κB activity could lead to an increase in ROS [293]. This mechanism for ROS induced DNA damage was investigated.

Reactive oxygen species (ROS) include oxygen ions such as superoxide, free radicals and peroxyls. These are molecules or molecular fragments that contain one or more unpaired electrons, which makes them extremely reactive. Oxidative stress is a

disruption in the balance maintained between production and removal of ROS. Excess ROS generation can cause damage to proteins, lipids and nuclei acids. DNA damage induced by ROS can result in base and sugar lesions, generation of strand breaks, release of bases from DNA and DNA-protein cross links. A set of enzymes whose function is to eliminate superoxide in cells are the superoxide dismutases (SODs). SODs convert superoxide to oxygen and hydrogen peroxide, which is further broken down into water and oxygen by catalases. There are three known SODs, (CuZnSOD) SOD1 in the cytoplasm, MnSOD (SOD2) in the mitochondria and the extracellular, SOD3. Normally superoxide is not reactive towards DNA however if the hydrogen peroxide produced by catalases reacts with Iron according to the Fenton reaction:

$$Fe(II) + H_2O_2 \longrightarrow Fe(III) + {}^{\bullet}OH + OH^{-}$$

the highly reactive hydroxyl radical ($^{\bullet}OH$) will be produced [294, 295].

One of the most frequent mutations in DNA arising from oxidative stress is oxidation of guanine through the addition of a hydroxyl group to the 8th position producing 8-oxo-dG. The modified base, 8-oxo-dG, and adjacent residues are misread as a T residue resulting in increase of G:C to T:A transversions [296]. The DNA glycosylases are enzymes responsible for 8-oxo-dG removal[297, 298]. 8-oxo-dG glycosylases 1 (OGG1) null mice have five times as many 8-oxo-dG sites per 10^6 bases in the liver leading to a 2/3 fold increase in mutation frequency [299, 300].

Another type of oxidative DNA damage is apurinic and apyrimidinic sites (AP sites). AP sites are non-coding lesions that have lost their purine or pyrimidine base. AP sites result from destabilisation of the N-glycosyl linkage that links sugar backbone and base. This can occur via enzyme catalysed hydrolysis, damaging chemicals such as free radicals or spontaneously[301]. Glycosylases during removal of damaged bases in the process of DNA repair form AP sites. Free radical induced modifications to the N-glycosyl linkage generate a better leaving group moiety promoting base release. Under normal physiological conditions approximately 9,000 AP sites are formed in each cell per day

AP sites are mutagenic as they can promote incorporation of non complimentary nucleotides at higher frequencies for example adenine is paired opposite an abasic base and DNA polymerases skip the AP site resulting in nucleotide deletion[302, 303].

DNA is packaged into nucleosomes using the architectural histones proteins. The nucleosome is a subunit of the chromosome and consists of 146bp of DNA wrapped around a histone core. This histone core is an octamer of the four core histones H2A, H2B, H3 and H4 [65]. Variant histones are proteins containing the histone fold but show differences in amino acid sequence at the C and N-terminus. H2A.X is a variant histone and differs from other H2A histones in its longer C-terminus [304]. H2A.X is ubiquitously distributed and is expressed throughout the genome. In normal human fibroblasts it composes 10% of the H2A core. There are approximately $6X10^6$ molecules of H2A.X per cell [305]. The H2A.X C-terminus contains a serine glutamic acid (SQE) motif, which is a consensus site for ATM, ATR and DNA-PK. There is functional redundancy between these kinases for phosphorylation of H2A.X[306]. In response to IR ATM and DNA-PK phosphorylate H2A.X on ser139 (γH2A.X) at sites of double strand breaks (DSBs) [307, 308]. ATR phosphorylates H2A.X in response to replication arrest[309, 310]. The amount of γH2A.X per DSB found in cells corresponds to phosphorylation of H2A.X molecules covering a very large region, 2MBs of chromatin or thousands of nucleosomes. These are known as nuclear foci[305, 311, 312]. H2A.X deficiency in mice leads to chromosomal abnormalities, immune deficiency, increases radiation sensitivity and impaired DNA repair. H2A.X deficient cells show increased IR radiation sensitivity and genomic instability. H2A.X deficient mice show a small increase in thymic lymphoma [313]. However loss of H2A.X and p53 has a synergistic effect the mice develop B and T cell lineage lymphomas and solid tumors[314, 315].

Subsequent to phosphorylation of H2A.X assembly of additional proteins involved in DNA repair and/ or checkpoint activation occurs on γH2A.X foci. The exact function of H2A.X at the site of DSBs is not clear although it may be an anchor holding the two broken chromosomal ends together [316]. At the site of these DSBs γH2A.X can interact

with 53BP1, which binds DNA and also NBS1, which can interact with other repair factors. Immunocytochemistry for γH2A.X has become the gold standard for assessing DSBs as γH2A.X foci represent one double strand break[305, 312].

In summary the pathway proposed is *Rb* loss activates E2F. This increases the levels of $p19^{ARF}$, which through an unknown mechanism activates ATR. This activated ATR via Chk1 induces a decrease in NF-κB activity leading to a decrease in MnSOD. This enables ROS accumulation, which damages the DNA. This increase in damage also leads to phosphorylation of H2A.X and p53 (Figure 4.3.1).

4.2 Results

4.2.1 ATR, the DNA damage response kinase, expression and localisation in hepatocytes

ATM and ATR are two PI3 like kinases known as sensors of DNA damage. ATM responds to changes in chromatin structure. ATR is switched on in response to stalled replication forks and the presence of single stranded DNA (ssDNA)[253]. Both kinases can be switched on simultaneously as many types of damage result in both scenarios. ATR kinase activity does not need to be activated. ATR is segregated from its substrates; movement of ATR to the vicinity of damage determines the activity of the kinase[253]. In an unstressed cell, the binding partner of ATR is ATR interacting protein (ATRIP). ATRIP associates with replication protein A (RPA), which is an ssDNA binding protein. Upon a stress that causes ssDNA production RPA decorates the ssDNA. This facilitates ATRIP binding the ssDNA and brings alongside ATR. This moves ATR to the site of damaged DNA bringing into close proximity with its substrates enabling ATR to phosphorylate them[253].

In *Rb-/-*hepatocytes increases in $p19^{ARF}$ expression were observed with a peak in expression at 72 hours (Figure 3.2.6A). $p19^{ARF}$ is a nucleolar protein and is known to effect ATR activation [235]. Thus ATR expression and localisation were examined

In *Rb-/-* hepatocytes ATR levels fluctuate, expression at 48 hours is low increases at 72 hours where it peaks and at 96 hours the levels fall. In WT hepatocytes ATR expression is maintained at a constant level from 48 to 96 hours. Comparing levels detected in *Rb-/-* to WT hepatocytes, only at 72 hours post-plating is ATR expression in *Rb-/-* hepatocytes above WT. At both 48 and 96 hours post-plating levels in *Rb-/-* are below WT hepatocytes (Figure 4.2.1A).

ATR localisation in *Rb-/-* hepatocytes varies. ATR movement in *Rb-/-* and not in WT hepatocytes indicates it is active. In *Rb-/-*hepatocytes at 48 hours ATR is in the cytoplasm, between 48 and 72 hours ATR moves to the nucleolus. Both at 72 and 96 hours ATR was found in the nucleolus. In WT hepatocytes ATR is found in both the nucleoplasm and cytoplasm but not in the nucleolus (Figure 4.2.1B)

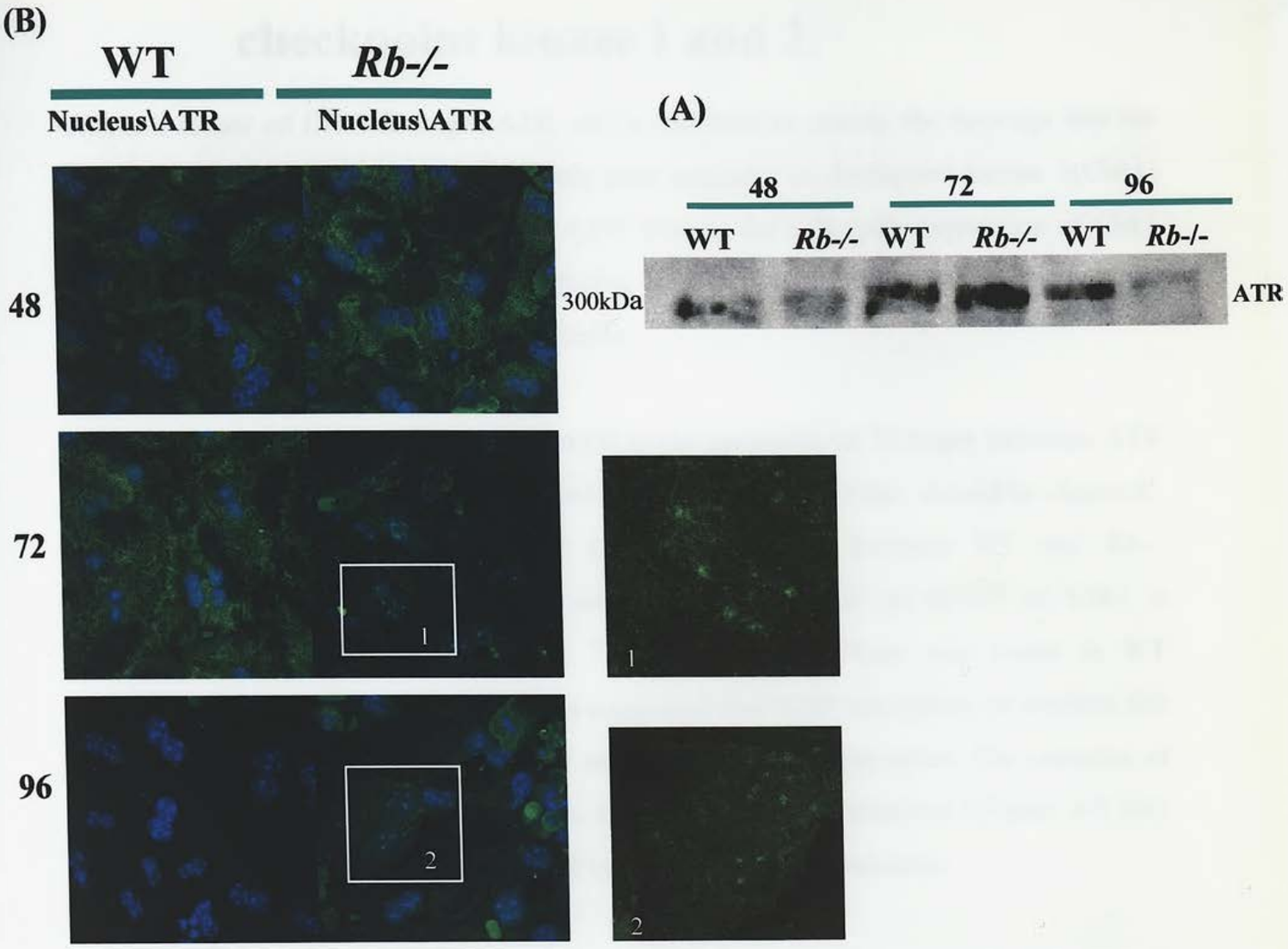


Figure 4.2.1: The expression of ATR in WT and *Rb-/-* hepatocytes

(A) Western blotting showing ATR expression in WT and *Rb-/-* hepatocytes at 48, 72 and 96 hours post-plating. 100μg of protein was loaded per lane, run on a gradient gel (4-20%) and transferred to a PVDF membrane. The membrane was probed with a rabbit polyclonal to ATR (1:10,000) (Abcam) followed by a donkey anti-rabbit HRP conjugated secondary (1:2,000) (Amersham). (B) Immunofluorescence showing ATR (Green) localisation of in WT and *Rb-/-*hepatocytes at 48, 72 and 96 hours post-plating. ATR was detected using the same rabbit polyclonal as in (A) at 1:100 followed by a goat anit-rabbit 488-fluor conjugated secondary (1:200). Nuclei (Blue) were stained with To-PRO 3 dye. The images were captured using a Zeiss axiovert confocal microscope. The experiment was repeated with consistent results.

4.2.2 Expression and phosphorylation of checkpoint kinase 1 and 2.

ATR is a sensor of DNA damage. ATR uses a mediator to convey the message that the DNA is damaged to effector kinases. One such mediator is checkpoint kinase 1(Chk1) and it is the most common substrate of ATR. During the cell cycle expression of Chk1 varies it is expressed in high amounts during S and G_2 phases and very low levels are detected in quiescent and differentiating cells.

In *Rb-/-* hepatocytes, the movement of ATR to the nucleolus at 72 hours indicates ATR is activated (Figure 4.2.1). If it is activated phosphorylation of Chk1 should be observed. No difference in expression of total Chk1 is observed between WT and *Rb-/-* hepatocytes (Figure 4.2.2A). The activating phosphorylation on ser317 of Chk1 is detected only in *Rb-/-* hepatocytes at 72 and 96 hours. None was found in WT hepatocytes at any timepoint tested. This suggested that ATR was active; to confirm this an inhibitor of ATR and ATM caffeine was added to the hepatocytes. The presence of caffeine eliminated phosphorylation on ser317 in *Rb-/-* hepatocytes (Figure 4.2.2A). This substantiates the evidence that ATR is active in *Rb-/-* hepatocytes.

In unstressed cells ATM exists as a homodimer. In response to DNA damage an intermolecular phosphorylation occurs disrupting this dimer, activating ATM function[249, 317]. The predominant mediator kinase of ATM is checkpoint kinase 2 (Chk2). Upon activation Chk2 similar to Chk1 can phosphorylate p53 and induce cell cycle arrest. Chk2 levels in hepatocytes appeared to decrease with time in WT and *Rb-/-* hepatocytes. Chk2 phosphorylation on thr68 was examined and none was detected in WT or *Rb-/-* hepatocytes at any timepoint (data not shown). This indicates ATM pathway may not be active in *Rb-/-* hepatocytes under these conditions.

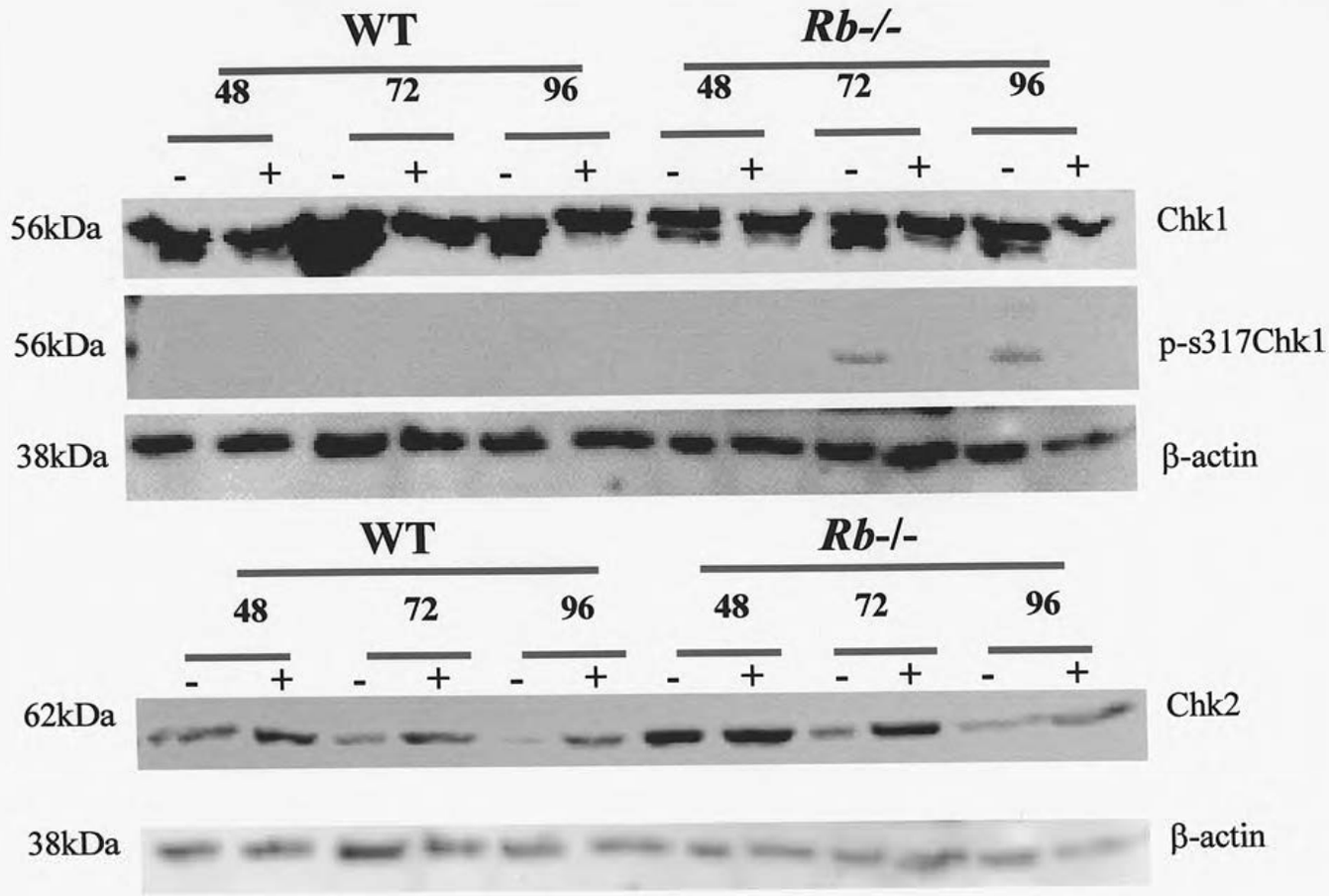


Figure 4.2.2: Expression of Chk1 and Chk2 in WT and *Rb-/-* hepatocytes in the absence and presence of 2mM caffeine

(A) Western blotting showing checkpoint kinase 1 (Chk1) expression in WT and *Rb-/-* hepatocytes in the absence (-) and presence (+) of caffeine at 48, 72 and 96 hours post-plating. In each western blot 100μg of protein was loaded per lane, run on a 10% gel and transferred to PVDF membrane The blots were probed with a rabbit polyclonal against Chk1 (1:1,000) to detect total Chk1 present (Top blot). The second blot was probed with a rabbit polyclonal against phosphorylated Chk1 at serine 317 (1:1,000) and β-actin (lowest blot) was used as the loading control. This was followed with a donkey anti-rabbit HRP conjugated secondary (1:2,000). (B) Immunoblot for total Chk2 protein in the absence (-) and presence (+) of caffeine over the same timepoints as in (A). A rabbit polyclonal to Chk2 (1:1,000) followed by the same secondary as in (A). In each immuno blot 100μg of protein was loaded per lane, run on a 10% gel and transferred to PVDF membrane. The experiment was repeated twice with consistent results

4.2.3 MnSOD expression is decreased in *Rb-/-* hepatocytes.

As both ATR and Chk1 were found activated downstream members of the proposed pathway were investigated. Expression of manganese superoxide dismutase (MnSOD) was examined as NF-kB can induce MnSOD expression[293]. MnSOD reduces superoxide anion produced in mitochondria to hydrogen peroxide and water which is further broken down by catalases. MnSOD expression was detected in WT hepatocytes at both 72 and 96 hours. In *Rb-/-* hepatocytes no MnSOD was observed at 48 and 72 hours. At 96 hours in *Rb-/-* hepatocytes a low level of expression was found (Figure 4.2.3). This is consistent with the results for the superoxide anion (Figure 4.2.5B).

It has been reported in the literature that in response to induction of ROS the human form of ARF, $p14^{ARF}$ dimerises. These $p14^{ARF}$ dimeric and trimeric forms diminished under reducing conditions and mutational studies showed the dimerisation is via cysteine residues. In the mouse form of ARF, $p19^{ARF}$, there are three cysteine residues downstream of the nucleolar localisation sequence the common one between mouse ($p19^{ARF}$) and human ($p14^{ARF}$) being cysteine 123[286]. In *Rb-/-* hepatocytes at 96 hours appearance of $p19^{ARF}$ homodimers was observed. (Figure 3.2.4). To confirm that these are homodimers, $p19^{ARF}$ expression was examined under reducing and non-reducing conditions. Under non-reducing conditions dimer bands of $p19^{ARF}$ were observed at 48 and 72 hours. Trimeric bands of $p19^{ARF}$ were observed at 96 hours post-plating (Figure 4.2.4). These homodimer bands decrease under reducing conditons. This supports the argument that these $p19^{ARF}$ homodimers are a response to an increase in ROS.

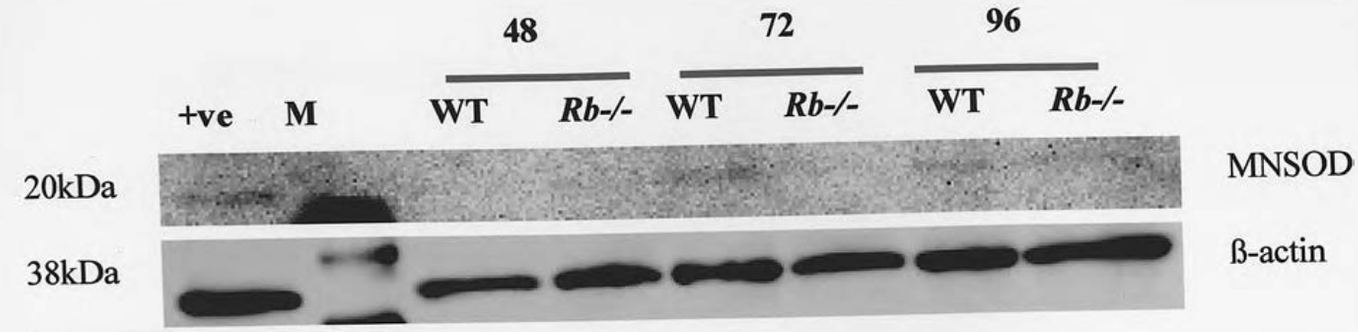


Figure 4.2.3: The expression of MnSOD in *Rb-/-* and WT hepatocytes

Western blotting showing the expression of MnSOD in WT and *Rb-/-* hepatocytes from 48 to 96 hours post-plating. 50µg of total cell lysate, with HELA cells used as the positive control were run on a 12% gel, and transferred to a PVDF membrane. The membrane was probed with a sheep polyclonal to MnSOD (1:1,000)(Calbiochem), followed by a Goat anti-rabbit HRP conjugated secondary (1:2,000) (Dako). A rabbit polyclonal to β-actin was used as the loading control. M represents molecular weight makers. This was repeated three times with consistent results.

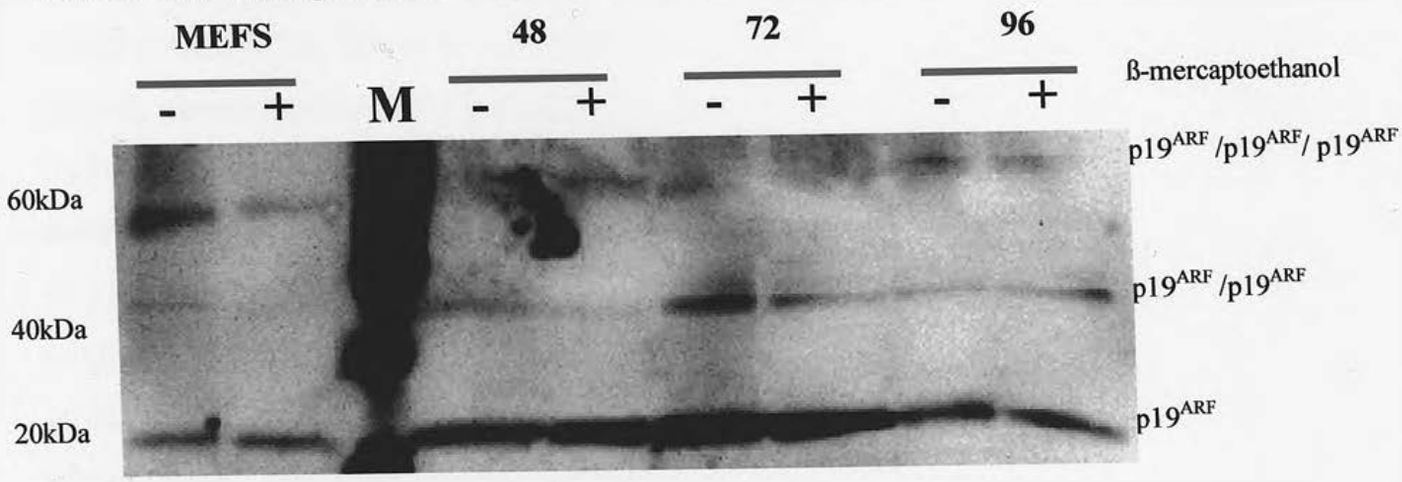


Figure 4.2.4: $p19^{ARF}$ homodimerises in *Rb-/-*hepatocytes

Immunoblot to show the presence $p19^{ARF}$ dimers in *Rb-/-* hepatocytes. 200µg of total cell lysate was heated in the absence (-) and presence (+) of β-mercaptoethanol, a reducing agent run on a 12% gel and transferred to a PVDF membrane. Mouse embryonic fibroblasts (MEFS) were used as the positive control and M represents molecular weight markers. The membrane was probed with a rabbit polyclonal to $p19^{ARF}$ (Abcam), followed by a donkey anti- rabbit HRP conjugated secondary (1:2,000) (Amersham). This was repeated twice with consistent results.

4.2.4 Reactive oxygen species (ROS) production is increased in *Rb-/-* cells and leads to an increase in DNA injury.

The decrease in MnSOD expression coupled with the presence of $p19^{ARF}$ dimers was an indicator that there was an upregulation of reactive oxygen species (ROS) in *Rb-/-* hepatocytes. Quantification of ROS in WT and *Rb-/-* hepatocytes was done using two fluorescence methods. One method used 5-(and 6-) chloromethyl-2', 7'-dichlorodihydrofluorescein diacetate, acetyl ester (CM-H_2DCFDA), a cell permeable diacetate ester. The other method used Dihydroethidium (DHE), a chemically reduced form of ethidium bromide.

CM-H_2DCFDA is a diacetate ester that upon entering the cell is cleaved by an esterase, which retains it in the cell. CM-H_2DCFDA measures hydrogen peroxide, hydroxyl radical, peroxyl radical and peroxynitrite anion. After reaction with these ROS CM-H_2DCFDA fluoresces green. At 24 hours post-plating there was a significant ROS decrease ($p=0.0017$) detected with CM-H_2DCFDA in *Rb-/-* hepatocytes compared to WT (Figure 4.2.5A). No differences in ROS levels between WT and *Rb-/* -hepatocytes were detected at 48 hours. At 72 hours a rise in ROS levels was observed in hepatocytes with a significant difference ($p=0.0130$) between WT and *Rb-/-* hepatocytes observed. Although WT and *Rb-/-* hepatocytes levels decreased at 96 hours, a higher amount of ROS was still maintained over the WT hepatocytes by the *Rb-/-* hepatocytes (Figure 4.2.5B).

The other method used dihydroethidium (DHE). DHE reacts with superoxide anion, which results in ethidium intercalating with the cells DNA. DHE detected significantly higher levels of superoxide anion in *Rb-/-*hepatocytes at both 24 ($p<.0001$) and 48 ($p=0.0156$) hours compared to WT. At 72 hours levels of superoxide anion peak with a

significant difference (p=0.0343) between WT and *Rb-/-* hepatocytes observed. At 96 hours there is a decreased level of ROS in *Rb-/-* hepatocytes while the levels in WT remained the same (Figure 4.2.5B). The main source of superoxide anions in cells is mitochondria. MnSOD is responsible for removal of superoxide anion in mitochondria. In hepatocytes MnSOD expression was examined and the increases in superoxide anion is consistent with these results (Figure 4.2.3).

At 72 hours both methods show a significant increase in ROS in *Rb-/-* hepatocytes compared to WT. As stated before 8-oxo-dG is formed through the oxidation of guanine and AP sites are formed via hydrolysis of the N-glycosyl bond. As these are both ROS induced types of DNA damage levels of both 8-oxo-dG and AP sites were assayed in the hepatocytes. This would determine if the increases observed in ROS were sufficient to actually cause damage to the DNA (Figure 4.2.6).

Quantification of 8-oxo-dG was done with an 8-oxo-dG specific elisa. At 48 hours no difference between WT and *Rb-/-* hepatocyte DNA was observed. At 72 hours in *Rb-/-* hepatocyte DNA levels of 8-oxo-dG rose and a significant (p=0.0465) difference between *Rb-/-* and WT hepatocyte DNA was observed. This corresponds to the associated increase in ROS with both dihydroethidum and CM-H_2DCFDA (Figure 4.2.5). WT and *Rb-/-* hepatocyte DNA showed an increase in 8-oxo-dG levels at 96 hours but there was no significant difference between them (Figure 4.2.6A). ROS can introduce modifications to DNA destabilising the N-glycosyl linkage generating a better leaving group. This promotes base release resulting in an AP site. In *Rb-/-* hepatocyte DNA at both 72 and 96 hours post-plating there was an increase in the number of AP sites (Figure 4.2.6B), although the difference was not significant.

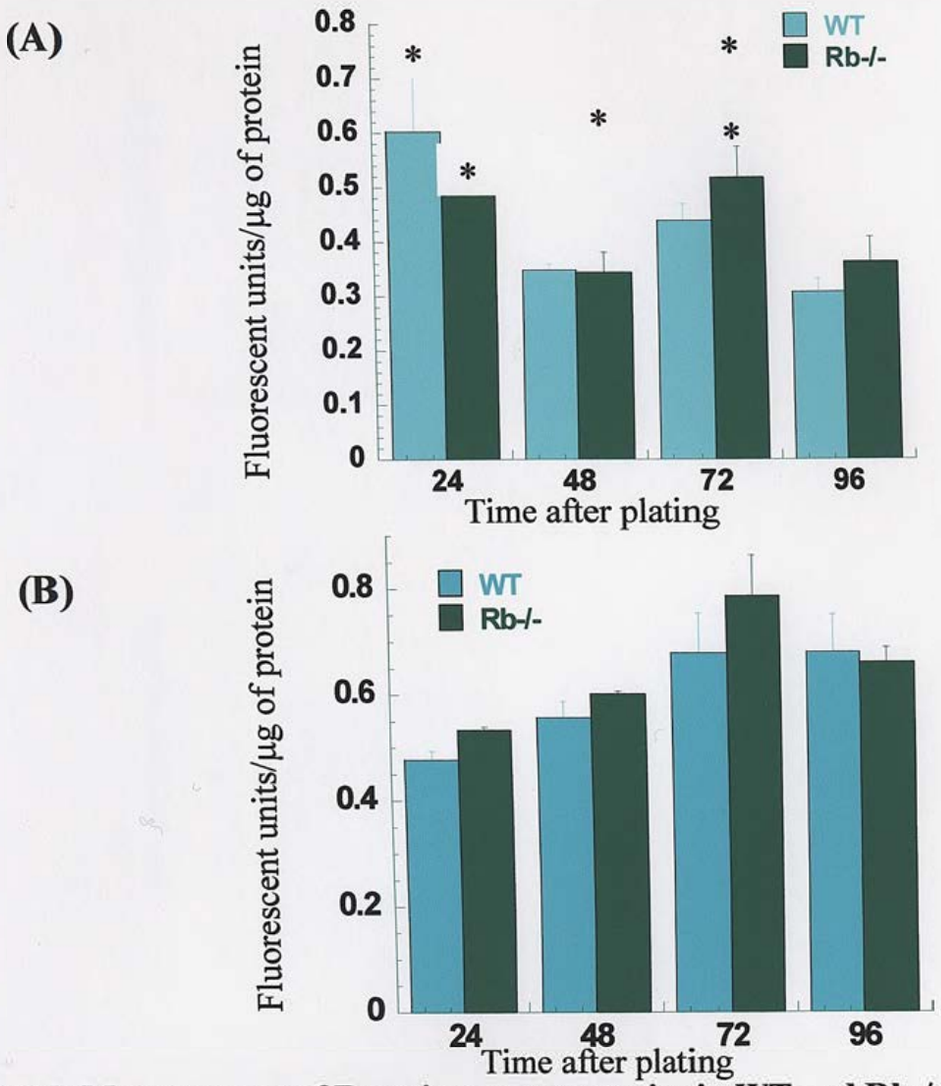


Figure 4.2.5: Measurement of Reactive oxygen species in WT and Rb-/-hepatocytes

(A)The amount of Reactive oxygen species (ROS) detected using CM-H_2DCFDA. A 100µM CM-H_2DCFDA stock solution was made in DMSO and further diluted to a 10µM final working solution in HBSS. Immediately after addition readings at 485nm and 510nm were taken on a fluorimeter (Thermo lifescience) every three minutes for a total period of one hour. (B) The amount of superoxide anion detected using DHE. A 31mM DHE stock solution was made using DMSO, diluted to a 100µM working solution in Chees's medium. Hepatocytes were incubated with DHE for four hours after which a single reading was taken at 480nm and 567nm. In both (A) and (B) the fluorescence was normalised for the amount of protein per well. Both assays were done in triplicate and repeated three times with consistent results. * Denotes significant difference using a two-tailed t-test. The inStat package was used for the statistical tests.

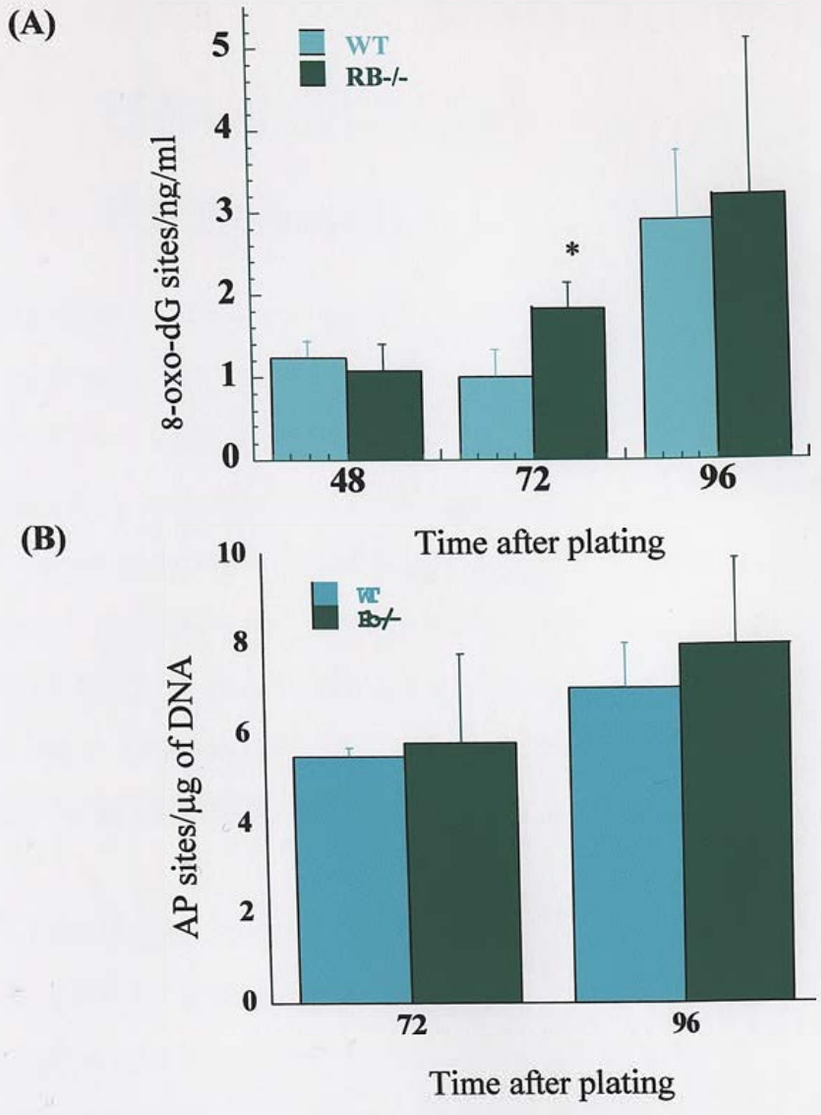


Figure 4.2.6: An increase in 8-oxo-dG and apurinic and apyrimidinic sites in *Rb-/-* compared to WT hepatocyte DNA

(A) The number of 8-oxo-dG sites in WT and *Rb-/-* hepatocyte DNA. In each well 20µg of DNA was added. A standard curve of known concentrations of 8-oxo-dG ranging from 0.125µg/ml to 10µg /ml was used to calculate the concentration of sites per ml. (B) The amount of apurinic and apyrimidic sites (AP sites) in WT and *Rb-/-* hepatocyte DNA. In each well DNA was added at a concentration of 0.5µg/µl. The assay is based on the AP sites reacting with an aldehyde reactive probe that has an intrinsic biotin, which is coupled to strepavidin. Both assays were performed in triplicate and repeated twice with consistent results. * Denotes significant difference using a two-tailed t-test. The inStat package was used for the statistical tests.

4.2.5 Two DNA damage response proteins, H2A.X and p53 are phosphorylated in Rb null cells

Phosphorylation of p53 and H2A.X are two markers of DNA damage. DNA damage kinases such as ATM and ATR are responsible for instigating phosphorylation of both p53 and H2A.X (γH2A.X). γH2A.X is a specific marker for double strand breaks (DSBs) in DNA with its C-terminus containing SQE, an ATM/ATR consensus motif[305]. In *Rb-/-* hepatocytes p53 is stabilised (Figure 3.2.1) but in order to be activated post-translational modifications need to occur. Phosphorylation on ser15 in p53 occurs in response to DNA damage. This disrupts the binding with MDM2 (Reviewed in section 1.6). In *Rb-/-* hepatocytes p53 is transcriptionally active. This is illustrated by the upregulation in expression of p21, a p53 responsive gene [283].

In *Rb-/-* hepatocytes phosphorylation on ser15 of p53 is detected at all timepoints tested. Levels of p53 phosphorylation on ser15 increase with time. WT hepatocytes showed no p53 phosphorylation on ser15 at any timepoints tested (Figure 4.2.7A). A kinase known to phosphorylate p53 on ser15 is Checkpoint kinase 1(Chk1). Chk1 lies downstream on the ATM/ATR pathway and both ATR and Chk1 are activated in *Rb-/-* hepatocytes (Figure 4.2.1 and Figure 4.2.2A). If these are responsible for p53 phosphorylation on ser15 caffeine addition, should eliminate p53 phosphorylation. The presence of caffeine did abolish p53 phosphorylation on ser15 at all timepoints tested in *Rb-/-* hepatocytes (Figure 4.2.7B). This demonstrates p53 phosphorylation was as a result of activation of either the ATM or ATR pathway.

In response to double strand breaks (DSBs) H2A.X becomes phosphorylated on ser139 (γH2A.X) and localises to the sites of these breaks[305]. γH2A.X is detected in *Rb-/-* hepatocytes at 48, 72 and 96 hours post-plating. The amount of γH2A.X increases with

time. No γH2A.X was detected in WT cells at any timepoint (Figure 4.2.8A). Having established that there was DSBs in the hepatocytes immunofluorescence was done to localise γH2A.X foci. γH2A.X was found throughout the nucleus in Rb-/-hepatocytes (Figure 4.2.8B). The immunofluorescence levels of γH2A.X in WT hepatocytes were consistent with western blotting at all timepoints tested.

To establish if either ATR or ATM were phosphorylating H2A.X a 2mM concentration of caffeine was added to the cells. In *Rb-/-* hepatocytes at 48 hours the presence of caffeine decreased γH2A.X levels. However at 72 and 96 hours no effect was observed with caffeine (Figure 4.2.9). This indicates that ATR or ATM may play a role in initiating the phosphorylation of H2A.X. However at later timepoints another kinase may be responsible for sustaining γH2A.X or there is functional redundancy with other kinases in hepatocytes[306].

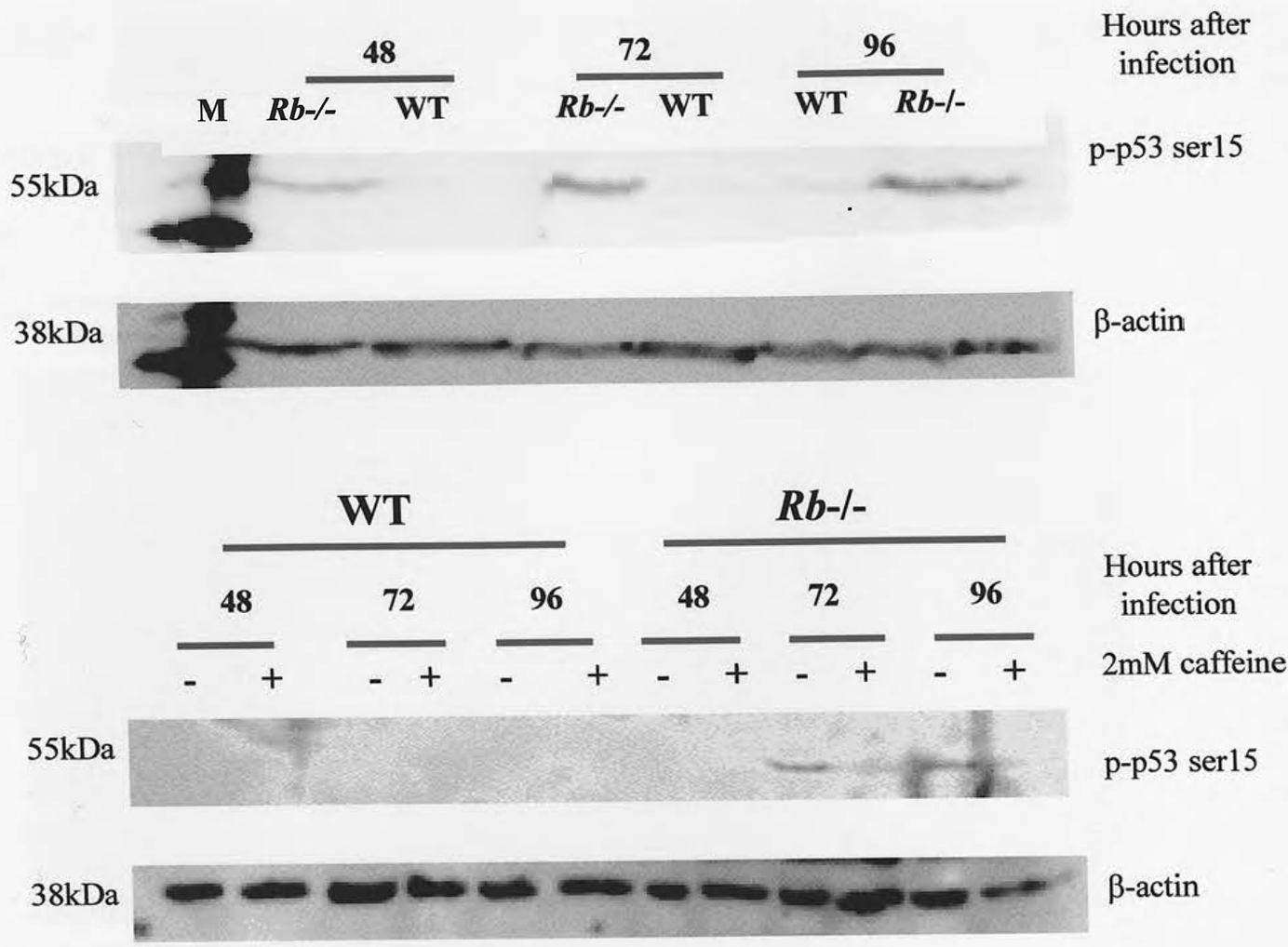


Figure 4.2.7: Phosphorylation of serine 15 of p53 in *Rb-/-* but not WT hepatocytes

(A) Western blotting showing an increase in phosphorylation of p53 on ser15 from 48 to 96 hours in WT and *Rb-/-* hepatocytes. 100μg of total cell lysate was run on a 10% gel, transferred to a PVDF membrane and probed with a rabbit polyclonal against p53 phosphorylated on ser15 (1:500) followed by a donkey anti-rabbit HRP conjugated secondary (1:2,000) (Amersham) (B) The phosphorylation of p53 on ser15 in the absence (-) and presence (+) of 2mM caffeine over the same timepoints in (A). The antibodies and conditions used were the same as in (A). The loading control used was β-actin. The experiment was repeated with consistent results.

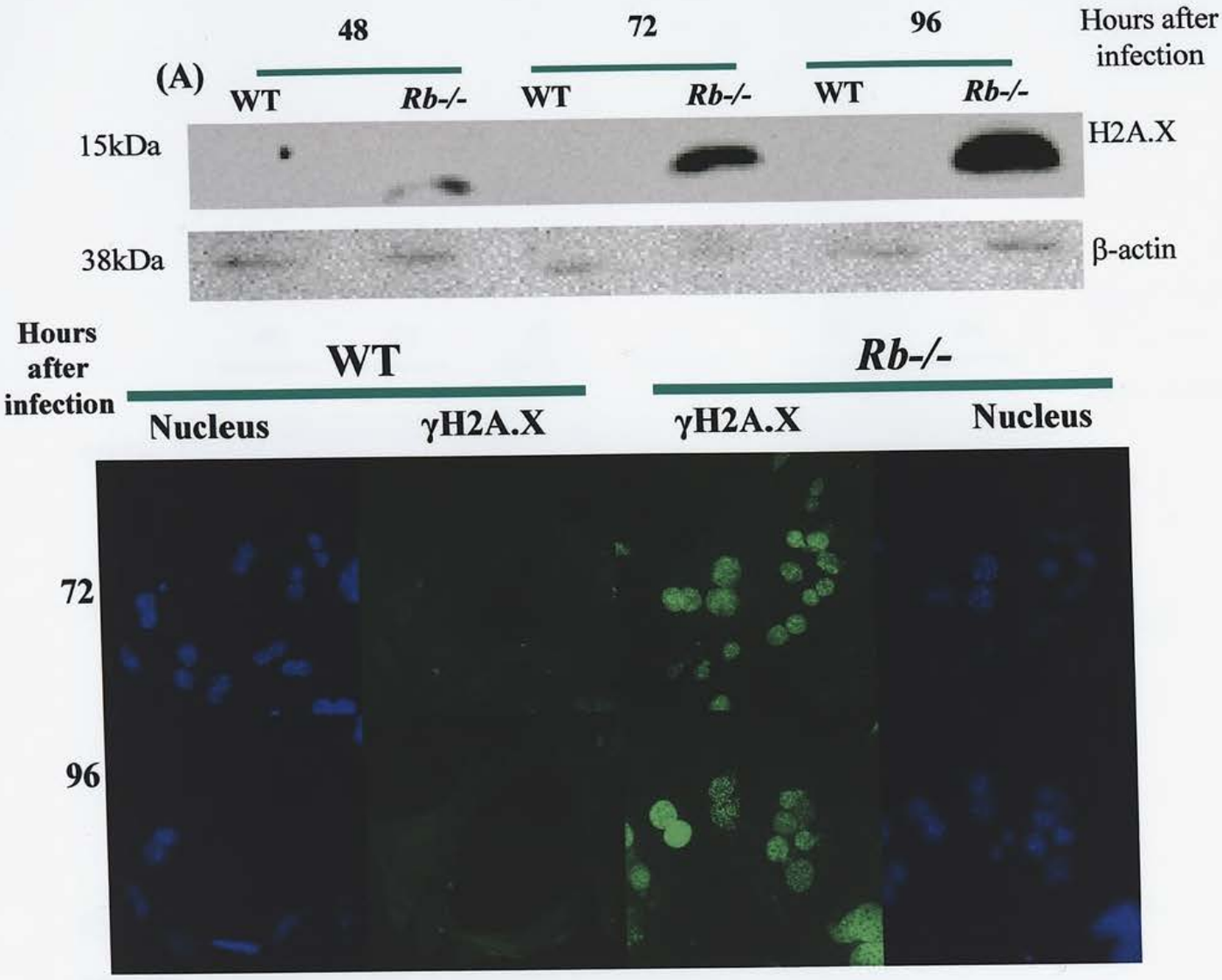


Figure 4.2.8: γH2A.X is present in Rb-/- but not WT hepatocytes

(A) Western blotting showing phosphorylation of H2A.X on ser139 from 48 to 96 hours in WT and Rb-/- hepatocytes. μg of acid extracted lysate was run on a 12.5% gel transferred to PVDF and probed with a mouse monoclonal IgG_{2A} against γH2A.X (1:700) followed by a goat anti-mouse HRP conjugated secondary (1:2,000) (Dako). β-actin was used as the loading control. (B) Immunofluorescence for γH2A.X (Green) at 72 and 96 hours post-plating. The same monoclonal antibody was used as in (A) (1:100) followed by a goat anti-mouse IgG_{2A} 488 fluor conjugated secondary (1:200) (Molecular Probes). The nucleus (Blue) was stained with TO-PRO-3. Both (A) and (B) were repeated three times with three different animals with consistent results. The images were captured using a Zeiss axiovert confocal microscope

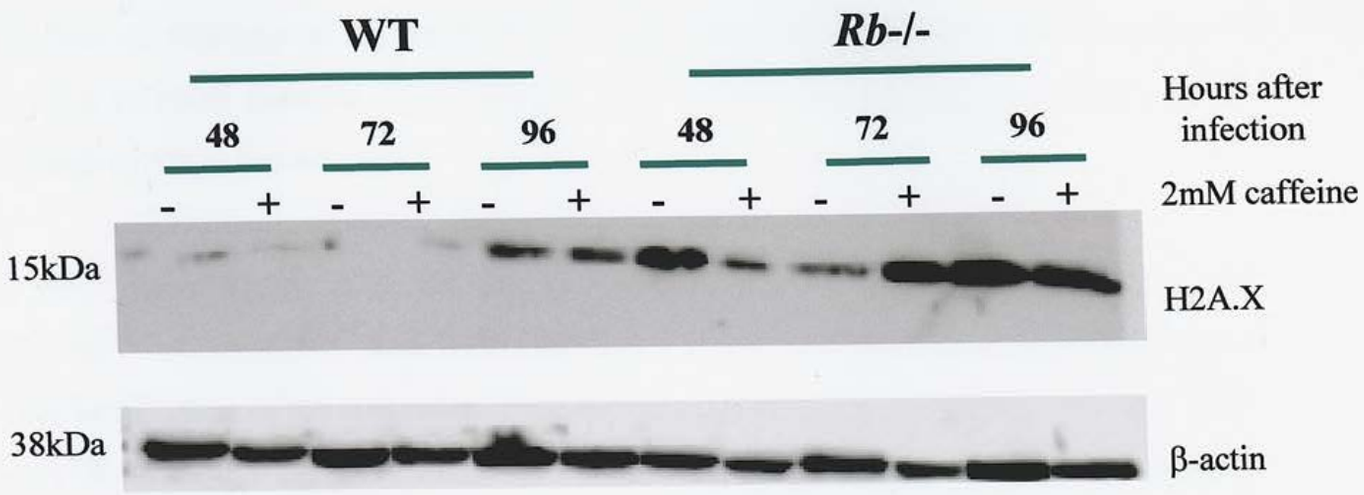


Figure 4.2.9: The presence of caffeine effects levels of γH2A.X in WT and *Rb-/-* hepatocytes

Immunoblot showing H2A.X phosphorylation on ser139 in the absence (-) and presence (-) of 2mM caffeine at 48, 72 and 96 hours post-plating in WT and *Rb-/-* hepatocytes. μg of acid extracted lysate was run on a 12.5% gel transferred to PVDF and probed with a mouse monoclonal IgG_{2A} against γH2A.X (1:700) followed by a goat anti-mouse HRP conjugated secondary (1:2,000) (Dako). The loading control used was β-actin. This was repeated three times with three different animals with consistent results. A mouse monoclonal IgG_{2A} to H2A.X was used.

4.3 Discussion

The aim of this part of my work was to invesitgate the hypothesis that there was an increase in ROS induced DNA damage and to establish the pathway leading to this increase in *Rb-/-* hepatocytes.

In *Rb-/-* hepatocytes, E2F activity is increased and $p19^{ARF}$ is upregulated (Figure 3.2.6A)[283]. In fact $p19^{ARF}$ and ATR expression peaks simultaneously and coincides with ATR localisation in the nucleolus. This implies $p19^{ARF}$ presence may be having an effect on ATR. Although the mechanism is undefined Rocha et al reported ATR activation by $p19^{ARF}$ [235]. Relocalistion of ATR to the vicinity of its substrates is reported to enable ATR to activate them and respond to DNA damage [253]. There are at least three lines of evidence to support that ATR is active in *Rb-/-* hepatocytes. Firstly, ATR relocalisation, secondly this relocalisation ties in with Chk1 phosphorylation on ser317 and p53 phosphorylation on ser15. Thirdly caffeine, an ATR/ATM inhibitor eliminated both phosphorylation of Chk1 and p53. $p19^{ARF}$ expression, ATR relocalisation and Chk1 phosphorylation is not observed in WT hepatocytes

ATR activation should enable the cell to halt the cell cycle and repond to DNA damage [318]. As ATR is activated in *Rb-/-* and not WT hepatocytes indicates this loss of Rb induces DNA damage in the cells. The reason why ATR is activated by $p19^{ARF}$ is not clear, as $p19^{ARF}$ itself can induce stabilisation of p53 [229, 230, 273]. In *Rb-/-* hepatocytes $p19^{ARF}$ binds to p53 and p53 has been found in the nucleolus (Figure 3.2.7) thus $p19^{ARF}$ could be bringing ATR and p53 into the same region of the nucleus. ATR activation could further enhance the transactivation activity of p53 through inducing post-translation modifications [319].

Previous reports have shown that Chk1 can phosphorylate NF-κB decreasing its transactivation activity [235]. As NF-κB induces MnSOD this could lead to a downregulation of MnSOD [293]. MnSOD, is a mitochondrial enzyme, responsible for catalsying the superoxide anion turnover into hydrogen peroxide and water. No expression of MnSOD levels was detected in *Rb-/-*hepatocytes at 72 hours which correlates with Chk1 phosphorylation. This indicates that Chk1 via NF-κB could be inducing a decrease in expression. In *Rb-/-* hepatocytes this decrease in MnSOD expression corresponded to the peak levels of superoxide anion in the hepatocytes at 72 hours. This is consistent with a previous report by Tanaka et al, which showed a downregulation in MnSOD lead to an increase in ROS [291]. Further evidence to support an increase in ROS is the number of $p19^{ARF}$ dimers increased in the absence of β-mercaptoethanol, a reducing agent. This confirms $p19^{ARF}$ is dimerising in the presence of ROS. In response to ROS dimer forms of $p14^{ARF}$, the human form have been found this has not previously been reported for the mouse form [286].

As stated above analysis of ROS levels in hepatocytes revealed *Rb-/-*hepatocytes had significant increases in both superoxide anion, hydroxides and peroxides at 72 hours post-plating compared to WT. Levels of 8-oxo-dG and AP sites revealed a significant increase in 8-oxo-dG at 72 hours post-plating in *Rb-/-* hepatocyte DNA, which is consistent with the ROS results. As these are both types of oxidative DNA damage and appear when there is a significant increase in ROS implies the increases in ROS observed is sufficent to cause DNA damage.

Examining H2A.X and p53 phosphorylation showed both to be phosphorylated at all timepoints tested in *Rb-/-* hepatocytes. No phosphorylation was detected in WT cells. H2A.X is phosphorylated as a result of DSBs and is used as a marker therefore this demonstrates DSB presence in *Rb-/-* hepatocytes[305]. These DSBs were found throughout the nucleus. Phosphorylation of p53 on ser15 is also a marker of DNA damage and substantiates two previous findings.

In summary, the evidence presented in this chapter is that in *Rb-/-* hepatocytes ATR, a DNA damage response kinase, is activated. ROS levels are increased and correlate with two types of oxidative DNA damage, 8-oxo-dG sites and AP sites in *Rb-/-*hepatocytes. In addition γH2A.X, a marker of DSBs and p53 phosphorylation at ser15 is detected only in *Rb-/-* hepatocytes and not WT hepatocytes. This evidence combined strongly supports the hypothesis that there is ROS induced DNA damage in *Rb-/-* hepatocytes.

In conclusion, *Rb* loss leads to ROS induced DNA damage. A pathway was proposed to show how *Rb* loss could lead to ROS increases in hepatocytes (Figure 4.3.1). $p19^{ARF}$ relocalises and activates ATR, with ATR moving and remaining in the nucleolus. An effector kinase of ATR, Chk1 is phosphorylated and activated. ATR also induces the formation of γH2A.X foci. The active Chk1 phosphorylates the transcription factor NF-κB on thr505 and decreases its transactivation function as well as phosphorylating $p53^{235}$. Expression of MnSOD, which has an NF-κB responsive promoter is downregulated as a result. This leads to an increase in ROS, which induces DNA damage.

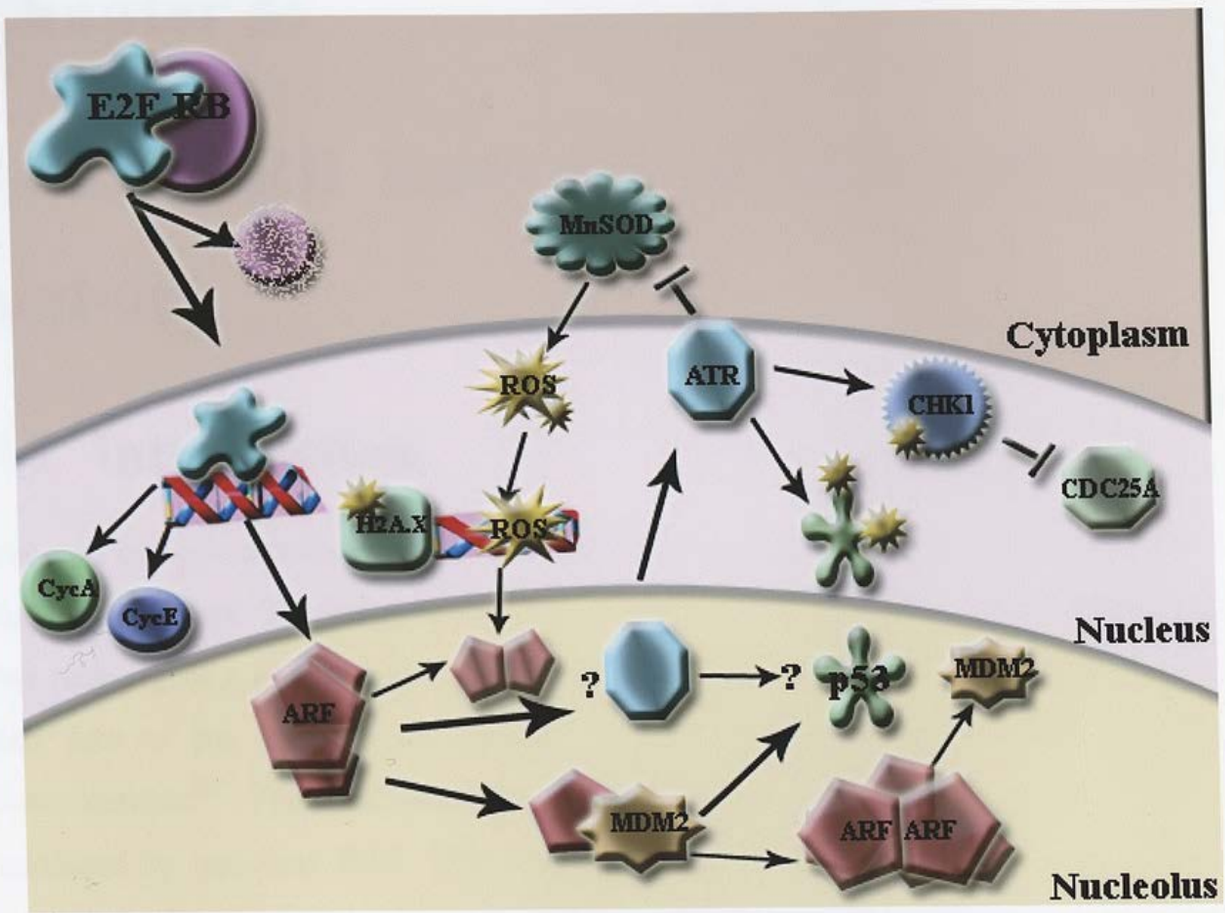


Figure 4.3.10: A model for the increase in ROS induced DNA damage in *Rb-/-*hepatocytes.

Upon *Rb* loss, E2F activity is increased. This leads to $p19^{ARF}$ upregulation, which activates ATR, which is drawn into the nucleolus. This activated ATR phosphorylates Chk1, p53 and H2A.X. The activated Chk1 downregulates MnSOD via NF-κB. This leads to ROS increases with the consequential DNA damage.

Chapter 5:

Loss of RB leads to aberrant cell cycle activity.

5.1 Introduction

The cell cycle is a coordinated network any loss in the harmony that exists predisposes the cell to cancer. The Rb pathway is an intricate part of this network and disruption in this pathway is a common event in liver cancer (Section 1.1). Previous studies indicate that loss of Rb leads to an increase in the number of chromosomal and nuclear abnormalities[283] .This was investigated further using a mini-macroarray, with the results validated by real-time PCR. This macro-array together with the real-time PCR results show a deviant content of certain cell cycle genes in *Rb-/-* cells compared to WT including the cyclin family, Mad2, GADD45a and CDC25a (Personal communication-Pin Lu). The aim of this chapter was to investigate the state of cell cycle control in *Rb-/-* hepatocytes.

The cyclin gene family are crucial to the maintenance and control of the cell cycle. Their production oscillates during the cell cycle and they are produced and destroyed in a co-ordinated manner. The synchronisation of the cell cycle from G1 right through to M-phase is controlled by the cyclins, beginning at G_0 with cyclin D stimulating the cells to enter the cell cycle, cyclin E and A promote entry into S-phase and the degradation of cyclin B by the APC complex signals the end of mitosis[151, 152]. The production of both cyclin A and E is under the control of the E2F transcription factor (Section 1.4.1). The

cyclins are only active when bound to their specific partners that are members of the cyclin dependent kinase family. The cyclin/CDK complexes activity is inhibited by numerous mechanisms, including phosphorylation, relocalisation of proteins and the direct binding of inhibitors. Any alteration in balance of this network predisposes to an increase in chromosomal instability.

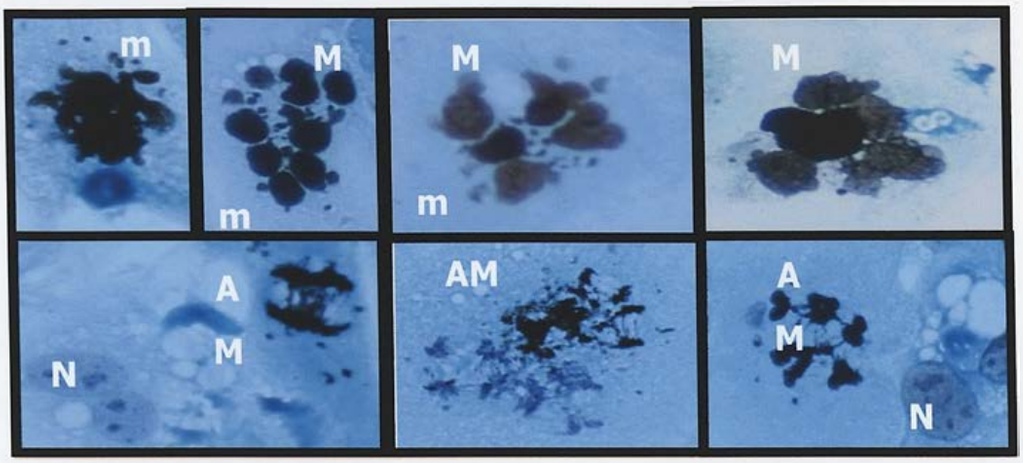
Mad2 is an E2F responsive gene activated in response to unattached kinetochores[320]. This initiates the binding of Mad2 to CDC20. This instigates the mitotic checkpoint, as binding of Mad2 to CDC20 sequesters it away from the APC thus preventing the activation of the ubiquitin ligase[321, 322]. The function of APC is to ubiquinate a number of components of the mitotic machinery including cyclin B1 and securin. This enables mitosis to progress to completion culminating in the separation of the two daughter cells[262].

The centrosome produces the mitotic spindle, which is responsible for the separation of the sister chromatids. The activity of the cyclin E/CDK2 complex merges the centrosome cycle to the DNA duplication cycle[97]. Any alteration in regulation of cyclin E/CDK2 may lead to an unregulated centrosome cycle with knock-on effects for mitosis. Increase in centrosome numbers through rereplication have been shown to lead too cancer[323].

The Cip/Kip family of CDK inhibitors predominantly targets complexes containing CDK2. It includes p27Kip1, which is a known inhibitor of cyclin A/CDK2 and cyclin E/CDK2[110]. It primarily works at the G1 transition but also works at the G2 transition by binding to cyclin B1/ CDK1. p27 binds across the cyclin/CDK complex at the ATP binding site. The phosphorylation of p27 on thr187 by the cyclin E/CDK2 complex is the signal for its degradation in the proteasome[98]. The regulation of the protein is extremely complex; it is regulated by transcription, translation, increased proteolysis and localisation.

Gadd45a and CDC25a are two important regulators of cyclin/CDK complex activity that have opposing effects. Dependent upon the circumstances of the cell they are active at both the G1/S-phase transition and also the G2/M transition. CDC25a is a member of the CDC25 phosphatase family and activates both cyclinE/CDK2 and cyclin B1/CDK1 complexes by dephosphorylating them[324]. In response to damage, levels of CDC25a decrease inducing a rapid halt in the cell cycle[325]. This contrasts with Gadd45a, which in response to damage is active at the G2/M checkpoint binding to CDK1 and removing it from cyclin B1 preventing mitosis from occurring[131].

(A)



(B)

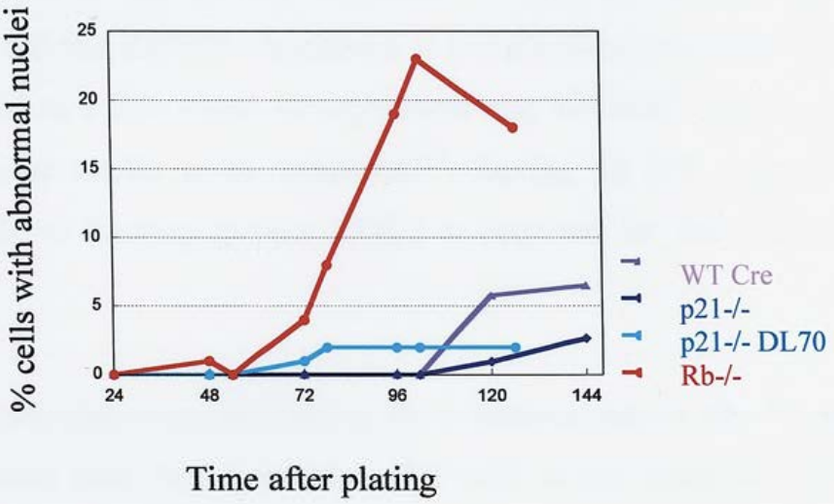


Figure 5.1.1: There is an increase in abnormal nuclei in *Rb-/-* hepatocytes

(A) An example of the mitotic and abnormal nuclei seen in the *Rb-/-* cells where N: normal nuclei, AM: abnormal mitosis and M: multinucleated (B) A graph showing the percentage increase in abnormal nuclei in *Rb-/-* cells compared to WT and p21-/- cells alone. (Taken from Sheahan at al[283]).

5.2 Results

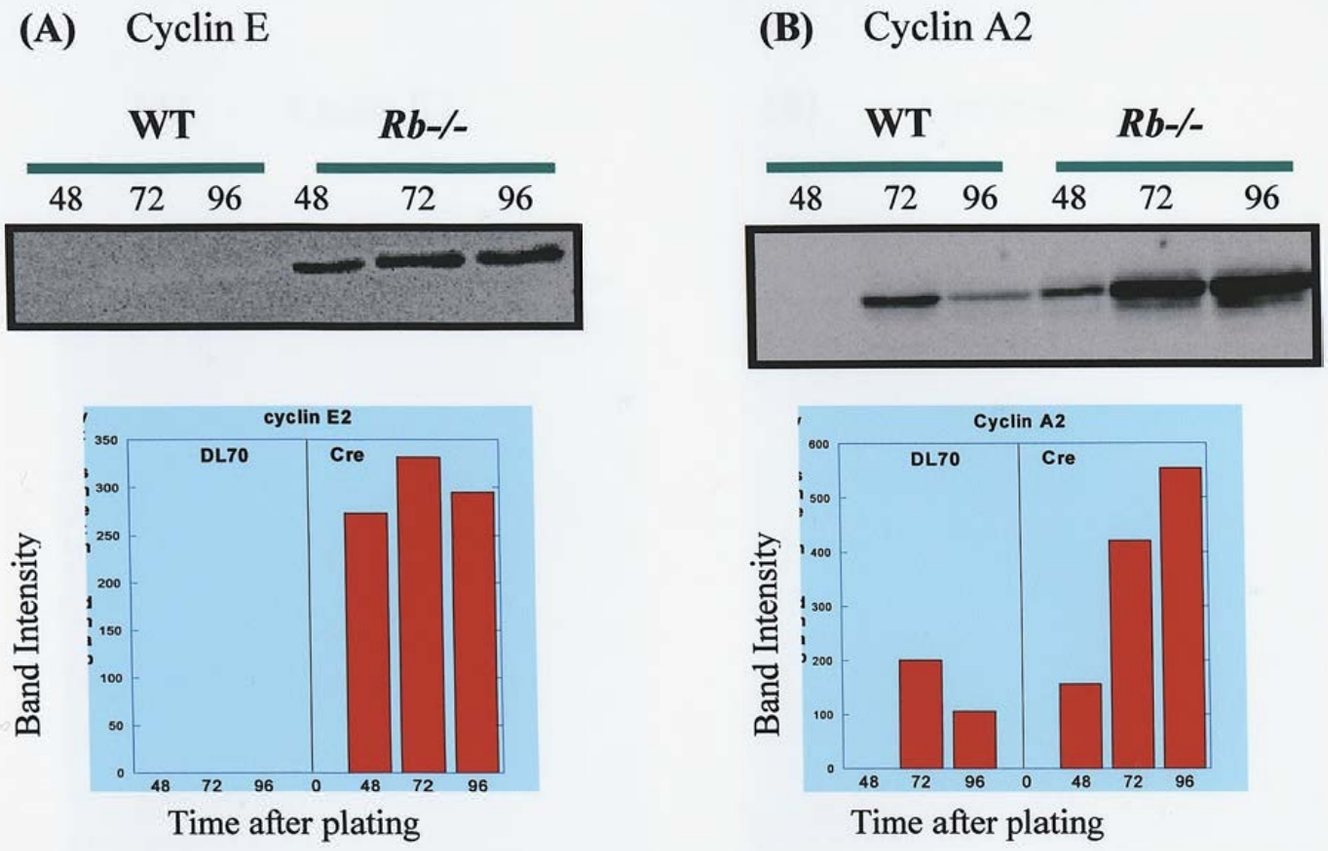
5.2.1 The expression of the cyclin family of proteins

The cyclins are a family of proteins that regulate the cell cycle together with their cyclin dependent kinase (CDK) partners, their levels are maintained by transcription and proteolysis. Once a cyclin is removed it indicates a stage of the cell cycle has come to an end enabling the cycle to advance. To try to ensure the maintenance of genomic integrity a system exists to ensure the sequential emergence of the cyclins[151, 152]. In an unperturbed cell the Rb/E2F checkpoint is a restriction point after it is passed the cells are committed to a full round of replication and division[83]. Cyclin E is the first post-restriction point cyclin to be produced[326], having an E2F responsive promoter and together with its binding partner CDK2 is required for the transcription of S-phase genes[327].

Cyclin E expression was detected in *Rb-/-* hepatocytes at 48, 72 and 96 hours post-plating however none was detected in WT cells at any timepoint (Figure 5.2.1). At all timepoints in *Rb-/-* hepatocytes cyclin E was localised to the nucleus indicating that it is active (Figure 5.2.2). The Cyclin E/CDK2 complex switches on the transcription of cyclin A, which binds to cyclin E segregating it from CDK2 preventing further activation of S-phase genes. Cyclin A is responsible for the initiation of DNA synthesis; a certain threshold level of cyclin A is produced before DNA replication begins. In *Rb-/-* cells the expression of cyclin A begins at 48 hours and increases up to 72 hours with the same levels maintained at 96 hours, compared to WT cells where expression peaks at 72

hours. In WT hepatocytes the levels of cyclin A decrease at 96 hours, which may indicate the WT cells are completing S-phase (Figure 5.2.1). These results for cyclin A are consistent with cyclin E expression, the superarray and BRDU data, which shows that the *Rb-/-* cells peak of proliferation is at 72 hours. Cyclin A is localised to the nucleus at both 72 and 96 hours corresponding to the peak of expression, only found there in WT cells at 72 hours (Figure 5.2.2).

The critical factor for the execution of mitosis is the cyclin B/CDK1 partnership, a minimum amount of the complex must be produced for initiation of mitosis and degradation by APC signals the end of mitosis. The presence of cyclin A2 /CDK1 prevents the premature activation of the APC complex, allowing the levels of cyclin B1 to accumulate for the initiation of mitosis. Cyclin B1 is detected in *Rb-/-* cells from 48 hours to 96 hours compared to WT cells where the levels are high only at 96 hours (Figure 5.2.1c). This is coherent with the cyclin A data as cyclin A is still present in high amounts which should prevent the activation of the APC complex and the degradation of the cyclin B1/CDK1 complex.



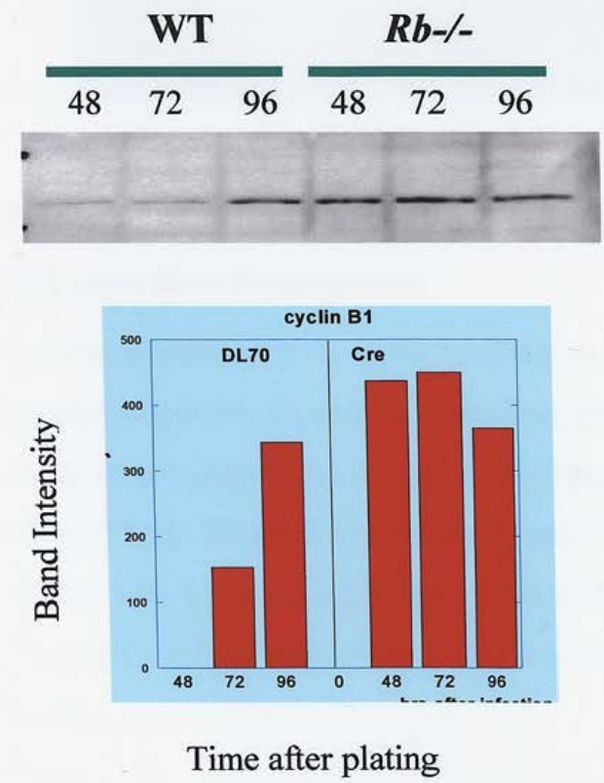


Figure 5.2.1: The expression levels of Cyclin A, E and B1.

(Done in conjunction with Mathew Parker)

Immunoblots showing expression of (A) cyclin E (B) cyclin A2 and (C) Cyclin B1 in WT and *Rb-/-* hepatocytes at 48, 72 and 96 hours post-plating. In each case a 100μg of protein was loaded, run on a 10% SDS gel and transferred to a PVDF membrane. The membrane was probed with rabbit polyclonals to each cyclin (1:100) (Abcam) followed by a donkey anti-rabbit HRP conjugated secondary (1:2,000). Below each blot is the densitometry of each of the bands normalised to β-actin expression. The western blotting was repeated three different times on three different animals and the results were consistent on each occasion.

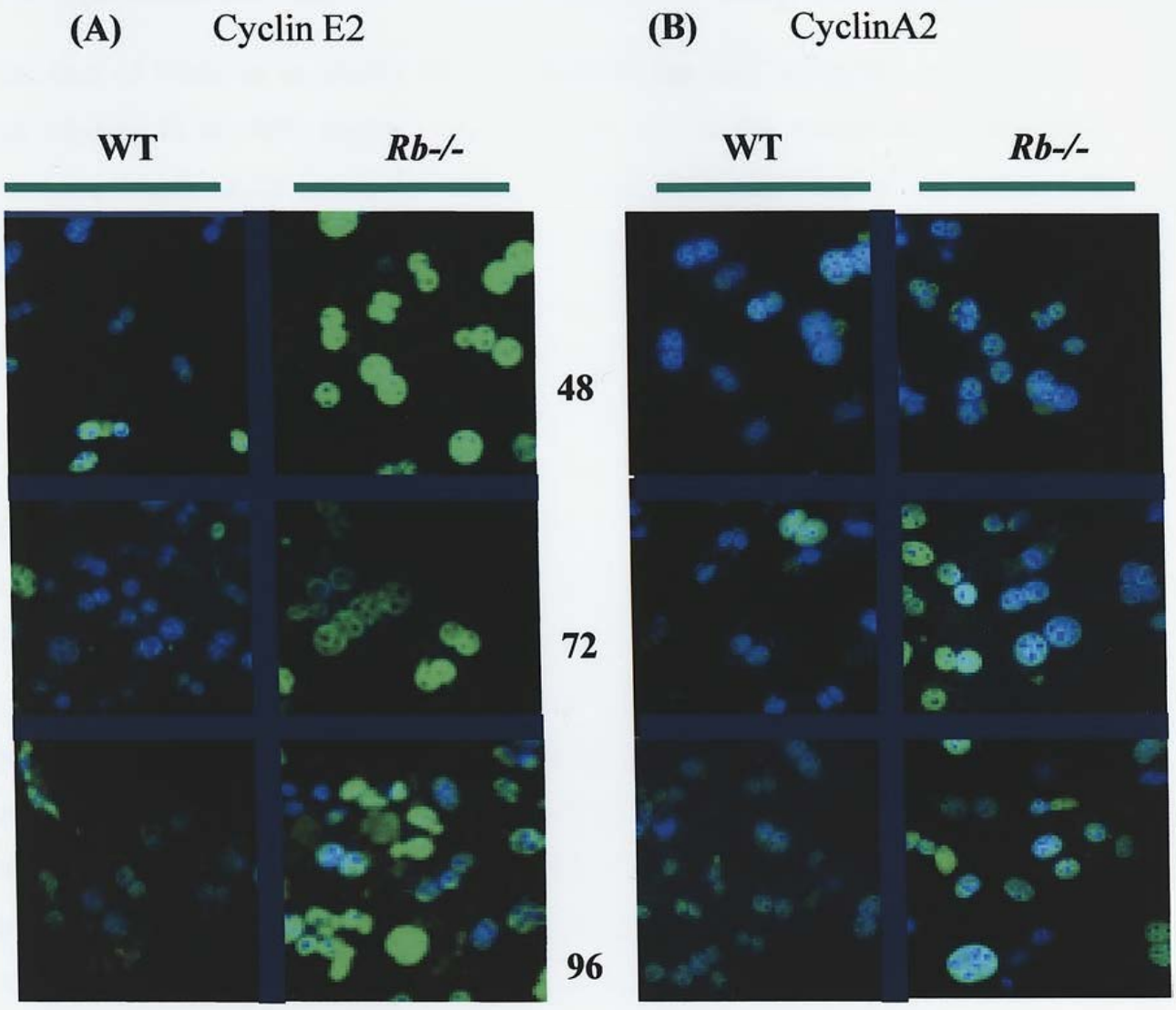


Figure 5.2.2: The localisation of Cyclin E and A with the proliferation of WT and *Rb-/-* hepatocytes.

Immunofluorescence to show localisation of Cyclin A and Cyclin E in WT and *Rb-/-* hepatocytes at 48, 72 and 96 hours post-plating. Staining for the cyclins was done using (A) a rabbit polyclonal to cyclin E2 (Green) and (B) a rabbit polyclonal to cyclin A2 (Green) both followed by a goat anti-rabbit 488-fluor conjugated secondary (1:200). TO-PRO3 was used to label the nucleus (Blue). Images were captured using a Zeiss Axiovert confocal microscope. The experiment was repeated three times with consistent results.

5.2.2 Centrosomes number and Mad2 expression in WT and *Rb-/-* hepatocytes

The function of Mad2 is to inhibit the activation of the APC complex, which it does through binding to an APC partner, cdc20. Mad2 acts in the metaphase to anaphase transition, a Mad2/cdc20 complex being assembled in the region of unattached kinetochores. The dissociation of cdc20 from Mad2 activates the APC. This activated APC results in securin and cyclin B1 being degraded and anaphase ensuing. Mad2 is undetectable in quiescent cells, in response to serum the levels increase after the cells enter S-phase, peaking at G2/M slightly after cyclin A. MAD2 is an E2F responsive gene and elevated levels of Mad2 in *Rb-/-* cells have been observed previously, this elevation leading to an increase in aneuploidy. In the case of the *Rb-/-*hepatocytes consistent with the previous publications the expression of Mad2 is increased at both the mRNA and protein level at all timepoints (Figure 5.2.3) [320].

An aberrant number of centrosomes could possibly account for the increase in the chromosomal abnormalities in the *Rb-/-* hepatocytes, as cyclin E overexpression is linked to increase in the number of centrosomes. Centrosomes are crucial to the mitotic stage of the cell cycle, generating two spindle poles at either end of the cell with microtubules that bind to the sister chromatids. During anaphase these microtubules retract separating the sister chromatids, ensuring that each daughter cell has the same number of chromosomes as the parent cell. The essential role of centrosomes in this phase of the cell cycle means that any dysregulation of centrosomes would be catastrophic.

The centrosomes were identified by immunofluorescence for γ-tubulin, a known centrosomal marker. The numbers quantified by manually counting the centrosomes in each cell. Approximately 80% of hepatocytes are binucleated, thus the number of hepatocytes was counted separately for mononucleated and binucleated. There was no

Significant difference in the number of centrosomes between WT and *Rb-/-* hepatocytes at any timepoint tested (Figure 5.2.4). This is for both mononucleated and binucleated demonstrating that it is not centrosome number that is leading to the abnormalities. The variation in number of centrosomes is due to the different stages of the cell cycle.

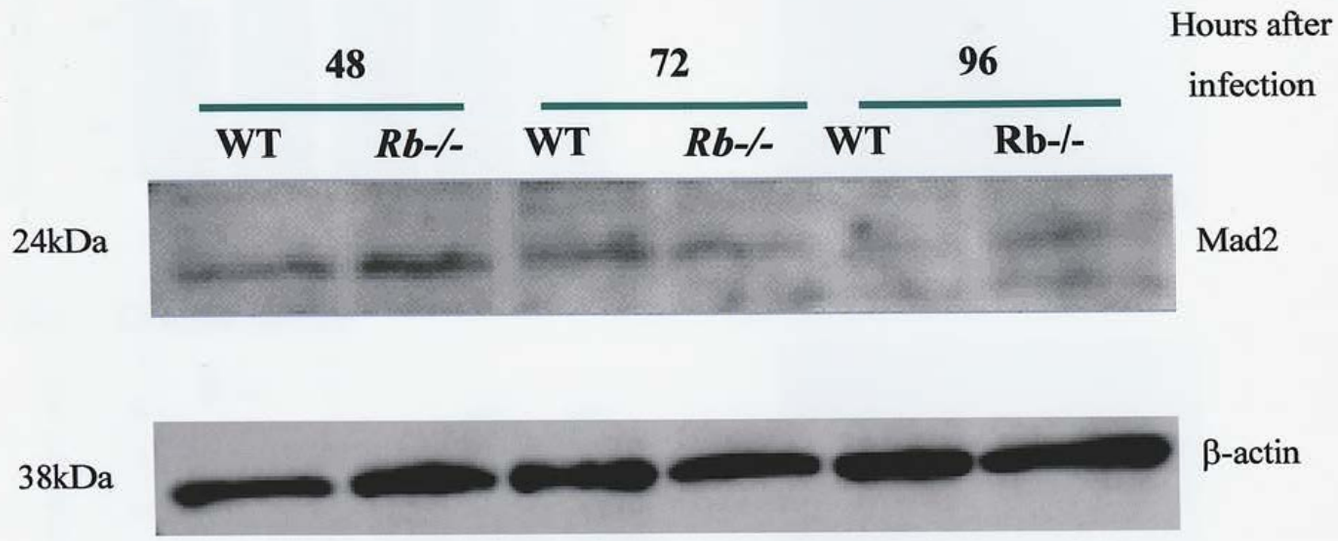


Figure 5.2.3: Increase in MAD2 expression in WT and *Rb-/-* hepatocytes

Western blotting for MAD2 from 48 to 96 hours post plating in WT and *Rb-/-*cells, 50μg of protein was loaded per lane, run on a 12% SDS gel and transferred to a PVDF membrane. The membrane was probed with a goat polyclonal to Mad2 (1:1,000) (Abcam) followed by a swine anti-goat HRP conjugated (Abcam) (1:2,000) secondary antibody was used. β-actin was used as the loading control.

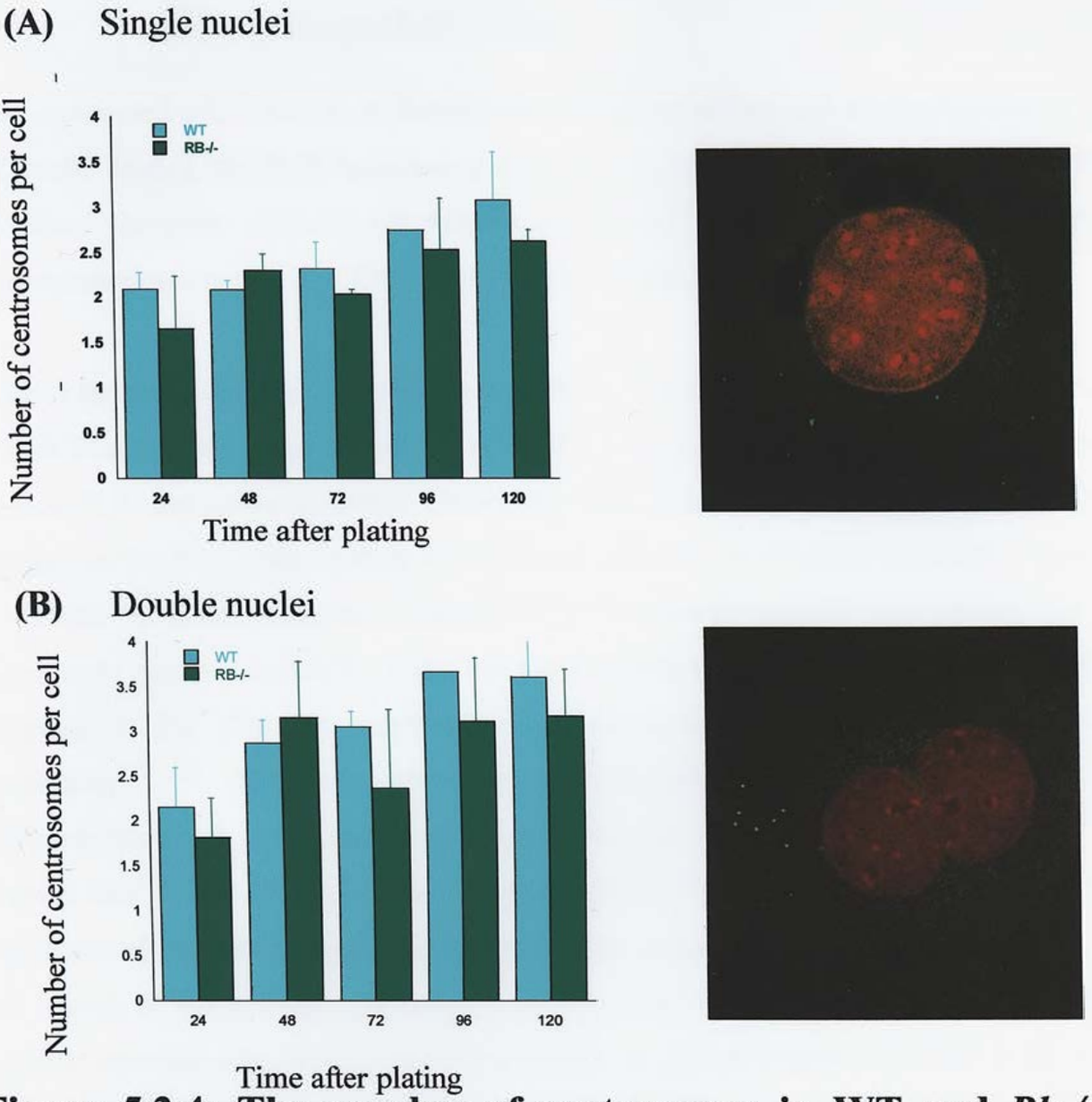


Figure 5.2.4: The number of centrosomes in WT and *Rb-/-* hepatocytes

Graphs showing the number of centrosomes in WT and *Rb-/-* hepatocytes for the indicated times post-plating in (A) for mononucleated cells and (B)binucleated cells. The centrosomes were stained with z mouse monoclonal against γ-tubulin (1:100), followed by a goat anti-mouse 488 conjugated secondary (1:200) antibody. At least 50 cells were counted per well per timepoint. Images were captured using a Zeiss Axiovert microscope. This experiment was repeated twice with consistent results and the error bars are the standard deviation of the mean.

5.2.3 A decrease in CDC25a is found in *Rb-/-* hepatocytes.

In an unstressed cell CDC25a, a phosphatase, functions at two critical checkpoints in the cell cycle. During the G1/S transition it activates cyclin E/CDK2 through removing the inhibitory phosphate allowing progression of S-phase. At the G2/M phase transition it dephosphorylates cyclin B1/CDK2 allowing the initiation of mitosis[324].

In *Rb-/-* hepatocytes, at all timepoints tested there is a significant decrease in the amount of CDC25a detected compared to WT (Figure 5.2.5). This is surprising, as it is known to have an E2F responsive promoter. Conversely there is an increase in the amount of DNA damage in the *Rb-/-* cells leading to the phosphorylation of checkpoint kinase 1 (Chk1) at 72 and 96 hours (Chapter 4 figure 4.2.2). Previously reports have shown that in response to genomic instability Chk1 has the ability to phosphorylate CDC25a on thr504 targeting it for ubiquitin mediated degradation, preventing the cell cycle from continuing[325, 328] also cells which are haploinsufficent for Chk1 show severely uncoordinated cell cycle and premature mitotic entry providing further evidence to support this[329]. The method of repression of CDC25a by Chk1 is rapid; it prevents the activation of S-phase and mitosis facilitating the repair of the damaged DNA, prior to the launch of the p53-p21 pathway[325]. This damage induced phosphorylation is Chk1 specific and not only does it have the ability to phosphorylate CDC25a it can also phosphorylate CDC25c, a member of the same family, on ser216[330]. The function of CDC25c is to dephosphorylate cyclin B1 bound CDK1 allowing for the initiation of mitosis, the phosphorylation by Chk1 removes CDC25c from the nucleus segregating it from potential binding partners resulting in the suppression of mitosis[331]. This increase in Chk1 activity most likely leads to the decrease observed in CDC25a in the *Rb-/-* cells. In both WT and *Rb-/-*cells the level of CDC25a begins to increase at 96 hours, although the level of CDC25a in the *Rb-/-*hepatocytes is still far less that in the WT cells. This is probably due to some cells entering mitosis at this timepoint.

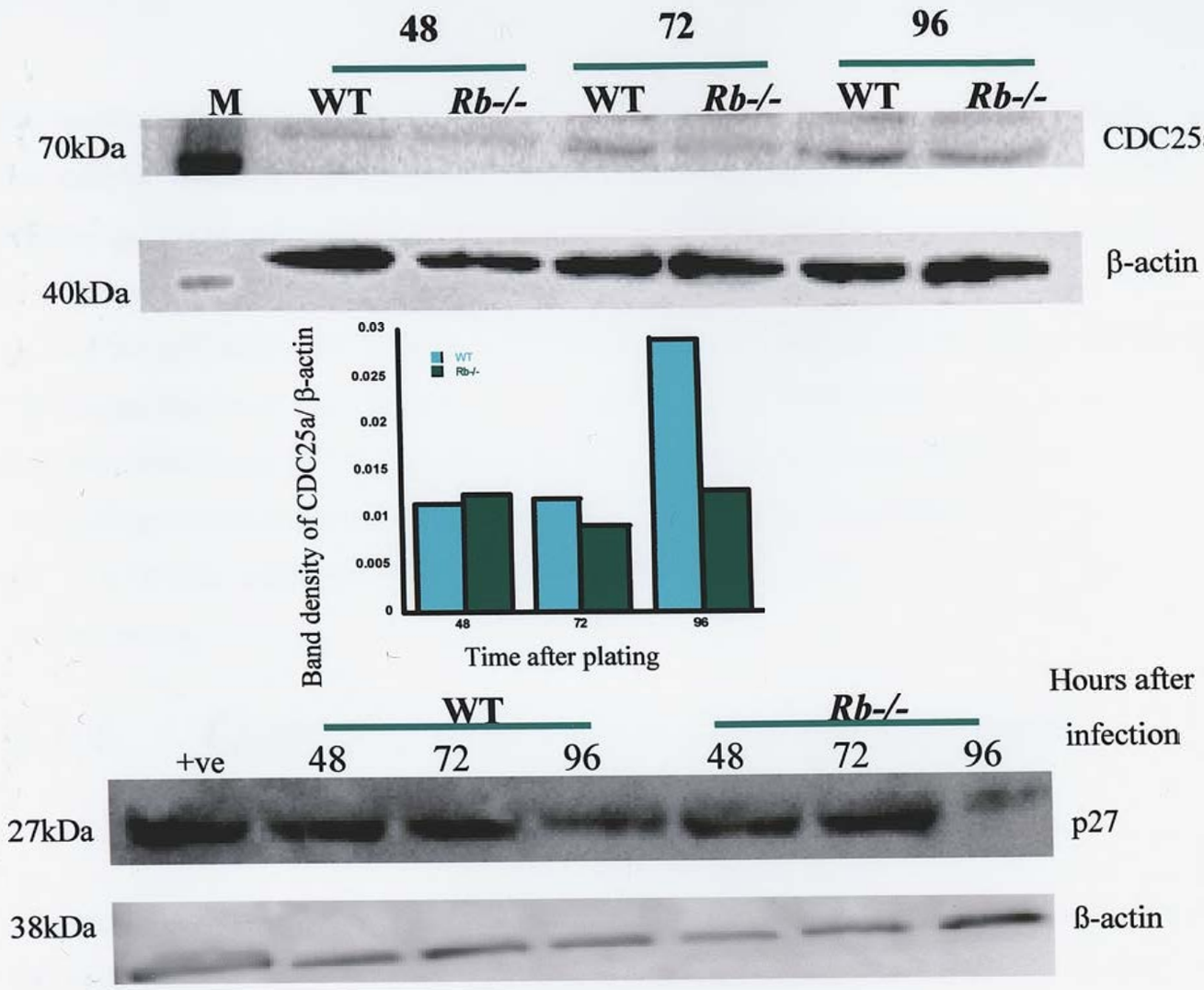


Figure 5.2.5: CDC25a and p27 expression in WT and *Rb-/-* hepatocytes

(A) CDC25a expression in WT and Rb-/- hepatocytes. 50μg of total cell lysate was loaded per lane, run on a 10% SDS gel and transferred to a PVDF membrane. A rabbit polyclonal to CDC25a (1:1,000) (cell signalling) was used to probe the membrane, followed by a donkey anti rabbit HRP conjugated secondary (1:2,000) (Amersham) antibody with β-actin used as a loading control. The graph shows the densitometry of the bands normalised with β-actin. The experiment was repeated three times using different animals with consistent results. (B) Western blotting showing a decrease in p27 in *Rb-/-* cells at 96 hours compared to WT. 100μg of protein was loaded per lane, run on a 10% SDS gel and transferred to a PVDF membrane. A rabbit polyclonal to p27 (1:2,500) (Abcam) was used to probe followed with the same secondary as in (A). β-actin was used as a loading control. The experiment was repeated once.

The function of p27 is to inhibit the cyclin E/CDK2 and the cyclin A/CDK2 complex. The mRNA levels of p27 stay the same during cell cycle progression. The CDK inhibitor p27 is targeted for degradation when associated and phosphorylated on thr187 by an active cyclin E/CDK2 complex during the G1/S phase transition[98]. In *Rb-/-* cells the level of p27 at 48 and 72 hours is comparable to the levels in the WT cells however at 96 hours the level declines(Figure 5.2.5B). Although the levels in the WT cells do drop the effect is not as dramatic as in the *Rb-/-* cells, which is most likely due to *Rb-/-* cells having a high amount of cyclin E as WT cells have no detectable levels, the small rise in CDC25a could be (Figure 5.2.5A) enabling the cyclin E/CDK2 complex to become active.

5.2.4 Gadd45a expression and localisation in the cytoplasm in *Rb-/-* hepatocytes

The growth arrest and DNA damage inducible protein (Gadd45a) was one of the first p53 responsive genes to be identified[332]. It is turned on in response to a variety of DNA damage agents including hydrogen peroxide[333, 334]. In unpertuRbed cells the levels are high in the G1 phase of the cell cycle and decrease during S-phase. In response to DNA-damage it acts in the G2/M phase of the cell cycle binding to CDK1 removing it from cyclin B1[131]. The free cyclin B1 is removed from the nucleus and targeted for degradation thereby preventing mitosis from occurring. Hollander et al generated a Gadd45a null mouse through gene targeting and showed that a lack of Gadd45a resulted in an increase in aneuploidy[130].

Gadd45a expression in both WT and *Rb-/-* hepatocytes is low, expression peaks at 48 hours in *Rb-/-* hepatocytes followed by a decline in expression at 72 hours. WT cells show a similar pattern, but with expression beginingg at 72 hours with a higher amount present and the corresponding decline is seen at 96 hours (Figure 5.2.6). Premature

activation of Gadd45a in *Rb-/-* hepatocytes is most likely due their advanced cell cycle, as they are known to enter S-phase at 72 hours. In response to oxidative stress Gadd45a levels are known to increase, a slight increase is seen at 96 hours in the Rb-/- hepatocytes. Immunofluorescence for Gadd45a is consistent with the western blotting results. In WT hepatocytes at 72 hours expression is seen in the nucleus, with none detected in *Rb-/-* hepatocytes. At 96 hours Gadd45a was detected in both WT and *Rb-/-* hepatocytes. WT cells show clearly Gadd45a expression in the nucleus, however it appeared to be excluded from the nucleus in the *Rb-/-*cells (Figure 5.2.7).

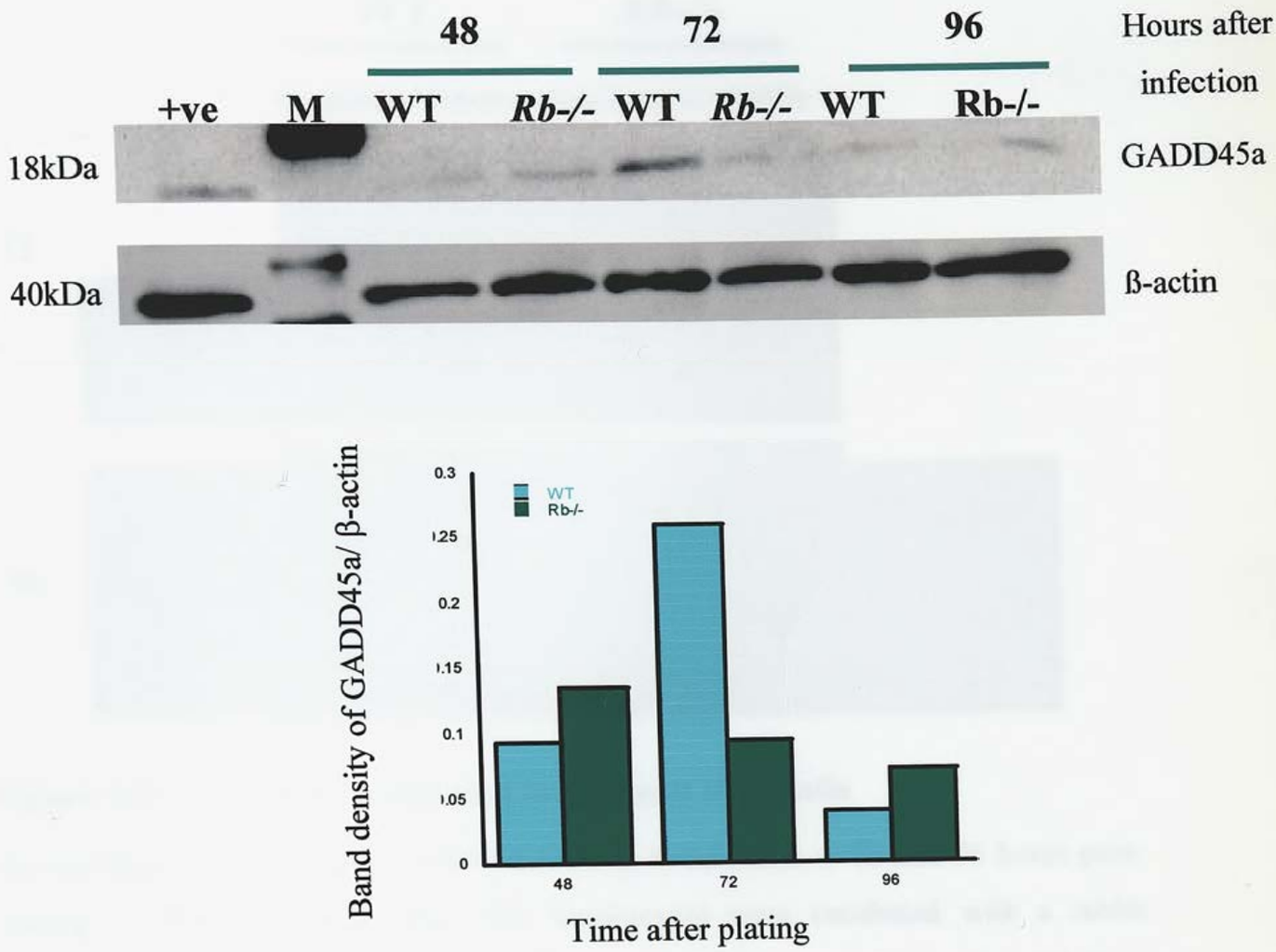


Figure 5.2.6: The expression of GADD45a in WT and *Rb-/-* cells

(A)Western blotting for Gadd45a from 48 to 96 hours post plating in WT and *Rb-/-* cells. 50μg of protein was loaded per lane on a 12% SDS gel with HELA cells used as a postive control and transferred to a PVDF membrane. A rabbit polyclonal to Gadd45a (1:1,000) was used to probe the membrane with β-actin was used as the loading control. A donkey anti-rabbit HRP conjugated (1:2,000) (Amersham) secondary was used. (B) The graph shows the densitometry analysis of the blot above. The density was measured using the quantity one software (Bio-rad™). Gadd45a denisty was normalised using β-actin density.

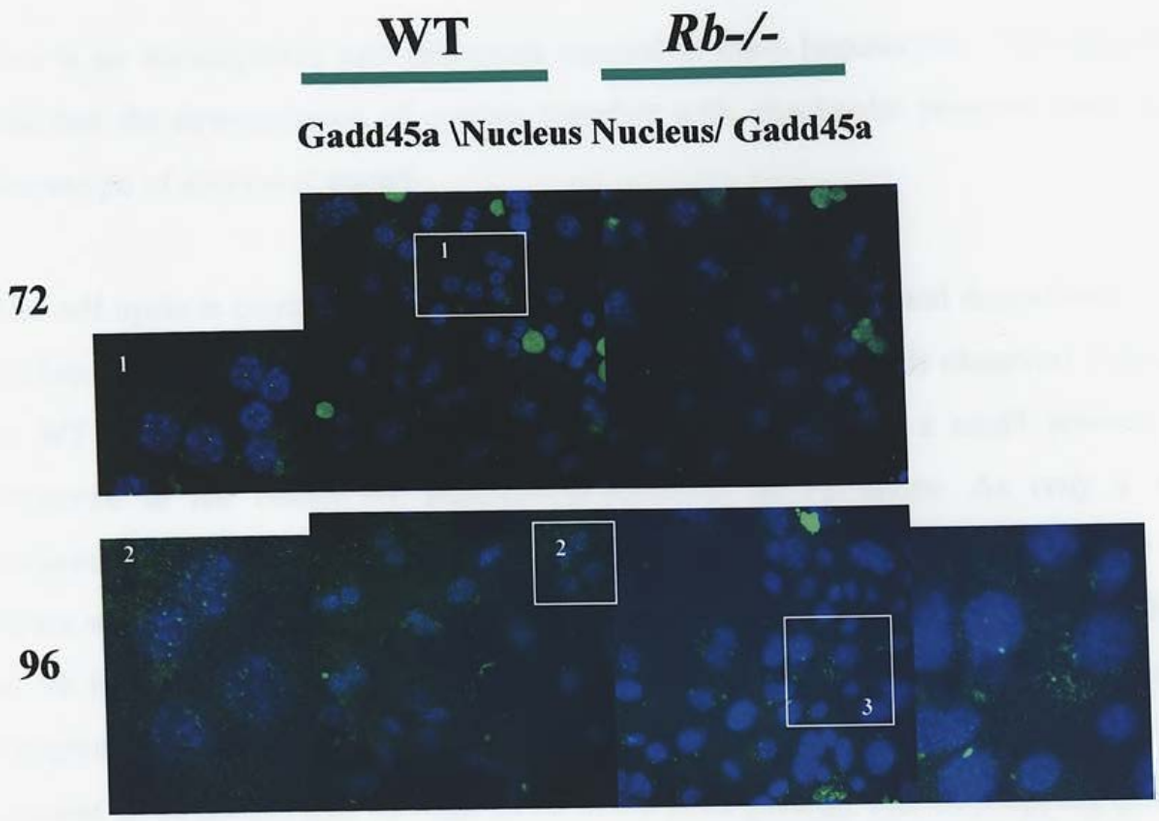


Figure 5.2.7: Gadd45 localisation in WT and *Rb-/-* cells

Immunofluoresence to show Gadd45a (Green) localisation at 72 and 96 hours post-plating in WT and *Rb-/-* cells. The hepatocytes were incubated with a rabbit polyclonal to Gadd45a (1:100) (Chemicon) followed by a goat anti-rabbit 488 fluor conjugated secondary antibody. The nuclues (Blue) was stained with TO-PRO3. The numbered boxes indicate the areas enlarged beside the respective image. The images were captured with a Zeiss axiovert confocal microscope. The experiment was repeated with consistent results.

5.3 Discussion

This is an investigation into cell cycle control in *Rb-/-* hepatocytes. The hypothesis was that the dysregulation of cyclins together with checkpoint proteins leads to the phenotype of abnormal nuclei.

The cell cycle is controlled through the systematic production and degradation of the cyclins[151, 152]. In WT cells sequential emergence of the cyclins is observed. Although in WT cells no cyclin E was detected by western blotting a small amount was observed in the nuclei by immunofluorescence at 72 hours. As only a small proportion of the cells are proliferating this may be sufficient. Cyclin A appears at 72 hours with the levels decreasing at 96 hours followed by the appearance of cyclin B1 at 96 hours (table 5.3.1). This indicates the WT hepatocytes are going through a programmed cell cycle. However in *Rb-/-* hepatocytes the three cyclins tested are all present at 48 hours right through to 96 hours post-plating. The overlapping presence of the cyclins in *Rb-/-* hepatocytes illustrates there is no control over their synthesis combined with a lack of degradation of the cyclins. Further investigation into the ubiquination pattern of the cyclins needs to be done to confirm this.

An explanation for the increase in cyclin E and A levels may be the increase in activity of E2F[283]. However both appear to be active due to their localisation in the nucleus. There are reports of an increase in cyclin E expression in many tumour cells indicating it may contribute to the development of carcinogenesis[99]

Cyclin	**Cyclin E**			**Cyclin A**			**Cyclin B**		
Time	48	72	96	48	72	96	48	72	96
WT	None detected			None	High	Low	None	None	Present
Rb-/-	Present			Low	High	High	Present		

Table 5.3.1 The expression levels of cyclin E, cyclin A and cyclin B during the cell cycle.

The phosphatase CDC25a is a regulator of both cyclin E and cyclin B1 complexes [324]. It is decreased in *Rb-/-* compared to WT hepatocytes at all timepoints tested. *Rb-/-*cells show an increase in the levels at 96 hours this combined with the high levels of cyclin E and B1 could be having a dramatic effect on the cell. The levels of p27 could be an indicator of this effect as once active, cyclin E could phosphorylates p27, inducing its degradation [98]. At 96 hours a drop in the amount of p27 is observed.

Mad2 regulates the APC ubiquitin complex. It prevents the activation of the complex in the presence of unattached kinetochores[321, 322]. Consistent with previous reports there are elevated levels of Mad2 in the *Rb-/-* hepatocytes compared to the WT hepatocytes [320]. In an unpertuRbed cell the expression of Mad2 peaks at the G2/M phase after cyclin A expression in S-phase. Observations in WT hepatocytes showed a low level of Mad2 present at 48 hours and 72 hours becoming undetectable at 96 hours. After Mad2 levels were undetectable accumulation of cyclin B1 was observed (Table 5.3.1). Cyclin B1 is not detected until Mad2 disappears indicating that both S-phase and the G2/M phase have been completed. However in the *Rb-/-* cells increased Mad2 levels were present at 48 and 72 hours compared to WT. This corresponded with cyclin B1 expression, in fact cyclin B1 was detected at all timepoints tested. The presence of Mad2 could prevent the activation of the early APC complex therefore allowing the accumulation of both cyclin B1 and cyclin A even before the cells have entered S-phase. Hernando et al reported that mitosis in *Rb-/-* cells took longer to complete, compared to WT, displaying marked differences in completing cytokinesis and showing frequent defects in chromosome segregation. This indicates that there is a delay in the degradation of securin and cyclin B1[320]. Thus an increase of Mad2 in the cells may lead to a hyperactive spindle checkpoint altering the sequence of mitotic events and the accuracy of chromosome transmission.

Time after Plating	WT	*Rb-/-*
	Mad2/Cyclin B1	Mad2/Cyclin B1
48 Hours	Present/None detected	High/High
72 Hours	Peak/ None detected	Present/ High
96 Hours	None detected/ Present	High/ High

Table 5.3.2: The expression levels of Mad2 and cyclin B at all timepoints tested.

Another regulator of the G2/M checkpoint is the DNA damage response protein, Gadd45a. It is activated in response to both elevated p53 and an increase in ROS[130]. The function of Gadd45a is to prevent the early accumulation of cyclin B1[131]. In an unstressed cell the levels are high in G1 phase of the cell cycle together with a decrease during S-phase. At 72 hours peak expression of Gadd45a is observed in the WT cells this decreases at 96 hours. However in the *Rb-/-* hepatocytes the levels of Gadd45a peak at 48 hours, although to a much lesser extent and decrease at 72 hours. This is consistent with the BRDU data[283], the WT cells entering S-phase later than the *Rb-/-* cells. In *Rb-/-* hepatocytes Gadd45a localised outside the nucleus but is in the nucleus in WT hepatocytes. This could be affecting the ability of Gadd45a to function; WT cells show no cyclin B1 until 96 hours, a time consistent with them entering mitosis. However in *Rb-/-* hepatocytes at 48, 72 and 96 hours there is a high level of expression of cyclin B1. Consistent with previous reports in the literature there is no significant difference in the number of centrosomes in WT and *Rb-/-* hepatocytes[335].

In conclusion in *Rb-/-* hepatocytes the lack of regulation of both the synthesis and degradation of the cyclins leads to a dysregulation of the cell cycle. This is coupled with an aberrant expression of checkpoint proteins responsible for maintenance of cyclin/ CDK complex activity. This superimposed on the DNA damage present in

the *Rb-/-* hepatocytes (Section 4.2.4) would predispose these hepatocytes to developing nuclear and mitotic abnormalities.

Chapter 6:

Final Discussion

The aim of this project was to understand how Rb contributes to the development of liver cancer. As Rb deletion is embryonic lethal, this project utilised the cre-lox system to remove Rb. This enabled the precise role of Rb to be analysed by comparing *Rb-/-* hepatocytes to WT hepatocytes with exactly the same genetic background. Pathways were investigated after removal of Rb that are involved in the regulation of p53, production of ROS and control of the cell cycle. The findings implicate NPM in the stabilisation of p53 through a previously unknown mechanism, show how increases in $p19^{ARF}$ levels could lead to increases in ROS and demonstrate how there is an absence of a cell cycle arrest in response to DNA damage in *Rb-/-* hepatocytes.

6.1 A novel mechanism for the transient stabilisation of p53 in *Rb-/-* hepatocytes

The stabilisation of p53 in *Rb-/-* hepatocytes has been reported[283]. This loss of *Rb* deregulates the transcription factor E2F1 increasing its transactivation activity[283, 292]. This would allow E2F to switch on the transcription of $p19^{ARF}$ [56]. $p19^{ARF}$ is reported to bind to and sequester MDM2 in the nucleolus leading to the stabilisation of p53 [229]. In *Rb-/-* hepatocytes, evidence is presented to support the hypothesis that $p19^{ARF}$ is stabilising p53. Firstly, there are high levels of $p19^{ARF}$ present in the *Rb-/-* cells prior to the upregulation of p53. Secondly, MDM2 localises to the nucleolus at 72 and 96 hours and binds to $p19^{ARF}$ at 72 hours post-plating. Thirdly, the levels of p53 peak at 72 hours.

In addition, an increase in ROS-induced DNA damage is observed following loss of Rb. In response to certain types of DNA damage, phosphorylation of p53 at ser15 is

induced by ATR, a DNA damage response kinase[179]. This disrupts the binding with MDM2, stabilising p53. $p19^{ARF}$ activation of ATR is reported although the mechanism has not been defined[235]. *Rb-/-* hepatocytes show phosphorylation of p53 at ser15 together with both p53 and ATR localisation to the nucleolus. Removal of this phosphorylation by caffeine, a known inhibitor of ATR, demonstrates that ATR is responsible for this phosphorylation of p53. Localisation of p53 in the nucleolus at 96 hours coupled with binding to $p19^{ARF}$ at 48 and 72 hours post-plating infers that ARF may be moving p53 to the nucleolus to bring it into close proximity with ATR. This enables further phosphorylation and stabilisation of p53. The induction of p53 sumoylation by $p19^{ARF}$ in the nucleolus with MDM2 present corroborates this argument[201].

The ROS produced in the *Rb-/-* hepatocytes could be having opposing effects on the levels of p53 stabilised. ROS have been reported to induce dimers of $p14^{ARF}$, the human form of $p19^{ARF}$ [286]. At 96 hours post-plating dimer forms of $p19^{ARF}$ are present in the *Rb-/-* hepatocytes. This dimerisation of $p19^{ARF}$, not previously reported in the mouse form of ARF, could be occurring in response to the presence of ROS. Supporting evidence for this is the presence of β-mercaptoethanol, a reducing agent, decreases the amount of $p19^{ARF}$ dimer bands. However, NPM, a $p19^{ARF}$ binding partner in *Rb-/-* hepatocytes, is known to promote the dimerisation of proteins. MDM2 and NPM compete for the same binding site within $p19^{ARF}$ [285] and dimerisation of $p19^{ARF}$ decreases the affinity of $p19^{ARF}$ for MDM2[286]. In *Rb-/-* hepatocytes, a combination of NPM binding and an increase in ROS could be inducing $p19^{ARF}$ dimers. This would allow NPM to bind to $p19^{ARF}$, releasing MDM2 and thus decreasing the stabilisation of p53. NPM promotes S-phase, thus the inhibition of $p19^{ARF}$ mediated stabilisation of p53 by NPM would allow cell cycle re-entry. NPM has been previously reported to set a threshold for p53 response to UV. In this situation, that is, in *Rb-/-* hepatocytes, NPM could also be moderating the p53 effect by binding to $p19^{ARF}$, resulting in a decrease in p53 stabilisation. Both NPM and $p19^{ARF}$ have been found upregulated in hepatocellular carcinoma[241, 260]. Combining this with a loss of control of the Rb pathway in a high percentage of hepatocellular carcinoma infers this *in vitro* system may reflect the *in vivo* state[260].

Liver cancers with a loss of both Rb and p53 are known to be particularly aggressive. In an Rb deficient background an important role for $p19^{ARF}$ is reported. Rb+/- $p19^{ARF}$ -/- mice develop pituitary tumours at a much higher frequency than either *Rb*+/- mice alone or *Rb*+/-p53-/-. Both *Rb*+/- and *Rb*+/- p53-/- mice show an increase in the levels of $p19^{ARF}$ [336]. Thus on a Rb deficient background the upregulation of $p19^{ARF}$ appears to provide a protective mechanism. In these hepatocytes which have lost Rb, there is also an upregulation of $p19^{ARF}$. The *Rb-/-* hepatocytes have an increase in proliferation, and selective pressure in the hepatocytes could lead to choosing cells with a higher proliferation potential such as those with mutated p53. Therefore it was important to investigate the mechanism leading to the transient increase in p53 in *Rb-/-* hepatocytes.

The suggested pathway is as follows: Loss of *Rb* enables the transcription factor E2F1 to upregulate $p19^{ARF}$. ARF binds to MDM2 relieving p53 of MDM2 mediated degradation. An upregulation in ROS induces the dimerisation of $p19^{ARF}$ and may impact on the activation of ATR through inducing DNA damage. As the dimerisation of $p19^{ARF}$ eliminates its ability to stabilise p53, this allows NPM to bind to $p19^{ARF}$, release MDM2 and promote S-phase. The outcome is a decrease in the levels of p53 (Figure 6.1). In conclusion, these results show a novel mechanism for a transient stabilisation of p53 in *Rb-/-* hepatocytes.

6.2. The response to the upregulation of ROS in *Rb-/-* hepatocytes

An increase in the number of chromosomal and nuclear abnormalities in *Rb-/-* compared to WT hepatocytes[283] led to DNA damage in the hepatocytes being investigated. As a link between the transcription factor E2F and the production of ROS was established previously, the levels of ROS in *Rb-/-* hepatocytes were

assessed and were higher than WT[291]. On an Rb deficient background, levels of ROS, AP sites and 8-oxo-dG have not been previously determined.

The proposed pathway for the increased production of ROS is the removal of Rb which leads to an increase in $p19^{ARF}$, activating ATR. ATR activates Chk1 on ser317 through phosphorylation. Activated Chk1 has been previously reported as phosphorylating the transcription factor NF-κB on thr504, inactivating its transactivation function (Figure 4.3.1). NF-κB is known to regulate MnSOD expression. MnSOD levels were found decreased in *Rb-/-* hepatocytes compared to WT. MnSOD is a mitochondrial enzyme whose function is to eliminate the ROS. Therefore a decrease in MnSOD could potentially lead to an increase in ROS in hepatocytes (Figure 6.1).

In addition to the increase in ROS, compared to WT both the levels of 8-oxo-dG and AP sites are found increased in *Rb-/-* hepatocytes. 8-oxo-dG is the most common mutagenic DNA product formed as a result of ROS increases. Thus this would correspond with the increase in ROS found in the hepatocytes. In fact, both the levels of 8-oxo-dG and the levels of ROS are significantly different between *Rb-/-* and WT cells at 72 hours post-plating. This infers that this DNA damage could result from increased levels of ROS. Levels of 8-oxo-dG in HCC have been assessed before, however 8-oxo-dG levels in non-tumour tissue were found to be above that in tumour tissue. The discrepancy could be explained in two ways. First, non-tumour tissue was more closely associated with the inflammatory cells. Second, the non-tumour and tumour tissue in this study was not from the same individual [337].

The results for the *Rb-/-* hepatocytes may help to explain why in the absence of inflammation mice expressing the HCV core protein show an increase in oxidative DNA damage[338]. HCV core protein is able to decrease the levels of RB and increase the activity of E2F1[11]. Inactivation of the RB pathway in HCC is well established. These results show that this may lead to an increase in ROS and ROS induced DNA damage. This increase, in combination with macrophages which infiltrate the liver post-viral infection that have the ability to produce ROS[339], would be extremely

deleterious for the liver. Transgenic mice that express HBV show chronic necroinflammation, an increase in hepatic oxidative damage and an increase in the rate of development of HCC. However a 100% liver cancer rate is observed in these mice when they are co-expressed with c-Myc and TGFα[340]. Cells that express c-myc have shown an upregulation of E2F1, which corresponded to an increase in ROS[291]. The fact that HBV alone was not sufficient to induce cancer but required c-myc and TGFα[340], further substantiates the argument that the ROS and the ROS induced damage in the *Rb-/-* hepatocytes could contribute to the development of HCC.

Pickering et al reported that E2F1 induced double strand breaks in their system independent of an increase in ROS, ATM/ Chk2, p53 or caspase-3 activity. However the levels of ROS were not directly measured, rather, the number of γH2A.X positive cells in the presence or absence of N-acetylcysteine, an antioxidant, was used[292]. This is in contrast with results presented herein and Tanaka et al, which both show an increase of ROS with an increase in E2F activity[291]. The method used by Pickering et al may not be as sensitive as the assays used either of these studies, which directly measure the levels of ROS.

γH2A.X was also used in this study, but as a marker of DSBs and an increase was found between *Rb-/-*and WT hepatocytes. In the *Rb-/-* hepatocytes caffeine did not eliminate all the γH2A.X phosphorylation but did eliminate phosphorylation of both p53 on ser15 and Chk1 on ser317. This could prevent p53 and Chk1 from eliciting their response to DNA damage. As other kinases besides ATR and ATM are able to phosphorylate H2A.X, damage may still be present and this could explain why the phosphorylation is not totally removed.

In conclusion the *Rb-/-* hepatocytes have an increase in ROS induced DNA damage that could contribute to the stabilisation of p53.

6.3 A lack of cell cycle arrest in *Rb-/-* hepatocytes

The normal response of WT cells to DNA damage is the induction of p53 leading to a halt in the cell cycle or apoptosis. Hepatocytes' response to DNA damage following p53 induction is not apoptosis, but arrest of the cell cycle [272]. In *Rb-/-* hepatocytes, the increase in ROS induced DNA damage does not lead to an arrest in the cell cycle. Progression of the cycle is normally halted at checkpoints that are activated if the DNA is found to haRbour mutations. *Rb-/-* cells are reported to evade checkpoints in the presence of DNA damage[244]. Important checkpoint proteins include ATR/ATM, Chk1, p53, CDC25A and Gadd45a [318]

Perfusing the liver primes the hepatocytes to enter G_1 therefore it is essentially a synchronised population. During the cell cycle, the emergence of the cyclins should follow a defined pattern. However in *Rb-/-* hepatocytes, Cyclin E, cyclin A and cyclin B were present at all timepoints tested, in contrast to the WT cells. The WT cells show a pattern of expression that reflects the BRDU data and therefore the stages of the cell cycle. This is consistent with *Rb-/-* fibroblasts, which also show an increase in cyclin E and A expression [341]. Having all three cyclins constantly present could lead to early progression to the next stage of the cell cycle as the limiting factor is available, thus enabling the *Rb-/-* hepatocytes to bypass certain cellular checkpoints. In addition, HBV and HCV effect the regulation of cyclins in hepatocytes. HCV core protein can upregulate the expression of cyclin E[342]. The cyclin A gene is on the HBV integration site. This can result in the N-terminal sequence of cyclin A being replaced with a viral sequence rendering the protein resistant to ubiquination and degradation via the proteasome pathway [343], similar to the outcome observed in the *Rb-/-* hepatocytes. An overexpression of cyclin E and CDK2 is implicated in promoting the progression of HCC [344]. This all demonstrates how important the proper regulation of the cyclins is in hepatocytes.

The phosphorylation of CDC25A by Chk1 is a rapid mechanism to halt the cell cycle as it induces the degradation of CDC25A[325]. This is prior to the activation of the p53/p21 pathway. CDC25A is an important mediator at two points of the cell cycle; it activates cyclin E-CDK2 at the G1/S and cyclin B1/CDK1 at G2/M transition allowing the initiation of mitosis[324]. *Rb-/-* hepatocytes show a decrease in the expression of CDC25A compared to WT. Relocalisation and activation of ATR in *Rb-/-*hepatocytes with the corresponding phosphorylation on ser317 of Chk1 implies that Chk1 is inducing the degradation of CDC25A. However the levels of CDC25A begin to increase at 96 hours post-plating. This may be due to the phase of the cell cycle or, as CDC25A is an E2F responsive gene[345], the levels of activated Chk1 may no longer be sufficient to induce degradation of all of the CDC25A. The order of CDC25A expression is opposite to p53 expression. A study observing the levels of CDC25A in liver tissue with HCV noted low levels of expression in cirrhotic tissue. In the corresponding HCC an increase in CDC25A was correlated with poor undifferentiated phenotypes[346]. Early stages of the disease have a more robust response to DNA damage and could be inducing the degradation of CDC25A. The high levels observed in both later stages of HCC and later timepoints in *Rb-/-* hepatocytes might be an indicator that the hepatocytes are losing the capacity to respond to the damage.

*Rb-/-*hepatocytes show a transient increase in p53. The p53 produced has transactivation function and induces expression of the cyclin-CDK inhibitor, p21 [283]. However another p53 responsive gene not upregulated is Gadd45a. In fact, the Gadd45a promoter is responsive to both p53 and ROS, specifically hydrogen peroxide. There is no increase in Gadd45a expression in *Rb-/-* hepatocytes compared to WT. Gadd45a functions in the nucleus at the G2/M transition and is involved in cyclin control. NPM, the protein previously implicated in p53 stabilisation also functions as a nuclear transport protein. One protein NPM is responsible for transporting to the nucleus is Gadd45a [347]. Localisation is crucial for Gadd45a function as it binds to CDK1 in the nucleus, removing it from cyclin B1. WT hepatocytes show Gadd45a inside the nucleus while in *Rb-/-* hepatocytes it is on the periphery of the nucleus. An explanation for this could be the ROS induced dimers of

ARF stimulate it to bind to NPM over MDM2. This binding of NPM to ARF sequesters NPM away from Gadd45a. A decrease in Gadd45a mRNA levels in HCC compared to matched cirrhosis controls have been found[348]. This supports the idea that a loss of expression of GADD45a, which regulates the cyclins, may be important in the progression of the disease.

In contrast to the movement of Gadd45a, there is no increase in centrosome numbers in *Rb-/-* hepatocytes, which is consistent with previous reports[335]. NPM is phosphorylated by Cyclin E/CDK2 phosphorylate during G1 phase.[97] This dissociates it from the centrosome allowing the centrosome to duplicate. Centrosome duplication and DNA replication are co-ordinated events during the cell cycle. Reassociation of NPM with the centrosome at the end of mitosis ensures the centrosome is duplicated once per cycle[97].

Degradation of the cyclins is another way in which the cyclins are regulated. It occurs in the proteasome following the ubiquination of certain residues in the F-box part of their C-terminus. Ubiquitin ligases, such as APC attach ubiquination tags. During mitosis APC targets cyclin B for degradation. This signals the end of mitosis. Mad2 is the negative regulator of the APC it prevents activation of the APC by binding to and sequestering CDC20, the activator of the APC. *Rb-/-* hepatocytes show an increase in expression of Mad2. This is consistent with previous reports [320] and the lack of APC activity may contribute the continual presence of the cyclins. The presence of Mad2 would extend the length of mitosis through inhibiting the degradation of cyclin B and activating the mitotic checkpoint.

In conclusion, lack of regulation of the cyclins combined with an absence of checkpoints enables the cell to continue through the cell cycle even in the presence of DNA damage.

6.4 Conclusion

The aim of this work was to assess the contribution Rb has to the development of liver cancer. This role of Rb was evaluated using an *in vitro* system that consisted of

primary murine hepatocytes which used conditional gene targeting to remove Rb. The main aims of this thesis were to understand how p53 was transiently stabilised, assess the extent and cause of DNA damage and evaluate the state of cell cycle control in *Rb-/-* hepatocytes. The findings presented showed that an upregulation of $p19^{ARF}$ contributed to the transient stabilisation of p53. This is further supported by $p19^{ARF}$ binding to MDM2 coinciding with p53 stabilisation and NPM binding to $p19^{ARF}$ corresponding to a decrease in stabilisation of p53. For the first time on a Rb deficient background, the levels of ROS, 8-oxo-dG sites and AP sites are found increased. The DNA damage found is correlated with an upregulation of ROS and a pathway for the production of ROS is proposed. This pathway includes $p19^{ARF}$, ATR, Chk1 and MnSOD. Cell cycle control is found lacking in the *Rb-/-* hepatocytes. In conclusion, the increase in DNA damage found should lead to an arrest of the cell cycle, but when the checkpoint proteins such as ATR, Chk1, $p19^{ARF}$ and p53 were analysed they had only a transient response to the DNA damage in *Rb-/-* hepatocytes. This superimposed on a background of an atypical cell cycle that has a lack of regulation of cyclins and p53 show how *Rb* loss could contribute to the development of liver cancer.

6.5 Future work

The addition of siRNA to $p19^{ARF}$ would determine if is directly responsible for the stabilisation of p53. Analysis of the phosphorylation status of NF-κB and binding to the MnSOD promoter would reveal if NF-κB is responsible for the downregulation of MnSOD. The addition of antioxidants would ascertain the exact contribution of ROS to DNA damage in *Rb-/-* hepatocytes. Analysis of the ubiquination status of the cyclins would reveal if it is both their synthesis and degradation is dysregulated in the *Rb-/-* hepatocytes. Further expansion on this work would be to look at other cell types and ascertain if the same pathways are abnormal on an *Rb* deficient background.

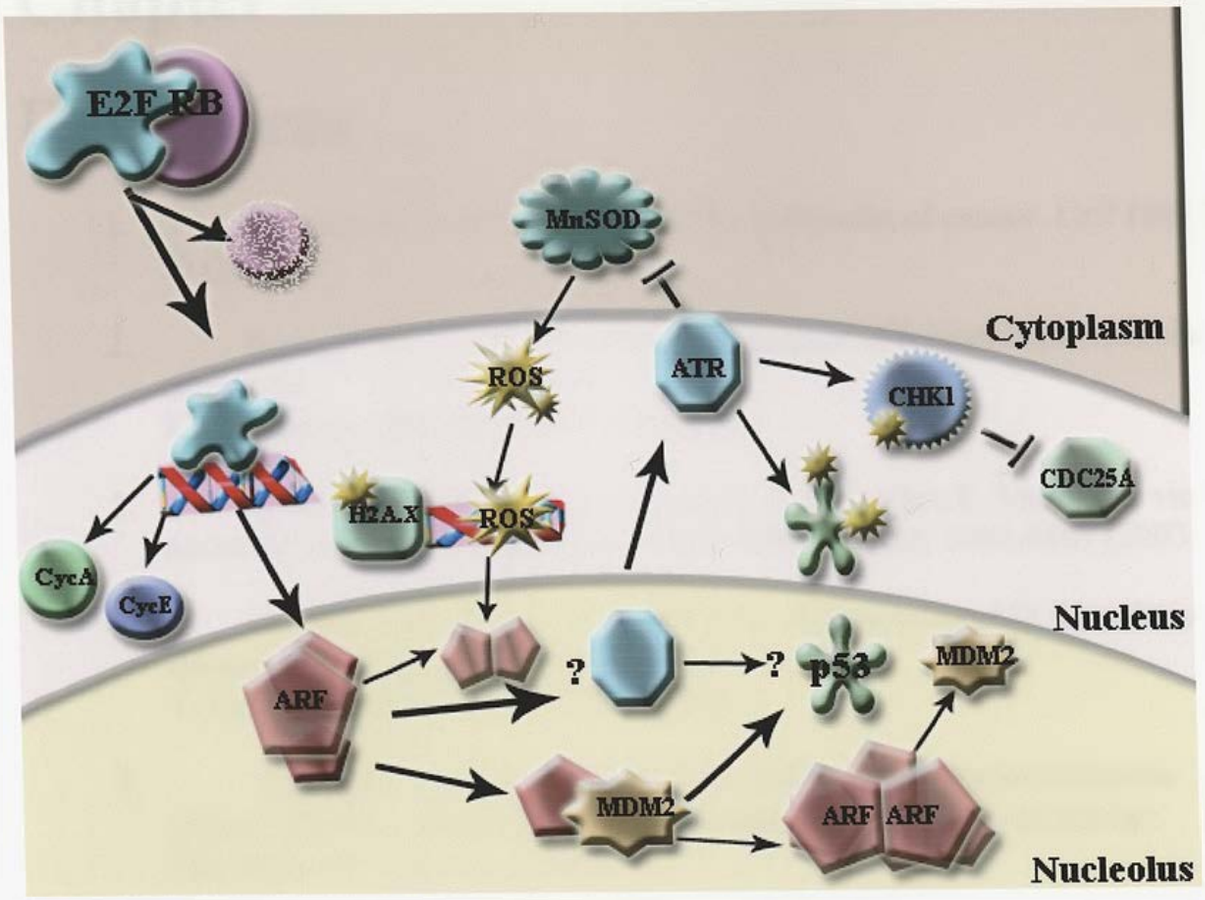


Figure 6.1- The impact of the loss of *Rb*

The lack of cell cycle control after loss of *Rb* induced on a background of an increase in DNA damage and absence of proper regulation of p53 predisposes the hepatocytes to neoplastic transformation

Chapter 7:

References

1. Hanahan,D. & Weinberg,R.A. The hallmarks of cancer. *Cell* **100**, 57-70 (2000).

2. Wang,X.W. *et al.* Molecular pathogenesis of human hepatocellular carcinoma
1. *Toxicology* **181-182**, 43-47 (2002).

3. Block,T.M., Mehta,A.S., Fimmel,C.J., & Jordan,R. Molecular viral oncology of hepatocellular carcinoma. *Oncogene* **22**, 5093-5107 (2003).

4. Kensler,T.W., Qian,G.S., Chen,J.G., & Groopman,J.D. Translational strategies for cancer prevention in liver
1. *Nat. Rev. Cancer* **3**, 321-329 (2003).

5. Azechi,H. *et al.* Disruption of the p16/cyclin D1/retinoblastoma protein pathway in the majority of human hepatocellular carcinomas. *Oncology* **60**, 346-354 (2001).

6. Edamoto,Y. *et al.* Alterations of RB1, p53 and Wnt pathways in hepatocellular carcinomas associated with hepatitis C, hepatitis B and alcoholic liver cirrhosis. *Int. J. Cancer* **106**, 334-341 (2003).

7. Ashida,K. *et al.* Loss of heterozygosity of the retinoblastoma gene in liver cirrhosis accompanying hepatocellular carcinoma. *J. Cancer Res. Clin. Oncol.* **123**, 489-495 (1997).

8. Tan,L. *et al.* Expression of p28GANK and its correlation with RB in human hepatocellular carcinoma. *Liver Int.* **25**, 667-676 (2005).

9. Lee,J.O., Russo,A.A., & Pavletich,N.P. Structure of the retinoblastoma tumour-suppressor pocket domain bound to a peptide from HPV E7. *Nature* **391**, 859-865 (1998).

10. Munakata,T., Nakamura,M., Liang,Y., Li,K., & Lemon,S.M. Down-regulation of the retinoblastoma tumor suppressor by the hepatitis C virus NS5B RNA-dependent RNA polymerase. *Proc. Natl. Acad. Sci. U. S. A* **102**, 18159-18164 (2005).

11. Cho,J. *et al.* HCV core protein modulates Rb pathway through pRb down-regulation and E2F-1 up-regulation
4. *Biochim. Biophys. Acta* **1538**, 59-66 (2001).

12. Choi,B.H., Choi,M., Jeon,H.Y., & Rho,H.M. Hepatitis B viral X protein overcomes inhibition of E2F1 activity by pRb on the human Rb gene promoter. *DNA Cell Biol.* **20**, 75-80 (2001).

13. Jacks,T. *et al.* Effects of an Rb mutation in the mouse. *Nature* **359**, 295-300 (1992).

14. Clarke,A.R. *et al.* Requirement for a functional Rb-1 gene in murine development. *Nature* **359**, 328-330 (1992).

15. Sternberg,N., Sauer,B., Hoess,R., & Abremski,K. Bacteriophage P1 cre gene and its regulatory region. Evidence for multiple promoters and for regulation by DNA methylation. *J. Mol. Biol.* **187**, 197-212 (1986).

16. Argos,P. *et al.* The integrase family of site-specific recombinases: regional similarities and global diversity. *EMBO J.* **5**, 433-440 (1986).

17. Mack,A., Sauer,B., Abremski,K., & Hoess,R. Stoichiometry of the Cre recombinase bound to the lox recombining site. *Nucleic Acids Res.* **20**, 4451-4455 (1992).

18. Vooijs,M., van,d., V, te,R.H., & Berns,A. Flp-mediated tissue-specific inactivation of the retinoblastoma tumor suppressor gene in the mouse. *Oncogene* **17**, 1-12 (1998).

19. Friend,S.H. *et al.* Deletions of a DNA sequence in retinoblastomas and mesenchymal tumors: organization of the sequence and its encoded protein. *Proc. Natl. Acad. Sci. U. S. A* **84**, 9059-9063 (1987).

20. Friend,S.H. *et al.* A human DNA segment with properties of the gene that predisposes to retinoblastoma and osteosarcoma. *Nature* **323**, 643-646 (1986).

21. Morris,N.R., Efimov,V.P., & Xiang,X. Nuclear migration, nucleokinesis and lissencephaly. *Trends Cell Biol.* **8**, 467-470 (1998).

22. Hu,N. *et al.* Heterozygous Rb-1 delta 20/+mice are predisposed to tumors of the pituitary gland with a nearly complete penetrance. *Oncogene* **9**, 1021-1027 (1994).

23. Wu,L. *et al.* Extra-embryonic function of Rb is essential for embryonic development and viability. *Nature* **421**, 942-947 (2003).

24. Sage,J., Miller,A.L., Perez-Mancera,P.A., Wysocki,J.M., & Jacks,T. Acute mutation of retinoblastoma gene function is sufficient for cell cycle re-entry. *Nature* **424**, 223-228 (2003).

25. Classon,M. & Dyson,N. p107 and p130: versatile proteins with interesting pockets. *Exp. Cell Res.* **264**, 135-147 (2001).

26. Mulligan,G. & Jacks,T. The retinoblastoma gene family: cousins with overlapping interests. *Trends Genet.* **14**, 223-229 (1998).

27. Beijersbergen,R.L., Carlee,L., Kerkhoven,R.M., & Bernards,R. Regulation of the retinoblastoma protein-related p107 by G1 cyclin complexes. *Genes Dev.* **9**, 1340-1353 (1995).

28. Cobrinik,D., Whyte,P., Peeper,D.S., Jacks,T., & Weinberg,R.A. Cell cycle-specific association of E2F with the p130 E1A-binding protein. *Genes Dev.* **7**, 2392-2404 (1993).

29. Smith,E.J., Leone,G., DeGregori,J., Jakoi,L., & Nevins,J.R. The accumulation of an E2F-p130 transcriptional repressor distinguishes a G0 cell state from a G1 cell state. *Mol. Cell Biol.* **16**, 6965-6976 (1996).

30. Paggi,M.G. & Giordano,A. Who is the boss in the retinoblastoma family? The point of view of Rb2/p130, the little brother. *Cancer Res.* **61**, 4651-4654 (2001).

31. Cobrinik,D. *et al.* Shared role of the pRB-related p130 and p107 proteins in limb development. *Genes Dev.* **10**, 1633-1644 (1996).

32. Lipinski,M.M. & Jacks,T. The retinoblastoma gene family in differentiation and development. *Oncogene* **18**, 7873-7882 (1999).

33. Stevaux,O. & Dyson,N.J. A revised picture of the E2F transcriptional network and RB function. *Curr. Opin. Cell Biol.* **14**, 684-691 (2002).

34. Logan,N. *et al.* E2F-7: a distinctive E2F family member with an unusual organization of DNA-binding domains. *Oncogene* **23**, 5138-5150 (2004).

35. Logan,N. *et al.* E2F-8: an E2F family member with a similar organization of DNA-binding domains to E2F-7. *Oncogene* **24**, 5000-5004 (2005).

36. Di Stefano,L., Jensen,M.R., & Helin,K. E2F7, a novel E2F featuring DP-independent repression of a subset of E2F-regulated genes. *EMBO J.* **22**, 6289-6298 (2003).

37. Christensen,J. *et al.* Characterization of E2F8, a novel E2F-like cell-cycle regulated repressor of E2F-activated transcription. *Nucleic Acids Res.* **33**, 5458-5470 (2005).

38. Maiti,B. *et al.* Cloning and characterization of mouse E2F8, a novel mammalian E2F family member capable of blocking cellular proliferation. *J. Biol. Chem.* **280**, 18211-18220 (2005).

39. Girling,R. *et al.* A new component of the transcription factor DRTF1/E2F. *Nature* **362**, 83-87 (1993).

40. Wu,L. *et al.* The E2F1-3 transcription factors are essential for cellular proliferation. *Nature* **414**, 457-462 (2001).

41. Helin,K., Harlow,E., & Fattaey,A. Inhibition of E2F-1 transactivation by direct binding of the retinoblastoma protein. *Mol. Cell Biol.* **13**, 6501-6508 (1993).

42. Lees,J.A. *et al.* The retinoblastoma protein binds to a family of E2F transcription factors. *Mol. Cell Biol.* **13**, 7813-7825 (1993).

43. Ross,J.F., Liu,X., & Dynlacht,B.D. Mechanism of transcriptional repression of E2F by the retinoblastoma tumor suppressor protein. *Mol. Cell* **3**, 195-205 (1999).

44. Brehm,A. *et al.* Retinoblastoma protein recruits histone deacetylase to repress transcription. *Nature* **391**, 597-601 (1998).

45. Strobeck,M.W. *et al.* BRG-1 is required for RB-mediated cell cycle arrest. *Proc. Natl. Acad. Sci. U. S. A* **97**, 7748-7753 (2000).

46. Hijmans,E.M., Voorhoeve,P.M., Beijersbergen,R.L., 't Veer,L.J., & Bernards,R. E2F-5, a new E2F family member that interacts with p130 in vivo. *Mol. Cell Biol.* **15**, 3082-3089 (1995).

47. Beijersbergen,R.L. *et al.* E2F-4, a new member of the E2F gene family, has oncogenic activity and associates with p107 in vivo. *Genes Dev.* **8**, 2680-2690 (1994).

48. Ginsberg,D. *et al.* E2F-4, a new member of the E2F transcription factor family, interacts with p107. *Genes Dev.* **8**, 2665-2679 (1994).

49. Vairo,G., Livingston,D.M., & Ginsberg,D. Functional interaction between E2F-4 and p130: evidence for distinct mechanisms underlying growth suppression by different retinoblastoma protein family members. *Genes Dev.* **9**, 869-881 (1995).

50. Lindeman,G.J., Gaubatz,S., Livingston,D.M., & Ginsberg,D. The subcellular localization of E2F-4 is cell-cycle dependent. *Proc. Natl. Acad. Sci. U. S. A* **94**, 5095-5100 (1997).

51. Dyson,N. The regulation of E2F by pRB-family proteins. *Genes Dev.* **12**, 2245-2262 (1998).

52. Takahashi,Y., Rayman,J.B., & Dynlacht,B.D. Analysis of promoter binding by the E2F and pRB families in vivo: distinct E2F proteins mediate activation and repression. *Genes Dev.* **14**, 804-816 (2000).

53. Dahiya,A., Wong,S., Gonzalo,S., Gavin,M., & Dean,D.C. Linking the Rb and polycomb pathways. *Mol. Cell* **8**, 557-569 (2001).

54. Narita,M. *et al.* Rb-mediated heterochromatin formation and silencing of E2F target genes during cellular senescence. *Cell* **113**, 703-716 (2003).

55. Leone,G. *et al.* Identification of a novel E2F3 product suggests a mechanism for determining specificity of repression by Rb proteins. *Mol. Cell Biol.* **20**, 3626-3632 (2000).

56. Aslanian,A., Iaquinta,P.J., Verona,R., & Lees,J.A. Repression of the Arf tumor suppressor by E2F3 is required for normal cell cycle kinetics. *Genes Dev.* **18**, 1413-1422 (2004).

57. Cartwright,P., Muller,H., Wagener,C., Holm,K., & Helin,K. E2F-6: a novel member of the E2F family is an inhibitor of E2F-dependent transcription. *Oncogene* **17**, 611-623 (1998).

58. Trimarchi,J.M., Fairchild,B., Wen,J., & Lees,J.A. The E2F6 transcription factor is a component of the mammalian Bmi1-containing polycomb complex. *Proc. Natl. Acad. Sci. U. S. A* **98**, 1519-1524 (2001).

59. Vandel,L. & Kouzarides,T. Residues phosphorylated by TFIIH are required for E2F-1 degradation during S-phase. *EMBO J.* **18**, 4280-4291 (1999).

60. Campanero,M.R. & Flemington,E.K. Regulation of E2F through ubiquitin-proteasome-dependent degradation: stabilization by the pRB tumor suppressor protein. *Proc. Natl. Acad. Sci. U. S. A* **94**, 2221-2226 (1997).

61. Marzio,G. *et al.* E2F Family Members Are Differentially Regulated by Reversible Acetylation. *J. Biol. Chem.* **275**, 10887-10892 (2000).

62. Martinez-Balbas,M.A., Bauer,U.M., Nielsen,S.J., Brehm,A., & Kouzarides,T. Regulation of E2F1 activity by acetylation. *EMBO J.* **19**, 662-671 (2000).

63. Muller,H. *et al.* E2Fs regulate the expression of genes involved in differentiation, development, proliferation, and apoptosis. *Genes Dev.* **15**, 267-285 (2001).

64. Nelson,D.A., Krucher,N.A., & Ludlow,J.W. High molecular weight protein phosphatase type 1 dephosphorylates the retinoblastoma protein. *J. Biol. Chem.* **272**, 4528-4535 (1997).

65. Luger,K. Structure and dynamic behavior of nucleosomes. *Curr. Opin. Genet. Dev.* **13**, 127-135 (2003).

66. Magnaghi-Jaulin,L. *et al.* Retinoblastoma protein represses transcription by recruiting a histone deacetylase. *Nature* **391**, 601-605 (1998).

67. Dahiya,A., Gavin,M.R., Luo,R.X., & Dean,D.C. Role of the LXCXE binding site in Rb function. *Mol. Cell Biol.* **20**, 6799-6805 (2000).

68. Ferreira,R. *et al.* Cell cycle-dependent recruitment of HDAC-1 correlates with deacetylation of histone H4 on an Rb-E2F target promoter. *EMBO Rep.* **2**, 794-799 (2001).

69. Nielsen,S.J. *et al.* Rb targets histone H3 methylation and HP1 to promoters. *Nature* **412**, 561-565 (2001).

70. Yamane,K. *et al.* JHDM2A, a JmjC-Containing H3K9 Demethylase, Facilitates Transcription Activation by Androgen Receptor. *Cell*(2006).

71. Yoshimoto,T. *et al.* The arginine methyltransferase PRMT2 binds RB and regulates E2F function. *Exp. Cell Res.*(2006).

72. Vandel,L. *et al.* Transcriptional repression by the retinoblastoma protein through the recruitment of a histone methyltransferase. *Mol. Cell Biol.* **21**, 6484-6494 (2001).

73. Hamamoto,R. *et al.* SMYD3 encodes a histone methyltransferase involved in the proliferation of cancer cells. *Nat. Cell Biol.* **6**, 731-740 (2004).

74. Esteller,M. CpG island methylation and histone modifications: biology and clinical significance. *Ernst. Schering. Res. Found. Workshop*115-126 (2006).

75. Kaneda,M. *et al.* Essential role for de novo DNA methyltransferase Dnmt3a in paternal and maternal imprinting. *Nature* **429**, 900-903 (2004).

76. Pradhan,S. & Kim,G.D. The retinoblastoma gene product interacts with maintenance human DNA (cytosine-5) methyltransferase and modulates its activity. *EMBO J.* **21**, 779-788 (2002).

77. Trouche,D., Le Chalony,C., Muchardt,C., Yaniv,M., & Kouzarides,T. RB and hbrm cooperate to repress the activation functions of E2F1. *Proc. Natl. Acad. Sci. U. S. A* **94**, 11268-11273 (1997).

78. Dunaief,J.L. *et al.* The retinoblastoma protein and BRG1 form a complex and cooperate to induce cell cycle arrest. *Cell* **79**, 119-130 (1994).

79. Sherr,C.J. D-type cyclins. *Trends Biochem. Sci.* **20**, 187-190 (1995).

80. Meyerson,M. & Harlow,E. Identification of G1 kinase activity for cdk6, a novel cyclin D partner. *Mol. Cell Biol.* **14**, 2077-2086 (1994).

81. Matsushime,H. *et al.* D-type cyclin-dependent kinase activity in mammalian cells. *Mol. Cell Biol.* **14**, 2066-2076 (1994).

82. Kato,J., Matsushime,H., Hiebert,S.W., Ewen,M.E., & Sherr,C.J. Direct binding of cyclin D to the retinoblastoma gene product (pRb) and pRb phosphorylation by the cyclin D-dependent kinase CDK4. *Genes Dev.* **7**, 331-342 (1993).

83. Weinberg,R.A. The retinoblastoma protein and cell cycle control. *Cell* **81**, 323-330 (1995).

84. Herber,B., Truss,M., Beato,M., & Muller,R. Inducible regulatory elements in the human cyclin D1 promoter. *Oncogene* **9**, 2105-2107 (1994).

85. Muller,H. *et al.* Cyclin D1 expression is regulated by the retinoblastoma protein. *Proc. Natl. Acad. Sci. U. S. A* **91**, 2945-2949 (1994).

86. Albanese,C. *et al.* Transforming p21ras mutants and c-Ets-2 activate the cyclin D1 promoter through distinguishable regions. *J. Biol. Chem.* **270**, 23589-23597 (1995).

87. Agami,R. & Bernards,R. Distinct initiation and maintenance mechanisms cooperate to induce G1 cell cycle arrest in response to DNA damage. *Cell* **102**, 55-66 (2000).

88. Shanahan,F., Seghezzi,W., Parry,D., Mahony,D., & Lees,E. Cyclin E associates with BAF155 and BRG1, components of the mammalian SWI-SNF complex, and alters the ability of BRG1 to induce growth arrest. *Mol. Cell Biol.* **19**, 1460-1469 (1999).

89. Zhang,H.S. *et al.* Exit from G1 and S phase of the cell cycle is regulated by repressor complexes containing HDAC-Rb-hSWI/SNF and Rb-hSWI/SNF. *Cell* **101**, 79-89 (2000).

90. Ekholm,S.V., Zickert,P., Reed,S.I., & Zetterberg,A. Accumulation of cyclin E is not a prerequisite for passage through the restriction point. *Mol. Cell Biol.* **21**, 3256-3265 (2001).

91. Won,K.A. & Reed,S.I. Activation of cyclin E/CDK2 is coupled to site-specific autophosphorylation and ubiquitin-dependent degradation of cyclin E. *EMBO J.* **15**, 4182-4193 (1996).

92. Yeh,K.H. *et al.* The F-box protein SKP2 binds to the phosphorylated threonine 380 in cyclin E and regulates ubiquitin-dependent degradation of cyclin E. *Biochem. Biophys. Res. Commun.* **281**, 884-890 (2001).

93. Morris,L., Allen,K.E., & La Thangue,N.B. Regulation of E2F transcription by cyclin E-Cdk2 kinase mediated through p300/CBP co-activators. *Nat. Cell Biol.* **2**, 232-239 (2000).

94. Moore,J.D., Yang,J., Truant,R., & Kornbluth,S. Nuclear import of Cdk/cyclin complexes: identification of distinct mechanisms for import of Cdk2/cyclin E and Cdc2/cyclin B1. *J. Cell Biol.* **144**, 213-224 (1999).

95. Moore,J.D., Kornbluth,S., & Hunt,T. Identification of the nuclear localization signal in Xenopus cyclin E and analysis of its role in replication and mitosis. *Mol. Biol. Cell* **13**, 4388-4400 (2002).

96. Furstenthal,L., Swanson,C., Kaiser,B.K., Eldridge,A.G., & Jackson,P.K. Triggering ubiquitination of a CDK inhibitor at origins of DNA replication. *Nat. Cell Biol.* **3**, 715-722 (2001).

97. Okuda,M. *et al.* Nucleophosmin/B23 is a target of CDK2/cyclin E in centrosome duplication. *Cell* **103**, 127-140 (2000).

98. Sheaff,R.J., Groudine,M., Gordon,M., Roberts,J.M., & Clurman,B.E. Cyclin E-CDK2 is a regulator of p27Kip1. *Genes Dev.* **11**, 1464-1478 (1997).

99. Akli,S. & Keyomarsi,K. Cyclin E and its low molecular weight forms in human cancer and as targets for cancer therapy. *Cancer Biol. Ther.* **2**, S38-S47 (2003).

100. Jung,Y.J. *et al.* Reciprocal expressions of cyclin E and cyclin D1 in hepatocellular carcinoma. *Cancer Lett.* **168**, 57-63 (2001).

101. Bell,S.P. & Dutta,A. DNA replication in eukaryotic cells. *Annu. Rev. Biochem.* **71**, 333-374 (2002).

102. Pines,J. & Hunter,T. Human cyclin A is adenovirus E1A-associated protein p60 and behaves differently from cyclin B. *Nature* **346**, 760-763 (1990).

103. Poon,R.Y. *et al.* Cell cycle regulation of the p34cdc2/p33cdk2-activating kinase p40MO15. *J. Cell Sci.* **107 (Pt 10)**, 2789-2799 (1994).

104. Erlandsson,F., Linnman,C., Ekholm,S., Bengtsson,E., & Zetterberg,A. A detailed analysis of cyclin A accumulation at the G(1)/S border in normal and transformed cells. *Exp. Cell Res.* **259**, 86-95 (2000).

105. Pagano,M., Pepperkok,R., Verde,F., Ansorge,W., & Draetta,G. Cyclin A is required at two points in the human cell cycle. *EMBO J.* **11**, 961-971 (1992).

106. Liu,D. *et al.* Cyclin A1 is required for meiosis in the male mouse. *Nat. Genet.* **20**, 377-380 (1998).

107. Murphy,M. *et al.* Delayed early embryonic lethality following disruption of the murine cyclin A2 gene. *Nat. Genet.* **15**, 83-86 (1997).

108. Henglein,B., Chenivesse,X., Wang,J., Eick,D., & Brechot,C. Structure and cell cycle-regulated transcription of the human cyclin A gene. *Proc. Natl. Acad. Sci. U. S. A* **91**, 5490-5494 (1994).

109. Zwicker,J. *et al.* Cell cycle regulation of the cyclin A, cdc25C and cdc2 genes is based on a common mechanism of transcriptional repression. *EMBO J.* **14**, 4514-4522 (1995).

110. Zerfass-Thome,K. *et al.* p27KIP1 blocks cyclin E-dependent transactivation of cyclin A gene expression. *Mol. Cell Biol.* **17**, 407-415 (1997).

111. Arooz,T. *et al.* On the concentrations of cyclins and cyclin-dependent kinases in extracts of cultured human cells. *Biochemistry* **39**, 9494-9501 (2000).

112. Booher,R.N., Holman,P.S., & Fattaey,A. Human Myt1 is a cell cycle-regulated kinase that inhibits Cdc2 but not Cdk2 activity. *J. Biol. Chem.* **272**, 22300-22306 (1997).

113. McGowan,C.H. & Russell,P. Human Wee1 kinase inhibits cell division by phosphorylating p34cdc2 exclusively on Tyr15. *EMBO J.* **12**, 75-85 (1993).

114. Takeda,D.Y. & Dutta,A. DNA replication and progression through S phase. *Oncogene* **24**, 2827-2843 (2005).

115. Coverley,D., Pelizon,C., Trewick,S., & Laskey,R.A. Chromatin-bound Cdc6 persists in S and G2 phases in human cells, while soluble Cdc6 is destroyed in a cyclin A-cdk2 dependent process. *J. Cell Sci.* **113 (Pt 11)**, 1929-1938 (2000).

116. Petersen,B.O., Lukas,J., Sorensen,C.S., Bartek,J., & Helin,K. Phosphorylation of mammalian CDC6 by cyclin A/CDK2 regulates its subcellular localization. *EMBO J.* **18**, 396-410 (1999).

117. Ishimi,Y., Komamura-Kohno,Y., You,Z., Omori,A., & Kitagawa,M. Inhibition of Mcm4,6,7 helicase activity by phosphorylation with cyclin A/Cdk2. *J. Biol. Chem.* **275**, 16235-16241 (2000).

118. Dutta,A. & Stillman,B. cdc2 family kinases phosphorylate a human cell DNA replication factor, RPA, and activate DNA replication. *EMBO J.* **11**, 2189-2199 (1992).

119. Pan,Z.Q., Amin,A.A., Gibbs,E., Niu,H., & Hurwitz,J. Phosphorylation of the p34 subunit of human single-stranded-DNA-binding protein in cyclin A-activated G1 extracts is catalyzed by cdk-cyclin A complex and DNA-dependent protein kinase. *Proc. Natl. Acad. Sci. U. S. A* **91**, 8343-8347 (1994).

120. Voitenleitner,C., Fanning,E., & Nasheuer,H.P. Phosphorylation of DNA polymerase alpha-primase by cyclin A-dependent kinases regulates initiation of DNA replication in vitro. *Oncogene* **14**, 1611-1615 (1997).

121. Rao,P.N. & Johnson,R.T. Mammalian cell fusion: studies on the regulation of DNA synthesis and mitosis. *Nature* **225**, 159-164 (1970).

122. Blow,J.J. & Hodgson,B. Replication licensing--defining the proliferative state? *Trends Cell Biol.* **12**, 72-78 (2002).

123. Nishitani,H. & Lygerou,Z. Control of DNA replication licensing in a cell cycle. *Genes Cells* **7**, 523-534 (2002).

124. Lukas,C. *et al.* Accumulation of cyclin B1 requires E2F and cyclin-A-dependent rearrangement of the anaphase-promoting complex. *Nature* **401**, 815-818 (1999).

125. Geley,S. *et al.* Anaphase-promoting complex/cyclosome-dependent proteolysis of human cyclin A starts at the beginning of mitosis and is not subject to the spindle assembly checkpoint. *J. Cell Biol.* **153**, 137-148 (2001).

126. Bastians,H., Topper,L.M., Gorbsky,G.L., & Ruderman,J.V. Cell cycle-regulated proteolysis of mitotic target proteins. *Mol. Biol. Cell* **10**, 3927-3941 (1999).

127. El Deiry,W.S. *et al.* WAF1, a potential mediator of p53 tumor suppression. *Cell* **75**, 817-825 (1993).

128. Yen,A. & Sturgill,R. Hypophosphorylation of the RB protein in S and G2 as well as G1 during growth arrest. *Exp. Cell Res.* **241**, 324-331 (1998).

129. Flatt,P.M., Tang,L.J., Scatena,C.D., Szak,S.T., & Pietenpol,J.A. p53 regulation of G(2) checkpoint is retinoblastoma protein dependent. *Mol. Cell Biol.* **20**, 4210-4223 (2000).

130. Hollander,M.C. *et al.* Genomic instability in Gadd45a-deficient mice. *Nat. Genet.* **23**, 176-184 (1999).

131. Jin,S. *et al.* The GADD45 inhibition of Cdc2 kinase correlates with GADD45-mediated growth suppression. *J. Biol. Chem.* **275**, 16602-16608 (2000).

132. Jin,S. *et al.* GADD45-induced cell cycle G2-M arrest associates with altered subcellular distribution of cyclin B1 and is independent of p38 kinase activity. *Oncogene* **21**, 8696-8704 (2002).

133. Zhan,Q. *et al.* Association with Cdc2 and inhibition of Cdc2/Cyclin B1 kinase activity by the p53-regulated protein Gadd45. *Oncogene* **18**, 2892-2900 (1999).

134. Gao,H. *et al.* B23 regulates GADD45a nuclear translocation and contributes to GADD45a-induced cell cycle G2-M arrest. *J. Biol. Chem.* **280**, 10988-10996 (2005).

135. Ishida,S. *et al.* Role for E2F in control of both DNA replication and mitotic functions as revealed from DNA microarray analysis. *Mol. Cell Biol.* **21**, 4684-4699 (2001).

136. Zhu,W., Giangrande,P.H., & Nevins,J.R. E2Fs link the control of G1/S and G2/M transcription. *EMBO J.* **23**, 4615-4626 (2004).

137. Kimura,K., Hirano,M., Kobayashi,R., & Hirano,T. Phosphorylation and activation of 13S condensin by Cdc2 in vitro. *Science* **282**, 487-490 (1998).

138. Lipinski,M.M. *et al.* Cell-autonomous and non-cell-autonomous functions of the Rb tumor suppressor in developing central nervous system. *EMBO J.* **20**, 3402-3413 (2001).

139. Morgenbesser,S.D., Williams,B.O., Jacks,T., & DePinho,R.A. p53-dependent apoptosis produced by Rb-deficiency in the developing mouse lens. *Nature* **371**, 72-74 (1994).

140. Macleod,K.F., Hu,Y., & Jacks,T. Loss of Rb activates both p53-dependent and independent cell death pathways in the developing mouse nervous system. *EMBO J.* **15**, 6178-6188 (1996).

141. Irwin,M. *et al.* Role for the p53 homologue p73 in E2F-1-induced apoptosis. *Nature* **407**, 645-648 (2000).

142. Stiewe,T. & Putzer,B.M. Role of the p53-homologue p73 in E2F1-induced apoptosis. *Nat. Genet.* **26**, 464-469 (2000).

143. Ziebold,U., Reza,T., Caron,A., & Lees,J.A. E2F3 contributes both to the inappropriate proliferation and to the apoptosis arising in Rb mutant embryos. *Genes Dev.* **15**, 386-391 (2001).

144. Tsai,K.Y. *et al.* Mutation of E2f-1 suppresses apoptosis and inappropriate S phase entry and extends survival of Rb-deficient mouse embryos. *Mol. Cell* **2**, 293-304 (1998).

145. Iavarone,A. *et al.* Retinoblastoma promotes definitive erythropoiesis by repressing Id2 in fetal liver macrophages. *Nature* **432**, 1040-1045 (2004).

146. Lasorella,A., Uo,T., & Iavarone,A. Id proteins at the cross-road of development and cancer. *Oncogene* **20**, 8326-8333 (2001).

147. Lasorella,A., Noseda,M., Beyna,M., Yokota,Y., & Iavarone,A. Id2 is a retinoblastoma protein target and mediates signalling by Myc oncoproteins. *Nature* **407**, 592-598 (2000).

148. Yokota,Y. *et al.* Development of peripheral lymphoid organs and natural killer cells depends on the helix-loop-helix inhibitor Id2. *Nature* **397**, 702-706 (1999).

149. Mori,S., Nishikawa,S.I., & Yokota,Y. Lactation defect in mice lacking the helix-loop-helix inhibitor Id2. *EMBO J.* **19**, 5772-5781 (2000).

150. Lasorella,A., Rothschild,G., Yokota,Y., Russell,R.G., & Iavarone,A. Id2 mediates tumor initiation, proliferation, and angiogenesis in Rb mutant mice. *Mol. Cell Biol.* **25**, 3563-3574 (2005).

151. Sanchez,I. & Dynlacht,B.D. New insights into cyclins, CDKs, and cell cycle control. *Semin. Cell Dev. Biol.* **16**, 311-321 (2005).

152. Deshpande,A., Sicinski,P., & Hinds,P.W. Cyclins and cdks in development and cancer: a perspective. *Oncogene* **24**, 2909-2915 (2005).

153. Lees,J.A., Buchkovich,K.J., Marshak,D.R., Anderson,C.W., & Harlow,E. The retinoblastoma protein is phosphorylated on multiple sites by human cdc2. *EMBO J.* **10**, 4279-4290 (1991).

154. Harbour,J.W., Luo,R.X., Dei,S.A., Postigo,A.A., & Dean,D.C. Cdk phosphorylation triggers sequential intramolecular interactions that progressively block Rb functions as cells move through G1. *Cell* **98**, 859-869 (1999).

155. Serrano,M., Hannon,G.J., & Beach,D. A new regulatory motif in cell-cycle control causing specific inhibition of cyclin D/CDK4. *Nature* **366**, 704-707 (1993).

156. Hannon,G.J. & Beach,D. p15INK4B is a potential effector of TGF-beta-induced cell cycle arrest. *Nature* **371**, 257-261 (1994).

157. Okuda,T. *et al.* Molecular cloning, expression pattern, and chromosomal localization of human CDKN2D/INK4d, an inhibitor of cyclin D-dependent kinases. *Genomics* **29**, 623-630 (1995).

158. Guan,K.L. *et al.* Growth suppression by p18, a p16INK4/. *Genes Dev.* **8**, 2939-2952 (1994).

159. Villacanas,O., Perez,J.J., & Rubio-Martinez,J. Structural analysis of the inhibition of Cdk4 and Cdk6 by p16(INK4a) through molecular dynamics simulations. *J. Biomol. Struct. Dyn.* **20**, 347-358 (2002).

160. Sherr,C.J. & Roberts,J.M. CDK inhibitors: positive and negative regulators of G1-phase progression. *Genes Dev.* **13**, 1501-1512 (1999).

161. Olashaw,N. & Pledger,W.J. Paradigms of growth control: relation to Cdk activation. *Sci. STKE.* **2002**, RE7 (2002).

162. Alt,J.R., Gladden,A.B., & Diehl,J.A. p21(Cip1) Promotes cyclin D1 nuclear accumulation via direct inhibition of nuclear export. *J. Biol. Chem.* **277**, 8517-8523 (2002).

163. Yang,B., Guo,M., Herman,J.G., & Clark,D.P. Aberrant promoter methylation profiles of tumor suppressor genes in hepatocellular carcinoma 1. *Am. J. Pathol.* **163**, 1101-1107 (2003).

164. Roncalli,M. *et al.* Methylation framework of cell cycle gene inhibitors in cirrhosis and associated hepatocellular carcinoma 1. *Hepatology* **36**, 427-432 (2002).

165. Piao,Z. *et al.* Homozygous deletions of the CDKN2 gene and loss of heterozygosity of 9p in primary hepatocellular carcinoma. *Cancer Lett.* **122**, 201-207 (1998).

166. Deane,N.G. *et al.* Hepatocellular carcinoma results from chronic cyclin D1 overexpression in transgenic mice 5. *Cancer Res.* **61**, 5389-5395 (2001).

167. Lu,Z.L., Luo,D.Z., & Wen,J.M. Expression and significance of tumor-related genes in HCC. *World J. Gastroenterol.* **11**, 3850-3854 (2005).

168. Honda,R., Tanaka,H., & Yasuda,H. Oncoprotein MDM2 is a ubiquitin ligase E3 for tumor suppressor p53. *FEBS Lett.* **420**, 25-27 (1997).

169. Appella,E. & Anderson,C.W. Signaling to p53: breaking the posttranslational modification code. *Pathol. Biol. (Paris)* **48**, 227-245 (2000).

170. Li,D., Cao,Y., He,L., Wang,N.J., & Gu,J.R. Aberrations of p53 gene in human hepatocellular carcinoma from China. *Carcinogenesis* **14**, 169-173 (1993).

171. Kew,M.C. Synergistic interaction between aflatoxin B1 and hepatitis B virus in hepatocarcinogenesis. *Liver Int* **23**, 405-409 (2003).

172. Ray,R.B., Steele,R., Meyer,K., & Ray,R. Transcriptional repression of p53 promoter by hepatitis C virus core protein. *J. Biol. Chem.* **272**, 10983-10986 (1997).

173. Okada,T. *et al.* Gene expression profile linked to p53 status in hepatitis C virus-related hepatocellular carcinoma. *FEBS Lett* **555**, 583-590 (2003).

174. Kwon,J.A. & Rho,H.M. Transcriptional repression of the human p53 gene by hepatitis B viral core protein (HBc) in human liver cells. *Biol. Chem.* **384**, 203-212 (2003).

175. Lee,S.G. & Rho,H.M. Transcriptional repression of the human p53 gene by hepatitis B viral X protein. *Oncogene* **19**, 468-471 (2000).

176. Shieh,S.Y., Ikeda,M., Taya,Y., & Prives,C. DNA damage-induced phosphorylation of p53 alleviates inhibition by MDM2. *Cell* **91**, 325-334 (1997).

177. Shieh,S.Y., Ahn,J., Tamai,K., Taya,Y., & Prives,C. The human homologs of checkpoint kinases Chk1 and Cds1 (Chk2) phosphorylate p53 at multiple DNA damage-inducible sites. *Genes Dev.* **14**, 289-300 (2000).

178. Hirao,A. *et al.* DNA damage-induced activation of p53 by the checkpoint kinase Chk2. *Science* **287**, 1824-1827 (2000).

179. Tibbetts,R.S. *et al.* A role for ATR in the DNA damage-induced phosphorylation of p53. *Genes Dev.* **13**, 152-157 (1999).

180. Khanna,K.K. *et al.* ATM associates with and phosphorylates p53: mapping the region of interaction. *Nat. Genet.* **20**, 398-400 (1998).

181. Wu,Z. *et al.* Mutation of mouse p53 Ser23 and the response to DNA damage. *Mol. Cell Biol.* **22**, 2441-2449 (2002).

182. Chao,C. *et al.* Cell type- and promoter-specific roles of Ser18 phosphorylation in regulating p53 responses. *J. Biol. Chem.* **278**, 41028-41033 (2003).

183. Craig,A.L. *et al.* Novel phosphorylation sites of human tumour suppressor protein p53 at Ser20 and Thr18 that disrupt the binding of mdm2 (mouse double minute 2) protein are modified in human cancers. *Biochem. J.* **342 (Pt 1)**, 133-141 (1999).

184. Pise-Masison,C.A., Radonovich,M., Sakaguchi,K., Appella,E., & Brady,J.N. Phosphorylation of p53: a novel pathway for p53 inactivation in human T-cell lymphotropic virus type 1-transformed cells. *J. Virol.* **72**, 6348-6355 (1998).

185. Waterman,M.J., Stavridi,E.S., Waterman,J.L., & Halazonetis,T.D. ATM-dependent activation of p53 involves dephosphorylation and association with 14-3-3 proteins. *Nat. Genet.* **19**, 175-178 (1998).

186. Buschmann,T. *et al.* Jun NH2-terminal kinase phosphorylation of p53 on Thr-81 is important for p53 stabilization and transcriptional activities in response to stress. *Mol. Cell Biol.* **21**, 2743-2754 (2001).

187. Bulavin,D.V. *et al.* Phosphorylation of human p53 by p38 kinase coordinates N-terminal phosphorylation and apoptosis in response to UV radiation. *EMBO J.* **18**, 6845-6854 (1999).

188. D'Orazi,G. *et al.* Homeodomain-interacting protein kinase-2 phosphorylates p53 at Ser 46 and mediates apoptosis. *Nat. Cell Biol.* **4**, 11-19 (2002).

189. Hofmann,T.G. *et al.* Regulation of p53 activity by its interaction with homeodomain-interacting protein kinase-2. *Nat. Cell Biol.* **4**, 1-10 (2002).

190. Zheng,H. *et al.* The prolyl isomerase Pin1 is a regulator of p53 in genotoxic response. *Nature* **419**, 849-853 (2002).

191. Zacchi,P. *et al.* The prolyl isomerase Pin1 reveals a mechanism to control p53 functions after genotoxic insults. *Nature* **419**, 853-857 (2002).

192. Ito,A. *et al.* p300/CBP-mediated p53 acetylation is commonly induced by p53-activating agents and inhibited by MDM2. *EMBO J.* **20**, 1331-1340 (2001).

193. Sakaguchi,K. *et al.* DNA damage activates p53 through a phosphorylation-acetylation cascade. *Genes Dev.* **12**, 2831-2841 (1998).

194. Nakamura,S., Roth,J.A., & Mukhopadhyay,T. Multiple lysine mutations in the C-terminal domain of p53 interfere with MDM2-dependent protein degradation and ubiquitination. *Mol. Cell Biol.* **20**, 9391-9398 (2000).

195. Kobet,E., Zeng,X., Zhu,Y., Keller,D., & Lu,H. MDM2 inhibits p300-mediated p53 acetylation and activation by forming a ternary complex with the two proteins. *Proc. Natl. Acad. Sci. U. S. A* **97**, 12547-12552 (2000).

196. Kawai,H., Nie,L., Wiederschain,D., & Yuan,Z.M. Dual role of p300 in the regulation of p53 stability. *J. Biol. Chem.* **276**, 45928-45932 (2001).

197. Luo,J. *et al.* Negative control of p53 by Sir2alpha promotes cell survival under stress. *Cell* **107**, 137-148 (2001).

198. Schmidt,D. & Muller,S. Members of the PIAS family act as SUMO ligases for c-Jun and p53 and repress p53 activity. *Proc. Natl. Acad. Sci. U. S. A* **99**, 2872-2877 (2002).

199. Megidish,T., Xu,J.H., & Xu,C.W. Activation of p53 by protein inhibitor of activated Stat1 (PIAS1). *J. Biol. Chem.* **277**, 8255-8259 (2002).

200. Weger,S., Hammer,E., & Heilbronn,R. Topors acts as a SUMO-1 E3 ligase for p53 in vitro and in vivo. *FEBS Lett.* **579**, 5007-5012 (2005).

201. Chen,L. & Chen,J. MDM2-ARF complex regulates p53 sumoylation. *Oncogene* **22**, 5348-5357 (2003).

202. Seeler,J.S. & Dejean,A. The PML nuclear bodies: actors or extras? *Curr. Opin. Genet. Dev.* **9**, 362-367 (1999).

203. Guo,A. *et al.* The function of PML in p53-dependent apoptosis. *Nat. Cell Biol.* **2**, 730-736 (2000).

204. Scotto,C., Delphin,C., Deloulme,J.C., & Baudier,J. Concerted regulation of wild-type p53 nuclear accumulation and activation by S100B and calcium-dependent protein kinase C. *Mol. Cell Biol.* **19**, 7168-7180 (1999).

205. Fakharzadeh,S.S., Trusko,S.P., & George,D.L. Tumorigenic potential associated with enhanced expression of a gene that is amplified in a mouse tumor cell line. *EMBO J.* **10**, 1565-1569 (1991).

206. Cahilly-Snyder,L., Yang-Feng,T., Francke,U., & George,D.L. Molecular analysis and chromosomal mapping of amplified genes isolated from a transformed mouse 3T3 cell line. *Somat. Cell Mol. Genet.* **13**, 235-244 (1987).

207. Oliner,J.D., Kinzler,K.W., Meltzer,P.S., George,D.L., & Vogelstein,B. Amplification of a gene encoding a p53-associated protein in human sarcomas. *Nature* **358**, 80-83 (1992).

208. Montes de Oca,L.R., Wagner,D.S., & Lozano,G. Rescue of early embryonic lethality in mdm2-deficient mice by deletion of p53. *Nature* **378**, 203-206 (1995).

209. Iwakuma,T. & Lozano,G. MDM2, an introduction. *Mol. Cancer Res.* **1**, 993-1000 (2003).

210. Fridman,J.S. *et al.* Tumor promotion by Mdm2 splice variants unable to bind p53. *Cancer Res.* **63**, 5703-5706 (2003).

211. Yang,Y. & Yu,X. Regulation of apoptosis: the ubiquitous way. *FASEB J.* **17**, 790-799 (2003).

212. Lee,J.C. & Peter,M.E. Regulation of apoptosis by ubiquitination. *Immunol. Rev.* **193**, 39-47 (2003).

213. Thrower,J.S., Hoffman,L., Rechsteiner,M., & Pickart,C.M. Recognition of the polyubiquitin proteolytic signal. *EMBO J.* **19**, 94-102 (2000).

214. Brazil,D.P. & Hemmings,B.A. Ten years of protein kinase B signalling: a hard Akt to follow. *Trends Biochem. Sci* **26**, 657-664 (2001).

215. Mayo,L.D. & Donner,D.B. A phosphatidylinositol 3-kinase/Akt pathway promotes translocation of Mdm2 from the cytoplasm to the nucleus. *Proc. Natl. Acad Sci U. S. A* **98**, 11598-11603 (2001).

216. Stambolic,V. *et al.* Negative regulation of PKB/Akt-dependent cell survival by the tumor suppressor PTEN. *Cell* **95**, 29-39 (1998).

217. Mayo,L.D., Dixon,J.E., Durden,D.L., Tonks,N.K., & Donner,D.B. PTEN protects p53 from Mdm2 and sensitizes cancer cells to chemotherapy. *J. Biol. Chem.* **277**, 5484-5489 (2002).

218. Stad,R. *et al.* Hdmx stabilizes Mdm2 and p53. *J. Biol. Chem.* **275**, 28039-28044 (2000).

219. Jackson,M.W., Lindstrom,M.S., & Berberich,S.J. MdmX binding to ARF affects Mdm2 protein stability and p53 transactivation. *J. Biol. Chem.* **276**, 25336-25341 (2001).

220. Quelle,D.E., Zindy,F., Ashmun,R.A., & Sherr,C.J. Alternative reading frames of the INK4a tumor suppressor gene encode two unrelated proteins capable of inducing cell cycle arrest. *Cell* **83**, 993-1000 (1995).

221. Zindy,F. *et al.* Myc signaling via the ARF tumor suppressor regulates p53-dependent apoptosis and immortalization. *Genes Dev.* **12**, 2424-2433 (1998).

222. Bates,S. *et al.* p14ARF links the tumour suppressors RB and p53. *Nature* **395**, 124-125 (1998).

223. Palmero,I., Murga,M., Zubiaga,A., & Serrano,M. Activation of ARF by oncogenic stress in mouse fibroblasts is independent of E2F1 and E2F2. *Oncogene* **21**, 2939-2947 (2002).

224. Groth,A., Weber,J.D., Willumsen,B.M., Sherr,C.J., & Roussel,M.F. Oncogenic Ras induces p19ARF and growth arrest in mouse embryo fibroblasts lacking p21Cip1 and p27Kip1 without activating cyclin D-dependent kinases. *J. Biol. Chem.* **275**, 27473-27480 (2000).

225. de Stanchina,E. *et al.* E1A signaling to p53 involves the p19(ARF) tumor suppressor. *Genes Dev.* **12**, 2434-2442 (1998).

226. Sugimoto,M., Kuo,M.L., Roussel,M.F., & Sherr,C.J. Nucleolar Arf tumor suppressor inhibits ribosomal RNA processing. *Mol. Cell* **11**, 415-424 (2003).

227. Harris,C.C. & Hollstein,M. Clinical implications of the p53 tumor-suppressor gene. *N. Engl. J. Med.* **329**, 1318-1327 (1993).

228. Kamijo,T., Bodner,S., van de,K.E., Randle,D.H., & Sherr,C.J. Tumor spectrum in ARF-deficient mice. *Cancer Res.* **59**, 2217-2222 (1999).

229. Weber,J.D., Taylor,L.J., Roussel,M.F., Sherr,C.J., & Bar-Sagi,D. Nucleolar Arf sequesters Mdm2 and activates p53. *Nat. Cell Biol.* **1**, 20-26 (1999).

230. Llanos,S., Clark,P.A., Rowe,J., & Peters,G. Stabilization of p53 by p14ARF without relocation of MDM2 to the nucleolus. *Nat. Cell Biol.* **3**, 445-452 (2001).

231. Kuo,M.L., den Besten,W., Bertwistle,D., Roussel,M.F., & Sherr,C.J. N-terminal polyubiquitination and degradation of the Arf tumor suppressor. *Genes Dev.* **18**, 1862-1874 (2004).

232. Bertwistle,D., Sugimoto,M., & Sherr,C.J. Physical and functional interactions of the Arf tumor suppressor protein with nucleophosmin/B23. *Mol. Cell Biol.* **24**, 985-996 (2004).

233. Itahana,K. *et al.* Tumor Suppressor ARF Degrades B23, a Nucleolar Protein Involved in Ribosome Biogenesis and Cell Proliferation. *Molecular Cell* **12**, 1151-1164 (2003).

234. Maiguel,D.A., Jones,L., Chakravarty,D., Yang,C., & Carrier,F. Nucleophosmin Sets a Threshold for p53 Response to UV Radiation. *Mol. Cell. Biol.* **24**, 3703-3711 (2004).

235. Rocha,S., Garrett,M.D., Campbell,K.J., Schumm,K., & Perkins,N.D. Regulation of NF-kappaB and p53 through activation of ATR and Chk1 by the ARF tumour suppressor. *EMBO J.*(2005).

236. Rocha,S., Campbell,K.J., & Perkins,N.D. p53- and Mdm2-independent repression of NF-kappa B transactivation by the ARF tumor suppressor. *Mol Cell* **12**, 15-25 (2003).

237. Tannapfel,A. *et al.* INK4a-ARF alterations and p53 mutations in hepatocellular carcinomas. *Oncogene* **20**, 7104-7109 (2001).

238. Tago,K., Chiocca,S., & Sherr,C.J. Sumoylation induced by the Arf tumor suppressor: A p53-independent function. *PNAS*0502978102 (2005).

239. Endo,K., Ueda,T., Ohta,T., & Terada,T. Protein expression of MDM2 and its clinicopathological relationships in human hepatocellular carcinoma. *Liver* **20**, 209-215 (2000).

240. Qiu,S.J., Ye,S.L., Wu,Z.Q., Tang,Z.Y., & Liu,Y.K. The expression of the mdm2 gene may be related to the aberration of the p53 gene in human hepatocellular carcinoma. *J. Cancer Res. Clin. Oncol.* **124**, 253-258 (1998).

241. Ito,T. *et al.* Alteration of the p14(ARF) gene and p53 status in human hepatocellular carcinomas. *J. Gastroenterol.* **39**, 355-361 (2004).

242. Herath,N.I. *et al.* Reciprocal relationship between methylation status and loss of heterozygosity at the p14(ARF) locus in Australian and South African hepatocellular carcinomas. *J. Gastroenterol. Hepatol.* **17**, 301-307 (2002).

243. Tannapfel,A. & Wittekind,C. Genes involved in hepatocellular carcinoma: deregulation in cell cycling and apoptosis. *Virchows Arch.* **440**, 345-352 (2002).

244. Bosco,E.E. & Knudsen,E.S. Differential role of RB in response to UV and IR damage. *Nucleic Acids Res.* **33**, 1581-1592 (2005).

245. Bentley,N.J. *et al.* The Schizosaccharomyces pombe rad3 checkpoint gene. *EMBO J.* **15**, 6641-6651 (1996).

246. Lin,W.C., Lin,F.T., & Nevins,J.R. Selective induction of E2F1 in response to DNA damage, mediated by ATM-dependent phosphorylation. *Genes Dev.* **15**, 1833-1844 (2001).

247. Peeper,D.S. *et al.* Phosphorylation of a specific cdk site in E2F-1 affects its electrophoretic mobility and promotes pRB-binding in vitro. *Oncogene* **10**, 39-48 (1995).

248. Jazayeri,A. *et al.* ATM- and cell cycle-dependent regulation of ATR in response to DNA double-strand breaks. *Nat. Cell Biol.*(2005).

249. Bakkenist,C.J. & Kastan,M.B. DNA damage activates ATM through intermolecular autophosphorylation and dimer dissociation. *Nature* **421**, 499-506 (2003).

250. Falck,J., Coates,J., & Jackson,S.P. Conserved modes of recruitment of ATM, ATR and DNA-PKcs to sites of DNA damage. *Nature* **434**, 605-611 (2005).

251. Liu,Q. *et al.* Chk1 is an essential kinase that is regulated by Atr and required for the G(2)/M DNA damage checkpoint. *Genes Dev.* **14**, 1448-1459 (2000).

252. Dart,D.A., Adams,K.E., Akerman,I., & Lakin,N.D. Recruitment of the cell cycle checkpoint kinase ATR to chromatin during S-phase. *J. Biol. Chem.* **279**, 16433-16440 (2004).

253. Zou,L. & Elledge,S.J. Sensing DNA damage through ATRIP recognition of RPA-ssDNA complexes. *Science* **300**, 1542-1548 (2003).

254. Post,S. *et al.* Phosphorylation of serines 635 and 645 of human Rad17 is cell cycle regulated and is required for G(1)/S checkpoint activation in response to DNA damage. *Proc. Natl. Acad. Sci. U. S. A* **98**, 13102-13107 (2001).

Appendix 1

Mitosis

The function of mitosis is to ensure that the each daughter cell gets a full set of chromosomes together with a centrosome. Mitosis is divided up into five distinct stages, prophase, prometaphase, metaphase, anaphase and telophase. It is regulated by cyclin B1 and the anaphase promoting complex (APC) targets cyclin B1 for degradation signalling the end of mitosis.

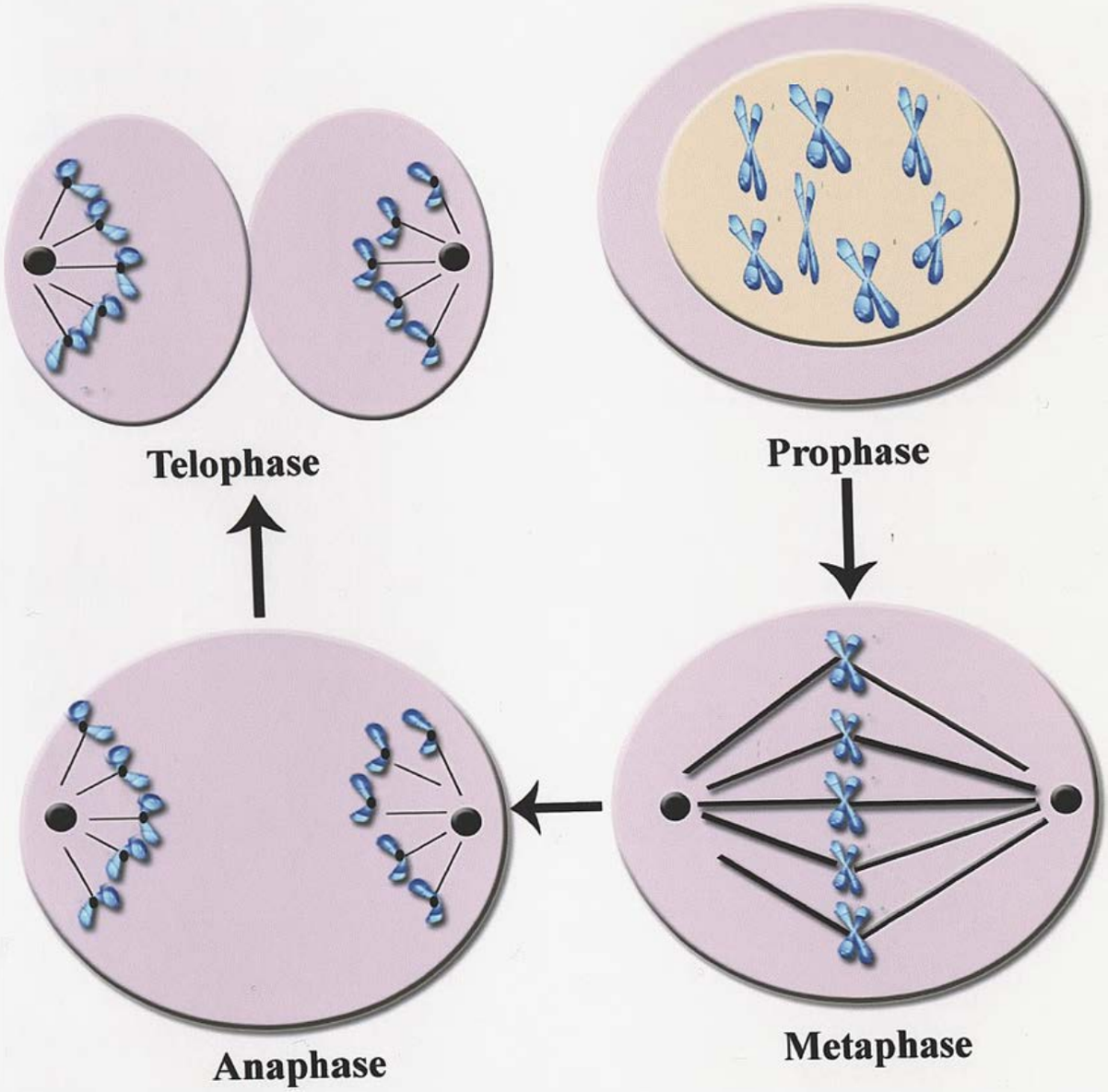


Figure 1: The four stages of mitosis

1. Prophase

The diffuse chromatin from interphase condenses into chromosomes. The chromosomes consist of a pair of sister chromatids joined together at a point known as the centromere. At the end of prophase the nuclear envelope breaks down into vesicles. The kinetochore, the point at which the sister chromatids are joined together recruits Bub1 and BUBR1. The nuclear envelope disassembly results in the chromosomes spilling out into the cytoplasm the mitotic checkpoint is activated at every unattached kinetochore.

2. *Metaphase*

The chromosomes are aligned at the midzone and are held in place by microtubules attached to the mitotic spindle. The sister chromatids are attached to the microtubules by their kientochore, the capture of both kinetochores of a duplicated chromatid pair by the microtubulues results in the mitotic checkpoint being silenced. After capture of the final chromatid pair the inhibitors that produce a 'wait anaphase" signal are removed, which includes cyclin B and securin.

3. *Anaphase*

The sister chromatid pairs are pulled apart and move towards opposite poles of the cell. The spindle elongates and invaginations of the plasma membrane around the midzone become apparent.

4. *Telophase*

Daughter chromosomes arrive at the poles and the microtubules disappear. The condensed chromatin expands and the nuclear envelope reforms. Cytokinesis is completed.

Appendix 2

Solutions:

Tissue culture stock solutions

0.36mg/ml Dexamethasone

1mg Dexamethasone (Sigma)

1ml absolute ethanol

27mls PBS

(Stored at -20°C in 500µl aliquots)

Insulin

5mls solution

Diluted to 72.5mls with dH_2O

(Stored at -20°C in 500µl aliquots)

10µg/ml Fibronectin

Top stock 1mg/ml fibronectin (sigma

Prior to use diluted 1/100 with sterile PBS

Stored at 4°C

PCR

PCR mastermixes

Gene	p53	Rb	ARF	ß-actin
dH_2O	17.25µl	24.75µl	35.75µl	35.75 µl
10X PCR buffer	5µl	5µl	5µl	5µl
Mg (50mM)	2µl	1.75µl	1.75 µl	1.75 µl
DNTP (1.25mM)	8µl	8µl	8µl	8µl
Primer (10µM)	2.5µl each	2.5µl each	2.5µl each	2.5µl each
Taq	0.25µl	0.5µl	0.25 µl	0.25 µl
DNA	5µl	5µl	2.5 µl	2.5 µl

Table 3: The concentrations and amounts of the various constituents in the specific PCR mastermixes

Immunofluoresence solutions

Mowiol

Mowiol, 2.4g, (Calbiochem 475904) was added to 6g of glycerol (Glycerol density =1.26g/ml – for 6g = 6/126 = 4.76mls). The mixture was stirred, 12mls of dH_2O added, and left overnight at room temperature. Tris pH8.5, was added to a final concentration of 90mM and the mixture was heated to 50°C for 1-2hours with occasional overtaxing. The tube was centrifuge at 2000rpm for 15minutes. 1,4-diazobicyclooctane (DABCO) was added to a final concentration of 2.5%. The solution was aliquoted and stored at -20 °C